

Distribution Agreement

In presenting this thesis or dissertation as a partial fulfillment of the requirements for an advanced degree from Emory University, I hereby grant to Emory University and its agents the non-exclusive license to archive, make accessible, and display my thesis or dissertation in whole or in part in all forms of media, now or hereafter known, including display on the world wide web. I understand that I may select some access restrictions as part of the online submission of this thesis or dissertation. I retain all ownership rights to the copyright of the thesis or dissertation. I also retain the right to use in future works (such as articles or books) all or part of this thesis or dissertation.

Signature:

William J. Kaiser

Date

DEVELOPMENTAL AND VIRAL CONTROL OF NECROTIC CELL DEATH

By

William J. Kaiser
Doctor of Philosophy

Graduate Division of Biological and Biomedical Science
Microbiology and Molecular Genetics

Edward S. Mocarski, Ph.D.
Advisor

Samuel H. Speck, Ph.D.
Committee Member

Tamara Caspary, Ph.D.
Committee Member

David S. Weiss, Ph.D.
Committee Member

Lawrence Boise, Ph.D.
Committee Member

Accepted:

Lisa A. Tedesco, Ph.D.
Dean of the James T. Laney School of Graduate Studies

Date

DEVELOPMENTAL AND VIRAL CONTROL OF NECROTIC CELL DEATH

By

William J. Kaiser
A.B, B.S, University of Georgia, 1998

Advisor: Edward S. Mocarski, Ph.D.

An abstract of
a dissertation submitted to the Faculty of the
James T. Laney School of Graduate Studies of Emory University
in partial fulfillment of the requirements for the degree of
Doctor of Philosophy
in Microbiology and Molecular Genetics.
2012

Abstract

DEVELOPMENTAL AND VIRAL CONTROL OF NECROTIC CELL DEATH

Apoptosis and necroptosis are complementary cell death pathways controlled by common signaling adaptors, kinases and proteases. Among the key players, caspase-8 stands out because this protease mediates tumor necrosis factor (TNF) family death receptor-induced apoptosis. TNF family receptors also control cytokine activation via NF- κ B activation. Recently, caspase 8 has been shown to suppress programmed necrosis mediated via receptor-interacting protein (RIP)1 and RIP3. Either apoptosis or necrosis can follow death receptor-activation, dependent on the level of caspase 8 activity. In this dissertation, I describe my work on establishing role of RIP3-dependent necrosis in host defense and the essential function caspase 8 plays in suppressing RIP3 during mammalian development.

Toll-like receptor (TLR) signaling is triggered by pathogen-associated molecular patterns, mediating cytokine activation pathways via NF- κ B and IRF3/IRF7 though how TLRs engage cell death pathways was unresolved. I found that caspase 8 is necessary to prevent RIP3-dependent programmed necrosis following TLR activation, and TLR3 or TLR4 signaling directly triggers programmed necrosis through the adapter protein TRIF interacting with RIP3. Thus, cell fate decisions following TLR activation depend on similar machinery as death receptor signaling in maintaining a balance between cytokine activation, apoptosis and necrosis.

Viral pathogenesis relies upon modulation of cell death pathways that contribute to host defense by eliminating infected cells. Infection by murine cytomegalovirus induces RIP3-dependent necrosis. Virus-induced programmed necrosis is death receptor- and TLR-independent but is dependent on the pathogen sensor protein DNA-dependent activator of interferon regulatory factors (DAI) which forms an antiviral pro-necrotic complex upon binding to RIP3. The viral inhibitor of RIP activation (vIRA, encoded by the viral M45 gene) suppresses programmed necrosis by disrupting DAI-RIP3 interactions. Importantly, the attenuation of vIRA-deficient virus in wild type mice is normalized in *RIP3*^{-/-} or *DAI*^{-/-} mice. Thus, vIRA function validates necrosis as central to the elimination of infected cells in host defense.

Germ line disruption of caspase 8 leads to embryonic lethality in mice. Conditional elimination of caspase 8 has revealed an essential role of this enzyme in a range of tissues and cell types. To determine whether caspase 8 naturally holds RIP3-dependent death pathways in check, I generated embryos lacking both caspase 8 and RIP3. Remarkably, these *Casp8*^{-/-} *Rip3*^{-/-} double mutant mice were viable, matured into fertile adults and appear immunocompetent although they develop lymphadenopathy marked by accumulation of abnormal T cells in the periphery, a phenotype reminiscent of mice with Fas-deficiency (*lpr/lpr*). Thus, caspase 8 contributes to homeostatic control in the adult immune system; however, RIP3 and caspase 8 are both completely dispensable for mammalian development.

DEVELOPMENTAL AND VIRAL CONTROL OF NECROTIC CELL DEATH

By

William J. Kaiser
A.B., B.S., University of Georgia, 1998

Advisor: Edward S. Mocarski, Ph.D.

A dissertation submitted to the Faculty of the
James T. Laney School of Graduate Studies of Emory University
in partial fulfillment of the requirements for the degree of
Doctor of Philosophy
in Microbiology and Molecular Genetics
2012

Acknowledgements

This thesis is dedicated to the memory of Lois Miller. Lois handed me my first set of pipets and introduced me to the joys of watching cells die through a microscope. I am indebted to Margaret Offermann and Ed Mocarski for their continued support, guidance, patience, and especially for the opportunity to pursue lines of investigation that I found fascinating. Importantly, Drs. Miller, Offermann, and Mocarski taught me to creatively pursue lines of scientific inquiry that fill critical gaps in our understanding. My gifted mentors have bestowed a solid template for me to model as I continue a career in science.

I greatly appreciate past and present members of the Mocarski lab, especially Linda Roback, Jason Upton, Devon Livingston-Rosanoff, Lisa Daley-Bauer, and Lynsey Crosby. I also wish to thank the Sam Speck and the members of his lab. I thank Tamara Caspary and Alyssa Long for guiding evaluation of embryos. I thank Vishva Dixit and Kim Newton (Genentech) for RIP3^{-/-} mice, Francis Chan (University of Massachusetts) for facilitating transfer of RIP3^{-/-} mice, Shizuo Akira (Osaka University) for *DAI*^{-/-} mice, John Silke (LaTrobe University) and Michelle Kelliher (University of Massachusetts) for RIP1^{-/-} MEFs, David Lembo (University of Turin) for M45/vIRA antibody, Stipan Jonjic (University of Rijeka) for MCMV IE1 antibody, Tillman Bückstümmer and Giulio Superti-Furga (CeMM) for anti-DAI antibody, and John Bertin and Peter Gough (GSK) for RIP3 inhibitors. I thank Louise McCormick, Andrew Kowalczyk, Rebecca Oas, Rafi Ahmed (Emory University), and Thomas Kaufmann (University of Bern) for insightful discussions and provision of reagents. I also thank Minida Dowdy and Jennifer Perry for animal husbandry, Laura Bender at the cell imaging and microscopy core at The Winship Cancer Institute and Hong Yi at the Emory School of Medicine Microscopy Core.

I finally would like to express my appreciation for my wife's enduring love and support.

Table of Contents

Abstract	<i>iii</i>
Acknowledgements	<i>v</i>
Table of Contents	<i>vi</i>
List of Figures and Tables	<i>vii</i>
Chapter 1: Introduction	1
Figures 1.1-1.4 and Table 1.1	11
Chapter 2: Pathogen subversion of RIP3-dependent necrosis	
A. Introduction.....	17
B. Results.....	21
C. Discussion	32
D. Conclusions.....	39
E. Materials and Methods.....	40
F. Figures 2.1-2.5 and 2.S1-S3.....	46
Chapter 3: RIP3 mediates the embryonic lethality of caspase-8-deficient mice	
A. Introduction and Summary	61
B. Results and Discussion.....	62
C. Materials and Methods	70
D. Figures 3.1-3.4 and 3.S1-3.S5	75
Chapter 4: DAI-RIP3 complex mediates virus-induced programmed necrosis	
A. Introduction.....	88
B. Results.....	92
C. Discussion	100
D. Materials and Methods	105
E. Figures 4.1-4.4 and 4.S1-4.S4.....	108
Chapter 5: Toll-like Receptor 3 induces RIP1-independent necrosis via a TRIF-RIP3 complex	
A. Introduction	119
B. Results.....	123
C. Discussion	129
D. Materials and Methods	134
E. Figures 5.1-5.6	136
Chapter 6: General Discussion and Future Possibilities	144
Figures 6.1 1.1	154
References	155

List of Figures and Tables

Figure 1.1.	Casp8 regulation of RIP1–RIP3 signaling pathways	11
Figure 1.2.	Viral modulation of cell death signals mediated by Casp8 activation and RIP1–RIP3 pathways	13
Figure 1.3.	MCMV modulation of cell death signals mediated by Casp8 activation and RIP1–RIP3 pathways	14
Figure 1.4.	Schematic representation of the domain architecture of the RHIM- containing proteins	15
Table 1.1.	Selected Viral Inhibitors of Apoptosis and Necrosis	16
Figure 2.1.	Role of MCMV M45 RHIM interactions in suppression of virus-induced death	46
Figure 2.2.	Cells sensitive to MCMV-associated programmed necrosis express high levels of RIP3	48
Figure 2.3.	MCMV RHIM-dependent suppression of RIP3-mediated necrosis	50
Figure 2.4.	RIP3 is required, and RIP1 is dispensable for MCMV-associated programmed necrosis	52
Figure 2.5.	M45mutRHIM attenuation <i>in vivo</i> is specifically normalized in RIP3- deficient mice	54
Figure 2.S1.	Generation of mutant MCMV viruses	56
Figure 2.S2.	Cell death induced by M45mutRHIM	58
Figure 2.S3.	Nec-1 does not block virus-induced necrosis	59
Figure 3.1.	Embryonic expression of <i>Rip3</i>	75
Figure 3.2.	<i>Casp8^{-/-}Rip3^{-/-}</i> mice are viable	77
Figure 3.3.	Sensitivity to DR-induced apoptosis, necroptosis and disease	78
Figure 3.4.	Immune compartment of 16-week-old DKO mice	79
Figure 3.S1.	Casp8 suppresses programmed necrosis	81
Figure 3.S2.	Embryonic lethality and RIP3 detection in Casp8-deficient mice	83
Figure 3.S3.	<i>Casp8^{-/-}Rip3^{-/-}</i> mice are viable	84
Figure 3.S4.	Susceptibility to LPS+GalN induced hepatitis in <i>Casp8^{+/+}Rip3^{+/+}</i> , <i>Casp8^{+/+}Rip3^{-/-}</i> , <i>Casp8^{-/-}Rip3^{-/-}</i> and control TRIF-deficient (<i>Ips2/Ips2</i>) mice.	85
Figure 3.S5.	DKO mice accumulate aberrant T-cells	86
Figure 4.1.	RIP3 levels differentially confer susceptibility to necroptosis and virus- induced programmed necrosis	108
Figure 4.2.	Increased DAI expression sensitizes resistant cells to virus-induced necrosis	110
Figure 4.3	DAI and RIP3 cooperate in virus-induced necrosis	111
Figure 4.4.	M45mutRHIM virus attenuation <i>in vivo</i> is reversed in DAI ^{-/-} mice	112
Figure 4.S1.	IFN β , but not MCMV infection induces DAI expression in NIH3T3 cells	113
Figure 4.S2.	Infection induced, DAI-mediated cell death displays characteristics of MCMV-induced programmed necrosis	116

Figure 4.S3.	Loss of DAI does not influence DR-induced necroptosis or apoptosis	117
Figure 4.S4.	M45mutRHIM disseminates poorly to SGs of <i>DAI</i> ^{-/-} mice, and remains attenuated in <i>IFNAR</i> ^{-/-} animals.....	118
Figure 5.1.	TLR stimulation in the presence of caspase inhibitor triggers cell death	136
Figure 5.2.	TLR3 stimulation triggers programmed necrosis dependent on TRIF and inhibited by MCMV vIRA.....	138
Figure 5.3	TLR3 activation induces a TRIF-RIP1 and TRIF-RIP3 complex	139
Figure 5.4.	TLR3 induced programmed necrosis requires RIP3	140
Figure 5.5.	Role of RIP3 kinase in TLR3-induced programmed necrosis.....	142
Figure 5.6.	Casp8 suppression of TLR3-mediated TRIF- and RIP3-dependent programmed necrosis	144
Figure 6.1.	Schematic of RHIM-dependent signal transduction induced by TLR3/4 and DAI.....	154

Chapter 1: Introduction¹

Programmed Cell Death. Regulated cell death is critical for metazoan life to sculpt body shape and to eliminate unnecessary or damaged cells. Importantly, cell death functions as an important host defense that destroys infected cells to limit the spread of intracellular pathogens. Apoptosis is a form of programmed cell death that follows well-defined pathways centering on a caspase-dependent proteolytic cascade that coordinates cell-membrane blebbing, nuclear condensation, and DNA fragmentation, while maintaining the dying cell's membrane integrity (Hengartner, 2000; Pop and Salvesen, 2009; Strasser et al., 2000; Thornberry and Lazebnik, 1998). In contrast, necrotic cell death is caspase-independent and involves cell rounding and cytoplasmic swelling and terminates with the loss of membrane integrity and cytoplasmic leakage (Yuan and Kroemer, 2010). Apoptosis is the prominent form of cell death that occurs naturally during development, and in human adults, tissue homeostasis is maintained by an estimated one million cells undergoing apoptosis per minute. Necrotic cell death is often associated with inflammatory abnormalities, especially in damaged or inflamed tissues. Though once regarded as an unregulated pathological endpoint, recent studies have revealed that necrotic cell death can be orchestrated by some of the same enzymes that control apoptosis.

Much of our understanding of programmed cell death derives from interrogation of the Tumor Necrosis Factor (TNF) signaling pathway. The search for TNF was inspired by over two centuries of anecdotal evidence that infections can sometimes cause tumor regression. Decades

¹ The chapter derives from a published paper entitled “Viral infection and the evolution of caspase 8-regulated apoptotic and necrotic death pathways Pathogen subversion of RIP3-dependent necrosis” (Mocarski et. al. 2011). Sections of this chapter have been reproduced in whole, or in part, with permission from the publisher.

of research focused on identifying this elusive necrotizing factor in 1975, Carswell et al. purified TNF from the serum of endotoxin-injected mice. TNF caused rapid necrosis of sarcoma in mice and killed some tumor cell lines (Balkwill, 2009; Carswell et al., 1975). The cytotoxicity TNF is the consequence of apoptosis or necrosis depending on cell type (Laster et al., 1988). The sarcoma necrotizing activity of TNF led to its discovery; however, gene induction, not cell death, appears the primary result of TNF stimulation. However, recent studies revealed that cell survival requires active suppression of a protein complex composed of the receptor interacting kinases (RIP)1 and RIP3 (Vandenabeele et al., 2010). It is now clear that multiple cell stress and host defense pathways prime cells for this programmed necrosis, and in the context of viral infection, elimination of infected cells benefits the host (Upton et al., 2010). In contrast, dysregulated pronecrotic kinase activity leads to vasculature defects, collapse in hematopoiesis, and lethal skin (Bonnet et al., 2011; Kaiser et al., 2011) and gut inflammation (Bonnet et al., 2011; Gunther et al., 2011). Additionally, RIP3 was recently shown to cause mortality in experimental models of sepsis. These findings suggest programmed necrosis may drive a spectrum of disease states, thus elevating expectations for therapies targeting necrotic cell death. This dissertation establishes how apoptotic and necrotic cell death pathways determine the fate of mammalian cells.

Apoptosis. The intrinsic apoptotic machinery eliminates excess cells during embryonic development and homeostasis and also purges stressed or damaged cells. This pathway depends on mitochondrial outer membrane permeabilization (MOMP) by the B cell lymphoma 2 (BCL2) family members BCL-2-associated X protein (BAX) and BCL-2 antagonist/killer (BAK). MOMP releases pro-apoptotic factors (such as cytochrome *c* and SMAC/DIABLO) into the cytosol, triggering activation of Casp9 and subsequent effector caspases such as Casp3/7. Caspase-mediated proteolysis of specific vital substrates dismantles the cell, and the resulting

debris is rapidly cleared by macrophages *in vivo* (Chipuk et al., 2010; Danial and Korsmeyer, 2004).

Extrinsic cell death pathways. Death receptors, including TNFR1 and FAS, mediate extrinsic cell death in mice and humans, to control three competing cellular responses: (i) a proinflammatory cytokine response dependent on nuclear factor κ B (NF- κ B) and mitogen activated protein kinases (MAPK), (ii) apoptosis and (iii) necroptosis (Gentle et al., 2011; Gerlach et al., 2011; Silke, 2011; Walczak, 2011; Wilson et al., 2009). Activation of NF- κ B-dependent transcription contributes to regulation of cell death as well as inflammation (Wajant and Scheurich, 2011), and the interplay of these proinflammatory and cell death processes influence disease outcome. Additional TNFR superfamily members drive activation of NF- κ B without contributing to cell death (Benedict et al., 2002). In the case of TNF, all three responses direct inflammation, clearance of microorganisms, and immunity. The intense study of the DRs revealed that cell death signals are typically muted via a filigreed molecular network favoring gene induction via activation of MAPK and NF- κ B over cell death. The death-promoting activity of TNF typically manifests only following inhibiting gene expression or through genetic deletion or pharmacologic inhibition of specific death suppressors within the TNF receptor signaling complex (RSC) network. These manipulations enable TNF signaling to activate Casp8 which then activates Casp3 and Casp7 either directly or indirectly following mitochondrial release of cytochrome c dependent upon the activation of the proapoptotic BCL2 family member BH3-interacting-domain death agonist (BID) and the action of Bax and Bak as described for intrinsic apoptosis (Kantari and Walczak, 2011).

Death receptor signaling and apoptosis. Ligation of TNFR superfamily members, promote the assembly of a Casp8- and FADD-containing complex to initiate apoptosis. Signaling via FAS, TRAILR1 or TRAILR2 direct interactions between receptor death domains and FADD to

form a receptor-associated death inducing signaling complex (DISC) (O'Donnell et al., 2011). The DISC recruits Casp8 via death effector domain (DED)-dependent interactions with FADD. Apoptosis ensues following Casp8 homodimerization and self-cleavage that unleashes the full activity of the enzyme (Ashkenazi and Dixit, 1998). cFLIP isoforms are noncatalytic paralogs of Casp8 that form heterodimers with Casp8 to suppress apoptosis (Irmeler et al., 1997) (Figure 1.1). Signaling via TNFR1 is more complex and involves death domain-dependent recruitment of TNFR1-associated via death domain (TRADD) and RIP1 into Complex I, driving activation of NF- κ B and MAPK, with the activation of NF- κ B transcription factors and prosurvival gene induction (Van Antwerp et al., 1996). Additionally, RIP1 kinase activity orchestrates the assembly of a DISC-like cytosolic Casp8–FADD–cFLIP complex (Wang et al., 2008b), called Complex II (Micheau and Tschopp, 2003), in which cFLIP isoforms are crucial for regulating apoptosis and necroptosis (Figure 1.1). In cells where levels of RIP3 are sufficient, in this complex cFLIP_L blocks; whereas, cFLIP_S promotes RIP1-RIP3 kinase-dependent necroptosis (Moquin and Chan, 2010; Vandenabeele et al., 2010b). This Casp8-FADD-cFLIP-RIP1 has been called a necrosome. In this way, TNFR1 signaling controls both anti-apoptotic NF- κ B and MAP kinase signaling as well as the choice of death pathway, either apoptosis or necroptosis.

Death receptor signaling and RIP1 kinase. Polyubiquitylation of RIP1 influences cell fate (Vucic et al., 2011; Walczak, 2011). RIP1 contributes to activation of NF- κ B and resultant expression of cell death suppressors that modulate the initiation and execution of cell death pathways (Hsu et al., 1996; Ting et al., 1996), including both cFLIP isoforms and cellular inhibitor of apoptosis proteins (cIAPs). cIAPs polyubiquitylate RIP1, a form of this protein kinase that promotes NF- κ B-dependent proinflammatory responses and suppresses both apoptosis (Bertrand et al., 2008; Ikner and Ashkenazi, 2011; Varfolomeev et al., 2008; Vince et al., 2009; Wang et al., 2008b) and programmed necrosis (Biton and Ashkenazi, 2011; He et al., 2009;

Vanlangenakker et al., 2011). When cIAPs are inhibited by natural pathways via SMAC–DIABLO (or experimentally using SMAC mimetic drugs), extrinsic death pathways become activated. Consistent with this, RIP1 deubiquitylation by proteins such as cylindromatosis (CYLD) favors death pathways over NF- κ B activation, by facilitating Complex II formation and activation of Casp8 (Wang et al., 2008b).

Phenotype of mice lacking DISC-components. Similar striking phenotypes emerge *in vivo* in mice with germ line disruption of Casp8 or FADD. The most dramatic impact of *Casp8*-deficiency in embryos is the disruption of endothelial cell organization leading to circulatory failure in the yolk sac between E10.5 and E11.5 at approximately the same time that the chorioallantoic placenta replaces the yolk sac (choriovitelline placenta) as the source of nutrient and gas exchange with the fetus. Defects in the yolk sac vasculature commonly lead to embryonic lethality between E9.5 and E11.5 (Sapin et al., 2001). The midgestational death of embryos with the Tie1-Cre or Tie2-Cre driven deletion of Casp8 reinforces the conclusion that a defect in endothelial cells or cells of hematopoietic origin underlies embryonic death in germline mutant (Kang et al., 2004) (Doug Green, personal communication). Moreover, tissue-specific disruption of Casp8 or FADD has revealed many examples where these genes are essential. Interferon-inducible disruption of Casp8 or FADD (Ben Moshe et al., 2007; Kang et al., 2004; Rosenberg et al., 2011) leads to the elimination of cells in various lineages, suppressing early and mid-stage hematopoietic development (Ben Moshe et al., 2007; Imtiyaz et al., 2006; Kang et al., 2004; Rosenberg et al., 2011). B cell (CD19)-specific disruption of Casp8 or FADD does not alter response to antigen although mutant cells fail to proliferate and die in response to TIR-domain-containing adaptor protein inducing IFN β (TRIF)-dependent Toll-like receptor 3 (TLR3) and TLR4 agonists (Beisner et al., 2005; Imtiyaz et al., 2006). Casp8 is required in T cells for survival and proliferation following T cell receptor stimulation (Salmena and Hakem, 2005).

Surprisingly, severe inflammatory abnormalities arise when Casp8 (or FADD) is compromised (Beisner et al., 2005; Ben Moshe et al., 2007; Imtiyaz et al., 2006; Kang et al., 2004; Kovalenko et al., 2009; Lee et al., 2009; Li et al., 2010; Rosenberg et al., 2011). Disruption of Casp8 in epidermis results in atopic dermatitis during the cornification process and has been used to model chronic skin disease (Kovalenko et al., 2009; Lee et al., 2009; Li et al., 2010). Furthermore, mice expressing a catalytically inactive Casp8 along with a single wild-type allele develop inflammation in internal organs and skin (Kang et al., 2008) and inflammation triggered by partial hepatectomy in Casp8-deficient hepatocytes impairs liver regeneration (Ben Moshe et al., 2007). All these observations point to the critical role of Casp8 in suppressing inflammation.

The ripoptosome and necroptosis. Consistent with the central role of Casp8 in TNF-induced apoptosis, inhibiting or eliminating Casp8 protects most cells from death; however, as noted previously, TNF triggers not only apoptosis but also necrosis (Laster et al., 1988; Vercammen et al., 1998a; Vercammen et al., 1998b). In a few outlier cell types, Casp8 inhibition or ablation does not result in cell survival, but conversion of apoptosis to necrosis. This toggling of death modalities was shown to depend the levels of Casp8 activity and on the adapter protein RIP1, indicating at least some forms of necrosis have a molecular basis (Holler et al., 2000). More recently, the protein RIP3 binds RIP1 to direct necroptosis (Cho et al., 2009; He et al., 2009; Zhang et al., 2009). The essential homeostatic, apoptotic death of billions of cells every day sustains human life, thus apoptosis is generally well tolerated. In contrast, necrotic death is proinflammatory and immunogenic, and in the context of TNF, is executed by a pronecrotic RIP1/RIP3 kinase complex. TNF-signaling can drive chronic inflammation, autoimmunity and even cancer, but the precise molecular controls regulating the outputs and how these controls are altered naturally are not clear (Yuan and Kroemer, 2010). Despite the gaps in our knowledge regarding the TNF-signaling pathway, Fig. 1 lists the pathogen sensor proteins that

engage the same inflammatory and cell death pathways. Even less is known about their regulation.

A cytosolic Casp8–FADD–cFLIP complex regulates initiation of necroptosis by RIP1. Whereas both cFLIP_L and cFLIP_S isoforms inhibit Casp8-induced apoptosis (Figure 1.1), the Casp8–cFLIP_L complex retains sufficient proteolytic activity (Boatright et al., 2004; Micheau et al., 2002; Oberst et al., 2010; Pop et al., 2011) to suppress RIP1-RIP3 signaling activities, thereby blocking necroptosis (Feoktistova et al., 2011; Oberst et al., 2011). When Casp8 activity is compromised, caspase-independent necrotic cell death initiates from the RIP1–RIP3 complex (Moquin and Chan, 2010; Vandenabeele et al., 2010b). This is consistent with evidence that catalytically active but noncleavable Casp8 retains the ability to suppress programmed necrosis (Oberst et al., 2011) as well as the embryonic lethality observed in Casp8-deficiency (Kang et al., 2008). Thus, Casp8 orchestrates apoptosis and necroptosis in association with its activator, FADD, as well as the full-length form of its modulator, cFLIP_L (Figure 1.1). Recent identification of the ripoptosome (Feoktistova et al., 2011; Tenev et al., 2011), containing RIP1, FADD, Casp8, and cFLIP, reveals a role for RIP1 in assembly of a cytosolic complex reminiscent of TNFR1-induced Complex II to regulate cell fate by a range of stimuli beyond death receptor signaling.

Recent investigations defined the ripoptosome while showing roles for both Casp8 and FADD in regulating necroptosis during stimulation via PRRs such as TLR3 (Feoktistova et al., 2011), as well as induction of genotoxic stress (Tenev et al., 2011). Initiation of TLR3-dependent (Figure 1.1b) or DNA damage-induced (Fig. 1d) signals promote formation of the ripoptosome. In TLR3 signaling TIR domain-containing adaptor inducing interferon- β (TRIF) recruits the ripoptosome through binding the RHIM in RIP1. TLR-mediated necroptosis has been implicated in the pathogenesis of acute bacterial inflammation under conditions where Casp8 activity is

compromised (Welz et al., 2011). Similarly, genotoxic stress can induce cIAP degradation, driving ripoptosome formation (Feoktistova et al., 2011; Tenev et al., 2011). This growing literature suggests that TCR stimulation also engages a ripoptosome-like complex (Ch'en et al., 2011; Lu et al., 2011), opening the potential for a variety of extra- and intracellular stimuli in regulating formation of this crucial pro-necrotic signaling complex.

Virus regulation of cell death. Viruses vest heavily in the fate of infected cells and some viruses encode cell death suppressors to increase viral spread by preventing clearance (Galluzzi et al., 2010; Krysko et al., 2006; Lamkanfi and Dixit, 2010; Roy and Mocarski, 2007). The existence of these suppressors provides tangible evidence that both apoptotic and necrotic death pathways are a benefit to host defence. It is possible to appreciate the compendium of critical biological pathways encountered by a viral pathogen through the suppressors they encode. Programmed necrosis becomes unveiled only when Casp8 activity is compromised, suggesting the abundance of viral Casp8 inhibitors (Table 1.1) may have driven the counteradaptation of programmed necrosis in host defence (Chan et al., 2003; Cho et al., 2009; Upton et al., 2010). The few viral inhibitors of programmed necrosis that have been identified and the one that has been shown to target RIP3 pathways in the natural host animal (Upton et al., 2010) (Table 1.1, Fig. 1.3) may soon be joined by additional examples.

Baculovirus-encoded p35 (Clem et al., 1991), adenovirus-derived E3-14.7 (Chen et al., 1998), a number of poxvirus-expressed serpins and viral FLIP (vFLIP) proteins (Taylor and Barry, 2006), gammaherpesvirus-derived vFLIPs (Lagunoff and Carroll, 2003), and viral inhibitor of Casp8 activation (vICA) encoded by cytomegaloviruses (McCormick, 2008) prevent Casp8 activation (Figure 1.3). Vaccinia virus-infected cells become susceptible to death receptor-induced necroptosis due to inhibition of Casp8 by a viral caspase inhibitor (Li and Beg, 2000),

when host cells have adequate levels of RIP3 (Cho et al., 2009). These features likely underlie susceptibility of RIP3-deficient mice to lethal vaccinia infection (Cho et al., 2009) as well as why necroptosis can be viewed as a trap door when Casp8 activity is compromised (Mocarski et al., 2011).

Cytomegaloviruses (CMVs) are evolutionarily ancient herpesviruses, with a complex pathogenesis and persistence in targeted host epithelial, myeloid and endothelial cells (Mocarski, 2007). Like other mammalian viruses, herpesviruses differ in pathogenesis and virulence in large part due to the elaboration of immune modulators to facilitate infection by undermining host intrinsic, innate and adaptive immunity. In all mammalian CMVs, the presence of well-conserved inhibitors of Casp8 activation and mitochondrial inhibitors of apoptosis that target BAX and BAK activation demonstrate that apoptotic cell death pathways contribute to viral clearance (Brune, 2011; Cicin-Sain et al., 2008; Manzur et al., 2009; McCormick, 2008; Skaletskaya et al., 2001).

By targeting Casp8, CMV-derived vICA reduces the impact of extrinsic death receptor-associated host control over the virus. Moreover, MCMV counteracts necrotic death by encoding vIRA, a product of the M45 gene that blocks RHIM-dependent signaling pathways, including death receptor-induced apoptosis (Rebsamen et al., 2009; Upton et al., 2008, 2010), TRIF-dependent apoptosis (Upton et al., 2010) and TRIF- or DAI-dependent NF- κ B activation (Kaiser et al., 2008; Mack et al., 2008; Rebsamen et al., 2009) (Figure 1.3). The RHIM-containing domain of M45, which is crucial for vIRA function, is not present in primate CMVs even though the gene is otherwise conserved. Rat CMV encodes a close homolog of vIRA, and, interestingly, an evolutionarily distant ortholog may be carried by herpes simplex virus 2 (Lembo and Brune, 2009). These, together with several classes of pathogen recognition receptors (PRRs), sculpt

inflammatory responses to microbial infection and assure the elimination of infected cells by induction of programmed cell death. Overlapping functions remains a major theme when considering pathogen recognition and death receptor signaling. In this thesis, we examine RHIM interactions drive necrotic death induced by pathogen sensors and how MCMV targets RHIM interactions for pathogenesis.

RIP1- and RIP3-dependent programmed necrosis (necroptosis). Necroptosis only emerges following a compromise in Casp8 activity (Chan et al., 2003; Feng et al., 2007; Lin et al., 1999; Lu et al., 2011; O'Donnell et al., 2011). The downstream events in the execution of necroptosis remain biochemically vague. Several candidate targets have emerged from screens (Zhang et al., 2009), although how these fit into execution pathways remains to be explored (Vandenabeele et al., 2010b). Recognition that a cytoplasmic RIP1- and Casp8-containing ripoptosome forms under a range of cell stress conditions opens additional avenues (Figure 1.1) of initiating RIP1/3 death signaling. In particular, we suspect that one this regulation of RIP1/3 by Casp8 may be crucial for mammalian development (Chapter 3) and necrosis may function as a trap door to eliminate infected cells.

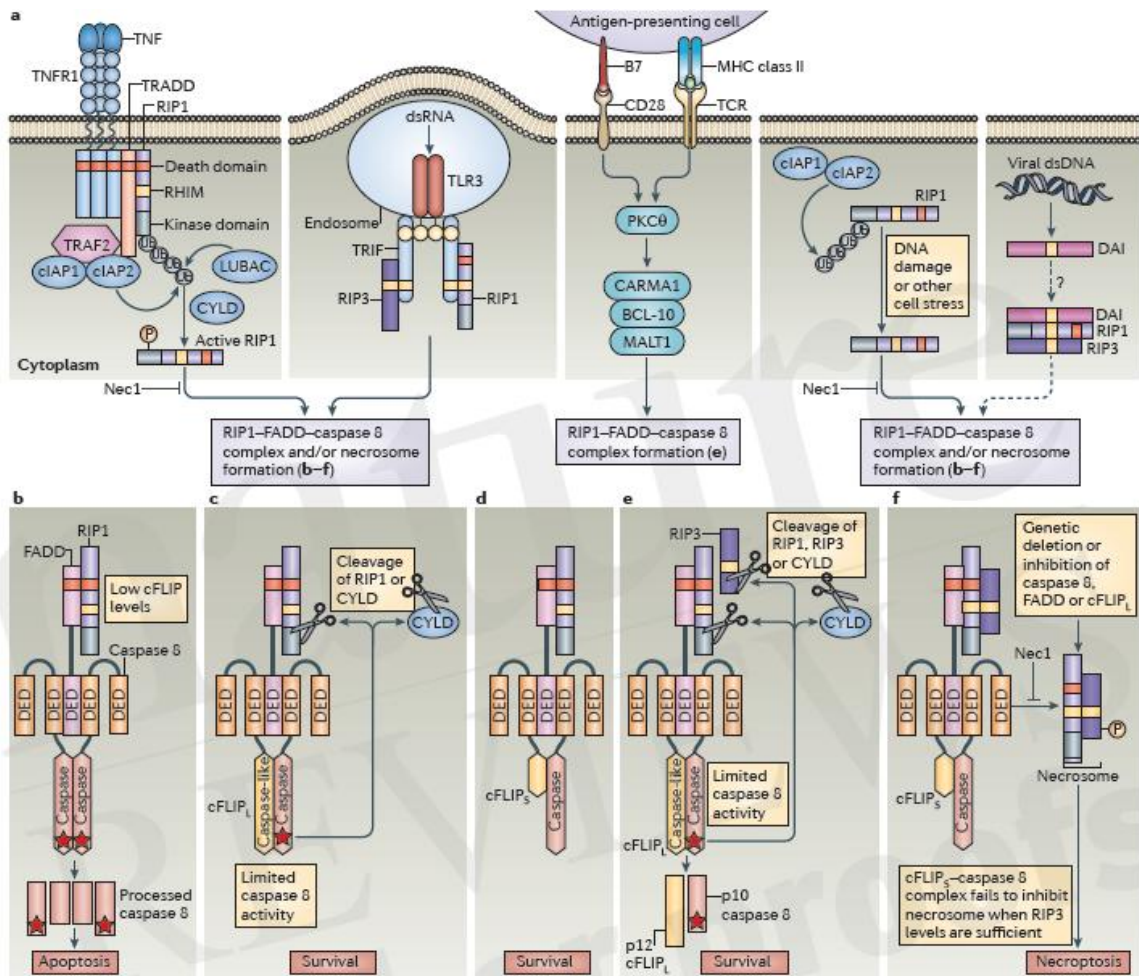


Figure 1.1. Casp8 regulation of RIP1–RIP3 signaling pathways. Following tumor necrosis factor (TNF) binding, RIP1 is recruited via a death domain to TNF receptor 1 (TNFR1). When polyubiquitylated by the E3 ligases cellular inhibitor of apoptosis 1 (cIAP1) and cIAP2, RIP1 promotes nuclear factor κ B (NF- κ B), which enhances cell survival by inducing the expression of cIAPs and cFLIP. In the absence of RIP1 polyubiquitylation (for example due to insufficient cIAP levels or deubiquitylation by proteins such as cylindromatosis (CYLD)), a RIP1 kinase activity facilitates assembly of alternative RIP1–FADD–Casp8 signaling platforms. When the levels of cFLIP_L or cFLIP_S are limiting, Casp8 homodimerization promotes enzymatic activity leading to autoprocessing and the execution of apoptosis through targeting BH3-interacting-domain death agonist (BID) and/or Casp3 (a). In the presence of sufficient cFLIP_L or cFLIP_S, a Casp8–cFLIP_L (b) or

(Figure 1.1 continued) Casp8–cFLIP_S (c) heterodimer forms, supporting survival. Importantly, the Casp8–cFLIP_L heterodimer retains sufficient proteolytic activity to cleave substrates such as RIP1 and CYLD to prevent necroptosis (d) without allowing Casp8 to induce apoptosis. When Casp8 activity is blocked, in conditions of elevated cFLIP_S (e) or in the presence of a Casp8 inhibitor, RIP1 binds RIP3 to form a kinase active necrosome (f) to initiate necroptosis. RIP1 kinase activity drives assembly of the cytosolic RIP1–FADD–Casp8 signaling platform as well as the necrosome. The RIP1 kinase inhibitor, necrostatin 1 (Nec-1) blocks both RIP1-dependent apoptosis and necroptosis. The levels of cFLIP, balance of cFLIP isoforms, and level of Casp8 activity determine whether apoptosis, necroptosis, or cell survival ensues. The TLR3 and TLR4 adaptor protein TIR-domain-containing adaptor protein inducing IFN β (TRIF) binds both RIP1 and RIP3 via RHIM interactions, bridging TLR3 signaling to the RIP1–FADD–Casp8 complex (ripiptosome). T cell survival and proliferation following stimulation of the TCR and CD28 requires FADD–Casp8–cFLIP_L-mediated inactivation of RIP1–RIP3 necroptosis (*iv*). Genotoxic damage or cell stress leads to cIAP1–cIAP2 degradation and formation of a ripoptosome. The cytosolic DNA sensor DAI directly engages RIP1 and RIP3 in RHIM-dependent complexes to potentially drive assembly and/or recruitment of a ripoptosome similar to TRIF. Stars indicate catalytically active Casp8 and red ovals denote the RHIM domains in RIP1, RIP3, TRIF, and DAI.

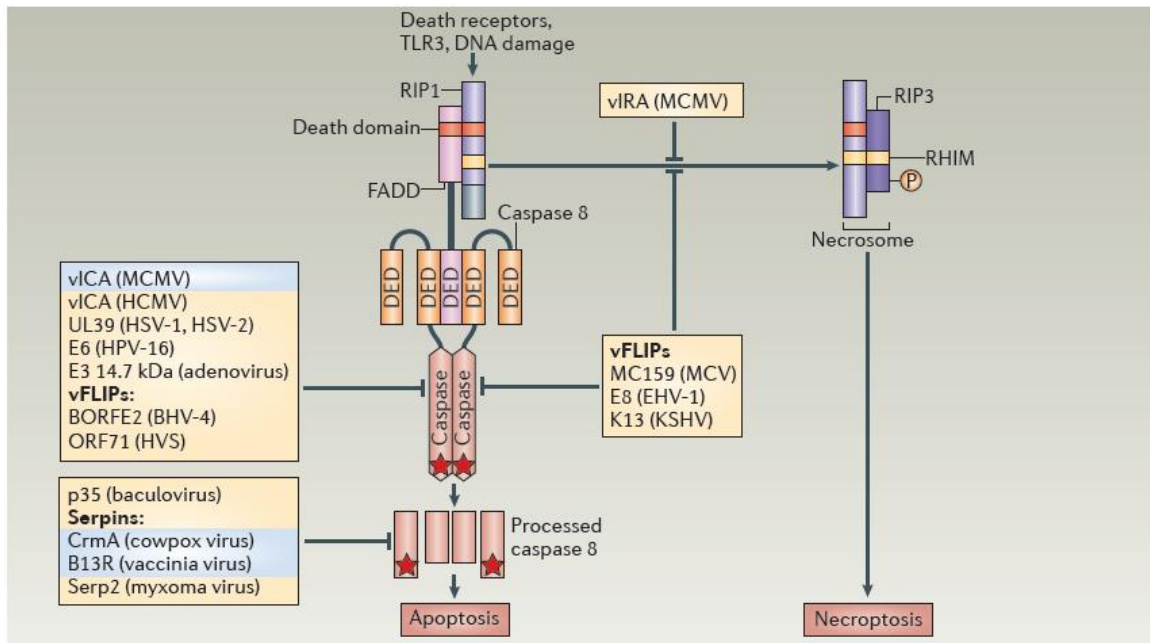


Figure 1.2. Viral modulation of cell death signals mediated by Casp8 activation and RIP1–RIP3 pathways. Viral genes directly targeting receptor-interacting protein 1 (RIP1), FAS-associated via death domain (FADD), and/or caspase 8 (Casp8) suppress signaling pathways activated via death receptors as well as pathogen recognition receptors (PRRs), such as Toll-like receptor 3 (TLR3) and cell stress, such as DNA damage. Many virally encoded proteins block Casp8-dependent apoptosis by interfering with Casp8, FADD, and/or RIP1 (Table 6.1). A number of poxvirus serpin family proteins bind directly to fully processed Casp8 to prevent apoptosis (green box), and some Casp8 inhibitors such as CrmA, B13R and viral inhibitor of Casp8 activation (vICA) sensitize cells to death receptor-induced necroptosis by disrupting Casp8 suppression of RIP1–RIP3 activity (noted in blue type). A subset of viral FLIP proteins (vFLIPs) including MC159 and E8 (blue box) as well as the murine cytomegalovirus (MCMV) protein vIRA (encoded by the M45 gene) block both apoptosis and RIP1–RIP3-mediated necrosis

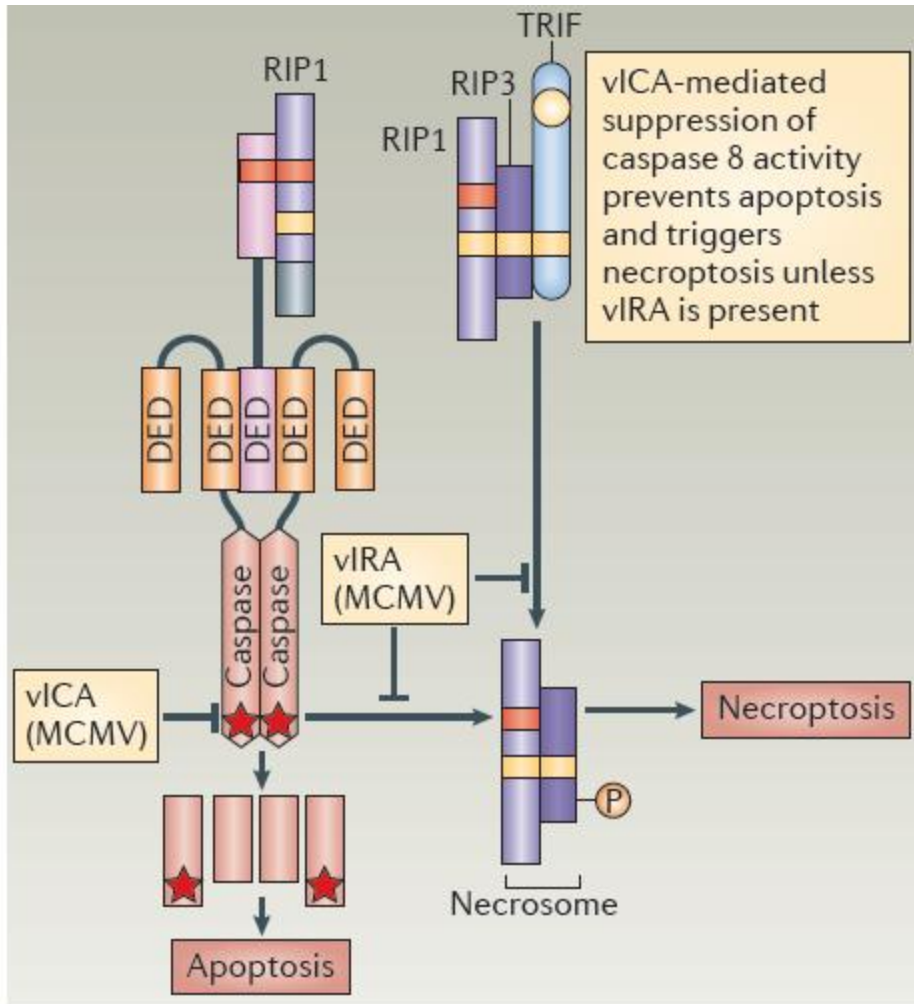


Figure 1.3. MCMV modulation of cell death signals mediated by Casp8 activation and RIP1–RIP3 pathways. MCMV vICA prevents Casp8 activation, sensitizing cells to death receptor-induced necroptosis. MCMV vIRA blocks necroptosis as well as MCMV-induced necrosis by inhibiting RHIM-dependent interactions. vIRA also inhibits RIP1- or TIR-domain-containing adaptor protein inducing IFN β (TRIF)-driven activation of Casp8.

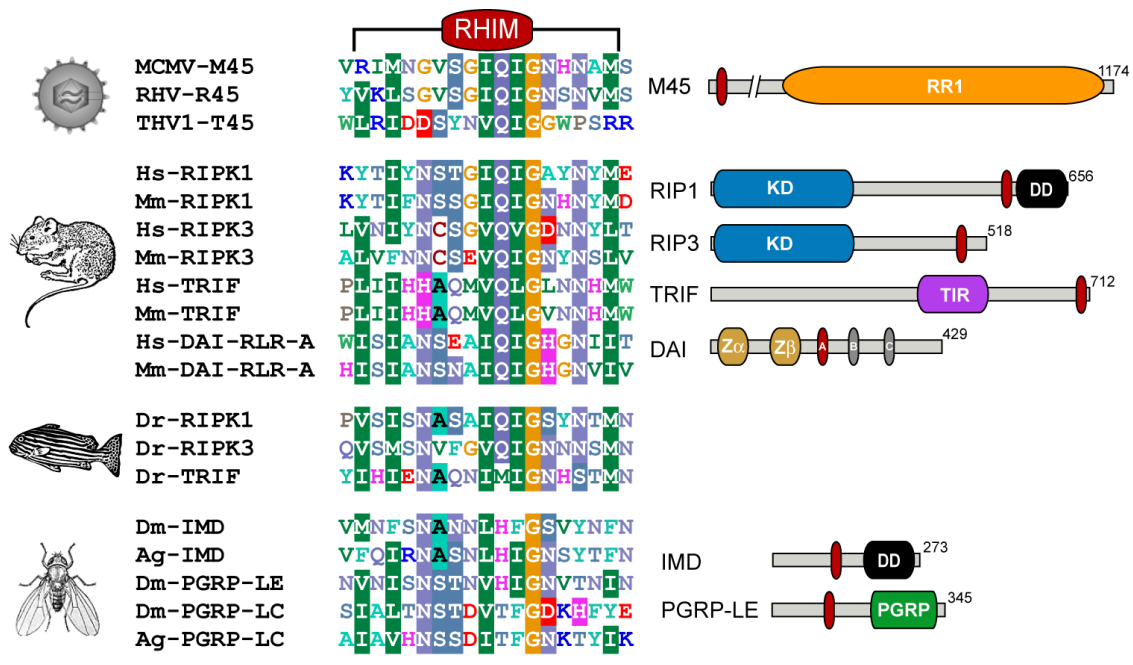


Figure 1.4. Schematic representation of the domain architecture of the RHIM-containing

proteins. DAI contains an amino-terminal Z α and Z β domain and three tandem stretches of

amino acids (labeled A, B, and C) that exhibit RHIM-like aa sequence homology. The motif in DAI

most similar to the RHIM is indicated by a red oval. RIP1 and RIP3 each have an amino-terminal

kinase domain (KD), and RIP1 also contains a carboxyl-terminal death domain (DD). TRIF

encodes a TIR domain, and M45 has a region of homology to a ribonucleotide reductase (RR1)

domain. PGRP-LE encodes a peptidoglycan recognition protein (PGRP) domain.

Type of inhibitor	Inhibitor	Virus	Known targets	Mechanism	Gene ID or accession number
<i>Inhibitors of apoptosis and programmed necrosis</i>					
cFLIP homologue	MC159	MCV	Caspase 8, FADD	Inhibits oligomerization	1487017
cFLIP homologue	K13	KSHV	Caspase 8	Prevents activation	4961494
cFLIP homologue	E8	EHV-1	Caspase 8	–	1461076
RHIM inhibitor	vIRA	MCMV	RIP1, RIP3, TRIF, DAI	Inhibits RHIM-mediated interactions	CAP08092.1
<i>Inhibitors of apoptosis</i>					
Caspase 8 inhibitor	vICA	CMV	Caspase 8	Prevents activation	3077442
Caspase 8 inhibitor	BORFE2	BHV-4	Caspase 8	–	1684940
Caspase 8 inhibitor	E3 14.7 kDa	Adenovirus	Caspase 8	Prevents activation	1460862
Caspase 8 inhibitor	UL39	HSV-1, HSV-2	Caspase 8	Prevents activation	2703361, 1487325
Serpin	CrmA	Cowpox virus	Caspases 1, 4, 5, 8 and 10, granzyme B	Inhibits activity	1486086
Serpin	B13R	Vaccinia virus	Caspases	–	3707572
Serpin	Serp2	Myxoma virus	Caspases	–	932102
Other	E6	HPV-16	Caspase 8, FADD	Inhibits oligomerization, degrades	1489078
Other	p35	Baculovirus	Caspases	Inhibits activity	1403968

Table 1.1. Selected Viral Inhibitors of Apoptosis and Necrosis (Chen et al., 1998; Galluzzi et al., 2010; Lamkanfi and Dixit, 2010). ¹ MCV, molluscum contagiosum virus; KSHV, Kaposi's sarcoma herpesvirus; EHV1, equine herpesvirus 1; MCMV, murine cytomegalovirus; CMV, cytomegaloviruses; BHV4, bovine herpesvirus 4; Ad, adenovirus; HSV1/HSV2, herpes simplex virus 1 and 2; HPV16, human papillomavirus type 16.

Chapter 2. Pathogen subversion of RIP3-dependent necrosis²

Upton JW*, Kaiser WJ*[‡], Mocarski ES. (2010) Virus Subversion of RIP3-dependent Necrosis. *Cell Host & Microbe*. 7(4): 302-13.

* authors contributed equally [‡] corresponding author

A. INTRODUCTION

Cellular sensing of viral pathogens by the host activates inflammatory gene expression and triggers cell death. These distinct cell-intrinsic response pathways directly control viral spread from the portal of entry and influence the quality of pathogen-specific adaptive immunity. Innate antiviral cytokines such as interferon (IFN) have long been considered central to control of viral spread (McCartney and Colonna, 2009; Roy and Mocarski, 2007; Takeuchi and Akira, 2009), with caspase-dependent apoptotic cell death viewed as a complementary, evolutionarily conserved clearance mechanism triggered by distinct signals. The importance of death has been reinforced by the widespread existence of apoptotic cell death suppressors, including those that viruses employ to subvert intrinsic clearance (Clem, 2005; D'Agostino et al., 2005; Kepp et al., 2009). These include (i) caspase inhibitors, such as baculovirus p35 (Bump et al., 1995; Clem et al., 1991), viral inhibitors of apoptosis (IAPs) (Crook et al., 1993), poxvirus crmA (Miura et al., 1993; Ray et al., 1992) and viral FLICE (caspase-8) inhibitory proteins (FLIPs) (Thome et al., 1997), as well as, (ii) mitochondrial cell death suppressors such as viral Bcl-2 homologs and other proteins encoded by large DNA viruses that block cytochrome *c* release from mitochondria (Galluzzi et al., 2008; Goldmacher, 2005; White, 2006). Although apoptosis is a well-established cell-intrinsic response to pathogens, caspase-independent cell death, or programmed necrosis, has recently emerged as an alternative death pathway that dominates under specific conditions

² The majority of the work in this chapter was performed by both William J. Kaiser and Jason W. Upton. The chapter derives from a published paper entitled "Pathogen subversion of RIP3-dependent necrosis" (Upton et. al. 2010). Sections of this chapter have been reproduced in whole, or in part, with permission from the publisher.

(Festjens et al., 2007; Hitomi et al., 2008). Necroptosis is a form of programmed necrosis induced by death receptors (DR), a subgroup of the tumor necrosis factor (TNF) superfamily, that is independent of caspases but dependent on the activity of the adaptors receptor interacting protein kinase 1 (RIP1) (Festjens et al., 2007; Meylan and Tschopp, 2005) and RIP3 (Cho et al., 2009; He et al., 2009; Zhang et al., 2009), two related RIP homotypic interaction motif (RHIM)-containing protein kinases (Sun et al., 2002). Programmed necrosis has been viewed as a back-up to apoptosis (Festjens et al., 2007; Festjens et al., 2006) because this pathway is activated by the same signals under experimental conditions where caspase-8 activation has been suppressed or is absent. It has recently been proposed that this alternative death pathway is another host counter-measure against invading pathogens (Cho et al., 2009). However, suppression of this pathway by a microbe for pathogenesis *in vivo* has yet to be established.

RIP1, the founding member of a serine-threonine protein kinase family related to interleukin 1 receptor-associated kinases, transduces inflammatory and cell death signals in cells following DR ligation, activation of pattern recognition receptors (PRRs), and DNA damage (Janssens et al., 2005; Meylan et al., 2004; Michallet et al., 2008; Stanger et al., 1995). An amino-terminal kinase domain in RIP1 is critical for DR-induced necroptosis (Holler et al., 2000) and is the target of necrostatin-1 (Nec-1) (Degterev et al., 2008; Degterev et al., 2005), a defining inhibitor of necroptosis. Other RIP family members share a kinase domain but carry different protein-protein interaction motifs. RIP1 has a carboxyl-terminal death domain (DD) that engages other DD-containing proteins and transduces signals from death receptors (Stanger et al., 1995) as well as a central (intermediate) domain important for NF- κ B activation (Festjens et al., 2007) and RHIM-dependent signaling (Sun et al., 2002). Three other cellular RHIM-containing adaptors interact with RIP1 to initiate gene activation and death pathways: (i) RIP3, the only

other RHIM-containing RIP family member (Sun et al., 2002), (ii) the toll-like receptor (TLR)3 and TLR4 adaptor TIR domain-containing adaptor-inducing IFN β (TRIF) (Kaiser and Offermann, 2005; Meylan et al., 2004), and (iii) DNA-dependent activator of IFN-regulatory factors (DAI, also termed DLM-1 or ZBP1) (Kaiser et al., 2008; Rebsamen et al., 2009), a candidate DNA sensor (Takaoka et al., 2007). RIP1 is recruited to TLR3 and TLR4 by TRIF (Meylan et al., 2004) via RHIM-dependent interactions. Signaling via TLR3, TLR4 or DAI activates proinflammatory, NF- κ B- and IRF3-dependent responses to endosomal dsRNA, lipopolysaccharide (LPS) or cytoplasmic dsDNA, respectively (Alexopoulou et al., 2001; Kawai and Akira, 2007; Takaoka et al., 2007). Thus, RIP1 is an important adaptor, balancing cellular signaling that results in inflammatory cytokine activation and influencing the initiation of programmed cell death pathways (Degterev and Yuan, 2008; Festjens et al., 2007; Meylan and Tschopp, 2005).

When first evaluated, RIP3 appeared to exert a negative modulatory role in TLR3-dependent or TNF α receptor NF- κ B activation (Meylan et al., 2004; Sun et al., 2002). More recently, RIP3 has been ascribed a positive impact on DAI-induced, RIP1 RHIM-dependent NF- κ B activation (Kaiser et al., 2008; Rebsamen et al., 2009) as well as in the RHIM-dependent initiation of necroptosis induced by TNF α (Cho et al., 2009; He et al., 2009; Zhang et al., 2009). RIP3- and RIP1-dependent necroptosis is triggered by death receptor stimulation when caspases are inhibited or absent (Ch'en et al., 2008; Cho et al., 2009; He et al., 2009; Holler et al., 2000; Vercaemmen et al., 1998a; Yu et al., 2004; Zhang et al., 2009), although the requirement for caspase inhibition to unveil necroptosis has limited observations of this cell death pathway in natural biological settings (Festjens et al., 2006). RIP3-deficient mice are viable and display no obvious developmental phenotypes or defects in NF- κ B signaling triggered by LPS or TNF α (Newton et al., 2004). One recent report highlighted decreased inflammation and liver

pathology in vaccinia virus-infected RIP3-deficient mice, processes that were ascribed to altered TNF α -induced necroptosis (Cho et al., 2009).

As obligate intracellular pathogens that remain latent for life, herpesviruses are heavily vested in cell fate decisions. Human cytomegalovirus (HCMV), the prototypic, medically significant β -herpesvirus, and murine cytomegalovirus (MCMV), a surrogate used to model viral pathogenesis, encode several cell death suppressors (Cicin-Sain et al., 2008; Goldmacher et al., 1999; Mack et al., 2008; McCormick et al., 2005; McCormick et al., 2008; Menard et al., 2003; Skaletskaya et al., 2001; Upton et al., 2008). The MCMV M45-encoded viral inhibitor of RIP activation (vIRA) is a viral structural protein (Lembo et al., 2004) originally identified as a tropism determinant required for endothelial cell-specific viral replication (Brune et al., 2001). MCMV mutants lacking vIRA induce premature death in some cell lines, although the mode and mechanism of death remains controversial. Both caspase-dependent and caspase-independent cell death pathways have been implicated (Brune et al., 2001; Mack et al., 2008), leaving the question of mechanism open for resolution. Recent reports showing the critical role of RIP1 and RIP3 in DR-induced necroptosis (Cho et al., 2009; He et al., 2009; Zhang et al., 2009), together with previous evidence that vIRA physically interacts efficiently with RIP3 as well as RIP1 (Upton et al., 2008), implicate vIRA suppression of cell death pathways via modulation of RIP3 and/or RIP1 to provide cell death suppression in sensitive cell types and enhance virus replication and dissemination. However, the specific contributions of RIP1-RIP3 interactions to the mutant virus phenotype have not been established. Here, we demonstrate that vIRA disrupts both the RHIM-dependent RIP3-RIP1 kinase complex that initiates TNF α -induced necroptosis as well as a novel RIP3 RHIM-dependent, RIP1-independent step in virus-induced necrosis. Importantly, the severe attenuation of vIRA-deficient virus is normalized when mice lack RIP3 function. These data

demonstrate that RIP3 mediates a necrotic death pathway independent of RIP1 and implicates viral control of this pro-necrotic adaptor protein in viral pathogenesis.

B) RESULTS

vIRA RHIM-dependent interactions suppress virus induced programmed necrosis and are required for pathogenesis. In order to explore the biological consequences of vIRA RHIM-specific interactions during viral infection, we generated a recombinant bacmid-derived mutant MCMV and evaluated its behavior in infected cells and animals. M45*mut*RHIM virus carried a tetra-alanine substitution (Figure 2.S1A, B) previously shown to eliminate the capacity for this protein to engage in RHIM-dependent interactions (Upton et al., 2008). Viral stocks were recovered by transfection of bacmid DNA into NIH3T3 fibroblasts, where mutant and wild type (WT) exhibited equivalent replication properties as elaborated previously (Brune et al., 2001; Mack et al., 2008). Viral genome integrity was affirmed by restriction enzyme digestion of bacmid and viral DNA (Figure 2.S1C, data not shown). Immunoblot analysis indicated MCMV mutant M45*mut*RHIM and WT viruses produced M45-proteins of comparable size and at similar levels of expression (Figure 2.1A). All samples contained equivalent amounts of β -actin as a loading control, and infected cells all expressed similar levels of viral immediate early (IE)1 protein. To investigate whether the *in vivo* behavior of vIRA RHIM-dependent interactions recapitulated the severe attenuation previously demonstrated for vIRA using null mutants (Lembo et al., 2004), we evaluated mutant and WT virus replication in immunodeficient as well as in immunocompetent mice. To evaluate the properties of viral replication, dissemination, and virulence independent of innate natural killer (NK) as well as adaptive T and B lymphocyte function, the behavior of WT and M45*mut*RHIM viruses was compared in severely immunocompromised nonobese diabetic (NOD), severe combined immunodeficient (scid), IL2 common γ chain^{-/-} (NSG) mice (Shultz et al., 2005). Mutant virus exhibited at least 1,000-fold reduced levels in spleen, 10,000-fold reduced levels in liver and 1,000,000-fold reduced levels in

salivary glands compared to WT virus (Figure 2.1B). To investigate viral pathogenesis, cohorts of NSG mice inoculated with WT or mutant virus were followed for 6 weeks. While mice infected with WT virus succumbed between 20 to 22 days post-infection, mutant virus infected animals showed no signs of CMV-disease up to 42 days (Figure 2.1C) and beyond (data not shown). We extended *in vivo* studies to include immunocompetent mice, demonstrating that WT was detected in the spleens of BALB/c mice at day 3 postinoculation when virus titers normally peak (Figure 2.1D); whereas mutant virus remained undetectable at day 3 (Figure 2.1D) as well as at day 5 (data not shown). These data show that the phenotype of the M45mutRHIM mutant virus is similar to previously characterized vIRA-deficient viruses (Lembo et al., 2004). Importantly, the attenuated phenotype of the tetra-alanine substitution mutant *in vivo* established the critical role of RHIM-dependent interactions in vIRA function, extending prior investigations that relied upon viral mutants which truncated or eliminated vIRA expression. This result implicates vIRA RHIM-dependent interaction partners, previously characterized as RIP1 or RIP3 using transient expression systems (Upton et al., 2008), as well as the significance of RHIM-dependent signaling in antiviral host defense.

We next sought to investigate the importance of vIRA RHIM-dependent interactions in cell tropism, cell-specific viral replication and induction of cell death. Consistent with previous reports using vIRA null viral mutants (Brune et al., 2001; Mack et al., 2008; Upton et al., 2008), M45mutRHIM virus was severely attenuated for growth in SVEC4-10 cells (Figure 2.1E) which died within 18 h after exposure to mutant (Figure 2.1F, right panel). WT virus replicated to levels that were similar to NIH3T3 cells and had no impact on cell viability. NIH3T3 fibroblasts retained sensitivity to TNF α -induced apoptosis (when not infected with MCMV). As expected from previous investigations (Mack et al., 2008), mutant virus-induced cell death was unaffected by addition of the broad-spectrum caspase inhibitor, zVAD-fmk (Figure 2.1F, right panel).

Additionally, the phenotype of two independently derived M45*mut*RHIM isolates was comparable (Figure 2.S2A), confirming that the tetra-alanine mutation in M45 was responsible for the phenotype. Thus, the behavior of RHIM mutant virus recapitulates the behavior of previously characterized M45-deficient viruses, and clearly demonstrated that RHIM-dependent interactions are integral to vIRA cell death suppression. These data are consistent with our previously proposed model (Upton et al., 2008) where RHIM-dependent interaction(s) with RIP3 and/or RIP1 controls the antiviral cell death pathway triggered shortly after viral infection. Thus, MCMV induces programmed caspase-independent death in susceptible cells and virus-encoded vIRA naturally suppresses this pathway by interfering with RHIM-dependent pathways.

Given the proposal that vIRA represents an endothelial growth determinant (Brune et al., 2001), we were surprised when M45*mut*RHIM virus failed to replicate efficiently (Figure 2.2A) and, instead, induced premature death in 3T3-Swiss albino (3T3-SA) cells, another immortal fibroblast line that is fully permissive for WT MCMV (Figure 2.S2B and data not shown). Exposure to mutant virus resulted in premature death similar to what was observed using SVEC4-10 cells, based on three independent lines of evidence: morphological evaluation (Figure 2.2B and Figure 2.S2), intracellular ATP levels (Figure 2.2C) and release of intracellular proteases (Figure 2.2D). Multiple isolates of M45*mut*RHIM induced death on SVEC4-10 and 3T3-SA cells (Figure 2.S2A). Like SVEC4-10 cells (Brune et al., 2001), 3T3-SA fibroblasts were fully susceptible to viral infection as assessed by expression of viral antigens (Figure 2.S2B). Death of mutant virus infected cells was first detected between 5 and 9 hpi and approached maximal levels by 18 hpi, accompanied by cytoplasmic swelling, cell detachment, propidium iodide inclusion, and membrane rupture (Figure 2.S2C, data not shown). This morphological evidence is most consistent with programmed necrosis (Festjens et al., 2006). To demonstrate that collapse in ATP levels (Figure 2.2C) was due to necrotic death rather than viral modulation of

cellular respiration, we assessed the release of intracellular proteases into the culture medium. The dramatic increase in released proteases (Figure 2.2D) was consistent with dramatic loss of plasma membrane integrity associated with necrotic death, rather than other changes in cellular physiology during viral infection. In contrast to the virus-induced necrotic death, TNF α plus CHX was employed to induce apoptosis, and ATP levels decreased without a dramatic rise in extracellular protease activity. To assure that the virus induced release of proteases occurred independent of apoptosis or autophagy, appropriate markers were assessed by IB analysis of infected 3T3-SA cells. Infected cells did not exhibit any evidence of caspase-3 activation at any time from 6 through 18 h post infection (hpi) with mutant virus (Figure 2.2E). In addition, the levels of LC3 II remained similar in uninfected or cells infected with mutant or WT viruses, compared to Bafilomycin A₁-treated controls. Ultrastructural analysis by electron microscopy (EM) failed to reveal evidence of membrane blebbing, nuclear condensation, or autophagosome formation in dying, mutant-infected cells compared to WT virus infection (Figure 2.2F and data not shown). Taken together with the caspase-independence, these observations indicate that the cell death pathway induced by mutant virus infection was unrelated to apoptosis or autophagy.

Given that recent studies have implicated high levels of RIP3 as a determinant in DR-induced necroptosis (Cho et al., 2009; He et al., 2009; Zhang et al., 2009), we next evaluated levels of the known vIRA interacting proteins, RIP1 and RIP3, in cells that were susceptible to virus-induced death (3T3-SA, and SVEC4-10) as well as in control NIH3T3 cells. IB analysis revealed that RIP3 levels were elevated in susceptible cells compared to control cells (Figure 2.2G); whereas, RIP1 levels were similar in all cell lines. SVEC4-10 and 3T3-SA cells were shown to be sensitive to TNF α and zVAD-fmk necroptosis (Figure 2.2H), paralleling susceptibility to virus-induced programmed necrosis. Together, these results suggested that, as is the case

reported for DR-induced necroptosis (He et al., 2009; Zhang et al., 2009), RIP3 expression is a common property of cells sensitive to virus-induced necrosis, which serves to clarify and add mechanistic insight to prior observations regarding the premature death of SVEC4-10 cells to infection with vIRA-deficient virus (Brune et al., 2001), as well as to evidence that the pathway is caspase-independent (Mack et al., 2008). Thus, high levels of RIP3 are the defining characteristic of cells that are sensitive to either virus-induced or DR-induced necrotic death, implicating this adaptor in necrosis induced by different stimuli.

vIRA suppresses necroptosis in a RHIM-dependent fashion. To establish the contribution of RIP1 and RIP3 to DR-induced necroptosis in SVEC4-10 and 3T3-SA cells, we employed specific shRNAs (RIP3-A and RIP3-B) to reduce expression levels of RIP3. This RNAi approach showed that RIP3 played a critical role in TNF α plus zVAD-fmk-induced necroptosis (Figure 2.3A and B). Addition of the RIP1-specific kinase inhibitor Nec-1 restored cell viability, consistent with prior studies (Degterev et al., 2008; Degterev et al., 2005) showing necroptosis to be RIP1 kinase-dependent (Figure 2.3B, bottom panel, Figure 2.S3E, F, right panels). The contribution of RIP3 and RIP1 to necroptosis was further evaluated in RIP1^{-/-} and control RIP1^{+/+} mouse embryonic fibroblasts (MEFs). RIP1^{-/-} MEFs were insensitive to TNF α plus zVAD-fmk-induced necroptosis (Figure 2.3C, top panel). However, as expected (Kelliher et al., 1998; Wong et al., 2009), RIP1-deficient cells exhibited an increased sensitivity to TNF α -induced, caspase-dependent, apoptosis (Figure 2.3C, upper panel). IB analysis of EV transduced RIP1^{-/-} and control MEFs showed similar levels of expression of endogenous RIP3 (Figure 2.3C, lower panel). To evaluate the impact of increasing RIP3 in the absence of RIP1, RIP1^{-/-} and control MEFs were transduced with epitope-tagged WT or kinase-deficient (KD) RIP3 (Figure 2.3C, lower panel). Elevated levels of WT, but not KD, RIP3 conferred increased sensitivity of control MEFs to TNF α plus zVAD-fmk induced necroptosis (Figure 2.3C, upper panel) and this was reversed by

Nec-1, showing a dependence on both RIP1 and RIP3 kinase activity. In contrast, overexpression of RIP3 in RIP1^{-/-} MEFs failed to enhance susceptibility to either necroptosis or TNF α -induced apoptosis. Taken together, these results indicate that RIP1 plays an essential role in induction of DR-associated necrotic death, that elevated levels of RIP3 are necessary for this pathway, and that overexpression of RIP3 does not overcome the requirement for RIP1 in DR-induced cell death. Furthermore, these data establishes the requirement for the protein kinase activity of both RIP1 and RIP3 in necrotic death induced following DR activation in sensitive cells. These independently derived results reaffirm the essential role of RIP3 and RIP1 in formation of an active RIP3-RIP1 kinase complex as well as the importance of their kinase domains to drive DR-induced necroptosis (Cho et al., 2009; He et al., 2009; Zhang et al., 2009).

Previously, vIRA was shown to suppress caspase-independent programmed cell death (Mack et al., 2008). To further investigate the role of vIRA in suppression of necroptosis and determine the contribution of RHIM-mediated interactions, SVEC4-10 cell lines stably expressing epitope-tagged WT (M45-myc) or mutant (M45*mut*RHIM-myc) vIRA were generated (Figure 2.3D, top panel) and compared to cells carrying an EV as control. As expected, expression of WT vIRA conferred protection to treatment with TNF α plus zVAD-fmk (Figure 2.3D, bottom panel) (Mack et al., 2008). Cells expressing M45*mut*RHIM-myc were as sensitive to death as EV control cells, indicating that vIRA is a potent RHIM-dependent suppressor of DR-induced necroptosis.

Given that both RIP1 and RIP3 contributed to the necroptosis pathway in the expected fashion (Cho et al., 2009; He et al., 2009, Zhang, 2009 #340), we sought to evaluate the potential role of vIRA as a competitor of RIP1-RIP3 complex formation. FLAG-RIP3 and myc-RIP1 were coexpressed in 293T cells in the presence of increasing amounts of either WT M45-FLAG or mutant M45*mut*RHIM-FLAG. IP followed by IB analysis revealed a RHIM-dependent vIRA-

mediated inhibition of RIP1-RIP3 complex formation (Figure 2.3E). This demonstration provides mechanistic insight into how vIRA suppresses the execution of necroptosis initiated by DR-signaling but leaves open whether RIP1, RIP3 or both are directly targeted by the viral cell death suppressor.

MCMV-induced programmed necrosis is RIP3-dependent, but RIP1-independent.

Having shown that vIRA suppresses necroptosis, which requires the expression and kinase activity of RIP3 and RIP1 as well as a RIP3-RIP1 complex (Cho et al., 2009; He et al., 2009; Zhang et al., 2009), we characterized the cellular requirements for MCMV-associated programmed necrosis. RIP3-knockdown rendered either 3T3-SA or SVEC4-10 cells resistant to programmed necrosis induced by mutant virus (Figure 2.4A and B), indicating a requirement for RIP3. To clarify the role of RIP3, control (RIP3+/+), heterozygous (RIP3+/-), and homozygous (RIP3-/-) deficient MEF cells were isolated, and assessed for virus replication and sensitivity to programmed necrosis. RIP3 levels were assessed by IB in cell lysates and shown to reflect gene copy (Figure 2.4D). WT MCMV replicated to comparable high titers in all MEF lines tested, and, as expected, *M45mutRHIM* virus was significantly attenuated in RIP3+/+ cells (Figure 2.4E, left panel) where RIP3 levels were the highest (Figure 2.4D). Mutant virus replication was fully rescued in RIP3-/- MEFs (Figure 2.4E, right panel). Consistent with a relationship between RIP3 levels and sensitivity to this death pathway (Figure 2.4D), replication levels and sensitivity to death were intermediate in RIP3+/- cells (Figure 2.4E, middle panel, and Figure 2.4G). Furthermore, RIP3+/+ MEFs died following mutant virus infection, whereas RIP3-/- cells survived, sustaining the evidence that RIP3 is required for virus-induced death to occur (Figure 2.4G). Here, RIP3 levels correlated with cellular sensitivity to virus-induced programmed necrosis as well as to the concomitant attenuation of viral growth. When RIP3-/- MEFs were reconstituted with WT, KD or mutant RHIM (mRHIM), RIP3 (Figure 2.4F, left panel) and infected

with mutant virus, only WT RIP3 reconstituted cells exhibited increased sensitivity to virus-induced necrosis (Figure 2.4F, right panel). These data are consistent with a direct role of RIP3, as well as a requirement for an intact RIP3 kinase domain and RHIM for cell death signal transduction in response to viral infection.

We showed that vIRA bound RIP3 in a RHIM-dependent manner when both were transiently overexpressed (Upton et al., 2008). Here we have revealed a requirement for RIP3 in virus-associated programmed necrosis. To formally demonstrate that vIRA directly targets RIP3 to modulate this death process during infection, we infected necrosis-sensitive 3T3-SA cells. Co-IP of M45 protein from infected cell lysates at 12 and 18 h postinfection with antibody to RIP3 is consistent with a physical interaction of vIRA with endogenous RIP3 (Figure 2.4C). The absence of detectable vIRA in RIP3 immunoprecipitates from M45*mut*RHIM virus-infected cells is consistent with this being a RHIM-dependent interaction. We were unable to detect an interaction between endogenous RIP3 and RIP1 during viral infection with either WT or mutant viruses (data not shown). These data suggest that virus-associated programmed necrosis is distinct from DR-induced necroptosis because the pathway does not involve RIP1.

To more formally investigate the role of TNF α as well as RIP1 in virus-associated programmed necrosis, we sought to interfere with mediators and adaptors known to play roles in necroptosis. First, infected cells were treated with TNF α -neutralizing antibody over a range of effective concentrations (Figure 2.S3D) without observing any impact on virus-induced necrosis in susceptible cell types (Figure 2.S3A, B, C). Second, infected cells were treated with the RIP1-specific kinase inhibitor Nec-1 to determine whether RIP1 kinase activity contributes to virus-induced DR programmed necrosis. Consistent with the inability to detect interactions between RIP3 and RIP1 during infection, treatment with Nec-1 over a range of doses failed to

restore viability of infected primary MEF, 3T3-SA, or SVEC4-10 cells (Figure 2.4G, grey bars; Figure 2.S3E, F, G). In contrast, Nec-1 treatment as low as 15-30 μ M was sufficient to suppress TNF α -induced necroptosis in these same cell lines (Figure 2.4G, 2.S3E, F), confirming both the sensitivity of these cells to DR-induced necroptosis and efficacy of Nec-1 as a RIP1 inhibitor that does not impact RIP3. Thus, RIP1 kinase activity is dispensable for virus-associated programmed necrosis, in contrast to its critical role in necroptosis. Since SV40-transformed MEFs, including both the RIP1^{+/+} and RIP1^{-/-} MEFs used in Figure 2.3C, were resistant to virus-induced cell death (data not shown), we knocked down RIP1 expression by RNAi in either primary MEFs or SVEC4-10 cells with multiple RIP1-specific hairpins (Figure 2.4I, J), and these cells failed to suppress virus-induced necrosis. This result was recapitulated using independently derived isolates of M45^{mut}RHIM mutant virus (Figure 2.4I, J). RIP3 scores as necessary whereas RIP1 appeared dispensable by either knockdown or chemical inhibition in virus-induced programmed necrosis. Thus, unlike TNF α -induced necroptosis, virus-induced necrosis does not rely on a RIP1/RIP3 kinase complex and instead appears to be a novel RIP3-dependent programmed necrosis pathway.

Normalization of M45 mutant virus phenotype in RIP3-deficient mice. Given that vIRA RHIM-deficient mutant MCMV induces a form of RIP3-dependent programmed necrosis that strongly attenuates viral pathogenesis, we inoculated RIP3^{-/-} as well as control RIP3^{+/+} C57BL/6 mice in order to follow initial inflammatory events induced by WT or mutant virus. Following footpad route of inoculation, WT virus replicates at the portal of entry, followed by dissemination to distal organs. This route allows for the assessment of virus-induced inflammation at the site of inoculation, which is influenced by the MCMV-encoded CC-chemokine homolog MCK-2 (Saederup et al., 2001). During infection, WT MCMV induces characteristic swelling of the footpad compared to uninfected controls, peaking at day 5 post-

infection and resolving by 14 days. Following inoculation, M45 mut RHIM virus infection induced swelling in RIP3 $-/-$ mice comparable to WT virus infection of either RIP3 $+/+$ or RIP3 $-/-$ mice, reaching greater than 50% increase in size over uninfected paws (Figure 2.5A). In contrast, mutant virus did not induce significant swelling in RIP3 $+/+$ mice, consistent with an attenuated phenotype. Thus, in the absence of RIP3 function, mutant virus infection recapitulated early inflammatory events characteristic of WT infection.

Given the importance of RHIM-mediated activity in suppressing virus-associated death as well as the observation that RIP3 associates with TRIF, we sought to determine whether this cellular RHIM adaptor (Kaiser and Offermann, 2005; Meylan et al., 2004) contributed to the inflammatory phenotype. TRIF is known to influence WT MCMV infection (Tabeta et al., 2004). Despite previous demonstration that vIRA is able to suppress RHIM-dependent cell death signaling relayed via TRIF (Upton et al., 2008), when inoculated in footpads, TRIF-mutant (Trif^{Lps2/Lps2}) mice (Hoebe et al., 2003) failed to exhibit any difference in behavior from WT mice (Figure 2.5A, right panel). Thus, vIRA plays a critical RIP3-dependent, TRIF-independent step in viral pathogenesis.

When explanted RIP3 $+/+$, RIP3 $-/-$, and Trif^{Lps2/Lps2} peritoneal exudate cells (PEC) were infected *ex vivo* with either WT or mutant virus, only RIP3 $-/-$ PECs were resistant to mutant virus-induced programmed necrosis (Figure 2.5B), consistent with the behavior of primary fibroblasts to mutant virus infection. Given that PECs express TLR3 and TLR4, this experiment excluded any contribution of TRIF-dependent TLR-signaling to RIP3-dependent virus-induced cell death. The TLR adaptor TRIF does not contribute to virus-induced programmed necrosis.

Finally, we sought to evaluate the role of RIP3 in viral pathogenesis. Mice were inoculated in footpads and sacrificed 14 days post infection, when salivary glands were

harvested and viral titers were determined by plaque assay. Salivary glands are the major site of secondary MCMV replication as well as the source of virus transmission between hosts. Virus levels in this organ remain a highly sensitive indicator of successful infection and dissemination to secondary organs in the intact host. Virus titers in salivary gland homogenates of RIP3^{-/-} mice were comparable to WT virus (Figure 2.5C). The complete normalization of mutant virus in RIP3^{-/-} mice provides formal proof that RIP3 is the relevant target of vIRA modulation under physiological conditions. In the absence of RIP3, vIRA function appears dispensable for normal WT levels of viral replication or dissemination. Consistent with the experiments in NSG and BALB/c mice, C57BL/6 mice were unable to support infection and dissemination of mutant virus and mutant virus was not able to disseminate to salivary glands of TRIF-defective mice (Figure 2.5C). WT MCMV disseminated at similar levels to salivary glands of control, RIP3^{-/-} and TRIF-defective C57BL/6 mice. Normalization of mutant virus behavior by elimination of a host determinant provides compelling and unambiguous evidence that RIP3 is the target of vIRA-mediated modulation during MCMV infection, and further suggests that RHIM-dependent suppression of RIP3 function in virus-associated cell death by vIRA is essential for MCMV pathogenesis.

C) DISCUSSION

Manipulation of host cytokine and cell death pathways affords pathogens the opportunity to maintain an environment necessary for efficient replication to establish a foothold within the host organism. In this work, which derives in part from the goal of elucidating mechanisms of cell death suppression by a natural pathogen of mice, we have demonstrated a critical role for RIP3 as a positive regulator of a cell-intrinsic antiviral programmed necrosis triggered during MCMV infection. Our results show a dependence on RIP3 function in both virus-associated programmed necrosis and DR-associated necroptosis. We also provide a clear mechanistic distinction between these two pathways. Whereas necroptosis is dependent on RIP1 and a RIP1-RIP3 signaling complex (Cho et al., 2009; He et al., 2009; Zhang et al., 2009), virus-induced death is dependent on RIP3 but not RIP1. MCMV encoded vIRA suppresses either of these necrotic death pathways in a RHIM-dependent fashion, suggesting that the common target of this viral cell death suppressor is RIP3. The dramatic differences in behavior of viruses expressing WT or RHIM-deficient form of vIRA, assayed *in vitro* and *in vivo*, demonstrate that this death suppressor is critical for MCMV replication and pathogenesis. The normalization of mutant virus behavior when RIP3 function is eliminated in the host formally establishes the biological significance of vIRA-RIP3 interactions. By revealing the commitment of a specific pathogen-encoded suppressor to necrotic death pathways, our data validates RIP3-dependent programmed necrosis as a central player in host defense, and reveal yet another cytomegalovirus immune escape mechanism contributing to viral pathogenesis.

The normalization of vIRA-deficient MCMV behavior in RIP3 deficient cells and mice provides unambiguous evidence that virus-induced inflammatory responses, viral replication and viral pathogenesis are all directly linked to RIP3-mediated events, and these most likely

revolve around the two pathways that vIRA blocks: virus-associated programmed necrosis and DR-associated necroptosis. Together with the surprising demonstration the RHIM-mediated vIRA function is independent of RIP1 as well as TRIF, these data strongly argue that RIP3 is a dominant adaptor controlling cellular necrotic pathways in viral pathogenesis.

Restoration of an attenuated vIRA viral mutant phenotype *in vivo* by the elimination of the host intracellular adaptor such as RIP3 has rarely been achieved in studies on viral pathogenesis. The most relevant to our studies is the demonstration that herpes simplex virus ICP γ 34.5 uniquely targets protein kinase R (Leib et al., 2000), an RNA binding adaptor protein that shuts down translation in virus-infected cells. The attenuation of ICP γ 34.5 mutant virus was completely normalized in protein kinase R-deficient mice. This strategy has also been employed to show the *in vivo* function of a number of herpesvirus immune evasion genes acting on the immune system. For example, MCMV m157 and m04 secreted gene products target the natural killer cell receptors Ly49H (Bubic et al., 2004) and Ly49P (Kielczewska et al., 2009), respectively, and murine gammaherpesvirus 68 regulator of complement activation (Kapadia et al., 2002) as well as herpes simplex virus glycoprotein C (Friedman et al., 1996; Lubinski et al., 1999; Lubinski et al., 1998) directly target complement factor C3 in pathogenesis. Here, we provide *in vivo* evidence that MCMV M45 gene product vIRA mediates its biological function by antagonizing the host necrosis-regulating kinase RIP3, and, furthermore, that the RIP3-dependent death pathway, as well as vIRA suppression, rely on RHIM-mediated interactions. Thus, our demonstration that virus carrying RHIM-deficient vIRA exhibited normalized replication in RIP3-deficient mice together with the evidence that restoration of WT RIP3 expression, but not KD or RHIM-deficient RIP3, sensitizes RIP3-deficient cells to virus-induced programmed necrosis, demonstrates the exclusive interplay of RIP3 and vIRA in MCMV pathogenesis.

Virus- and DR-associated programmed necrosis share a requirement for RIP3 kinase activity and RHIM-dependent interactions (Cho et al., 2009; Hitomi et al., 2008; Zhang et al., 2009). High levels of RIP3 remain the common feature that predicts sensitivity to necrotic death from either inducer. In addition, endothelial cell type (Brune et al., 2001), *per se* plays no role in susceptibility to premature death induced by vIRA mutant virus. The recent findings that high RIP3 levels confer sensitivity of human and murine cell lines to TNF α -induced necroptosis (He et al., 2009; Zhang et al., 2009), are entirely consistent with the results presented here. One characteristic of DR-induced necroptosis, the requirement for kinase activity and RHIM-dependent signaling of RIP1 (Christofferson and Yuan, 2009; Declercq et al., 2009; Festjens et al., 2007; Galluzzi and Kroemer, 2008) distinguishes this necrotic pathway from virus-induced necrosis. Nec-1 treatment inhibits the formation of a RIP1-RIP3 complex, RIP3 activation, and cell death in response to TNF α (Cho et al., 2009; He et al., 2009). Treatment with this RIP1-specific inhibitor has no impact on RIP3 activation or signaling in virus-induced necrosis. Overexpression of RIP3 has previously been reported to induce cell death (Kasof et al., 2000; Pazdernik et al., 1999; Sun et al., 1999; Yu et al., 1999), including in situations where RIP1 expression has been eliminated (Zhang et al., 2009). While this work indicated RIP3 alone may be sufficient to drive necrotic death, the data reported here show physiological relevance of a RIP3-dependent, RIP1 independent pathway. The cell death pathway induced by virus infection is naturally executed in cells that can also support DR-induced necroptosis. The RIP1 as well as TRIF-independence of virus-induced necrosis, raises a need to identify additional RHIM-dependent interactions of RIP3 as well as other downstream events in RIP3-dependent, RIP1-independent programmed necrosis.

vIRA likely triggers a range of events when complexed with RIP3 that may contribute to suppression of virus- or DR-associated necrosis. vIRA is composed of two distinct regions, a 277

amino terminal RHIM-containing region is sufficient for suppression of cell death (Upton et al., 2008) and a 801 aa region that contains the herpesvirus-conserved ribonucleotide reductase large subunit homology that has been assigned conflicting roles in suppression (Mack et al., 2008) and activation of NF- κ B expression (Rebsamen et al., 2009). The direct interaction of vIRA with RIP3 opens the way for other activities of vIRA to potentially contribute to parallel signaling pathways. Regardless of how downstream signaling proceeds, it is important to recognize that neither the carboxyl-terminus nor other regions of vIRA can mediate suppression of virally induced programmed necrosis when RHIM-dependent interactions are disrupted.

The cellular death response to infection with vIRA-deficient MCMV was initially characterized as apoptosis (Brune et al., 2001) with caspase-independence only recognized recently (Mack et al., 2008). Here, we have formally demonstrated that a four amino acid substitution to prevent RHIM-dependent interactions recapitulates the expected behavior of vIRA-null mutant phenotype (Brune et al., 2001), and conclusively show, by morphological, biochemical, and cell biological criteria, that the cell death pathway is RIP3-dependent programmed necrosis. Molluscum contagiosum, equine herpesvirus-2 and Kaposi's sarcoma-associated herpesvirus encode proteins that can suppress DR-induced necroptosis (Chan et al., 2003), although the mechanisms by which these viral genes suppress necroptosis, and their specific role(s) in pathogenesis, remain undetermined. Comparison to investigations on the RIP3-dependence of vaccinia-induced liver pathology, inflammation and viral replication in mice (Cho et al., 2009) reveals potential parallels and differences. The behavior of vaccinia has been interpreted to be a consequence of TNF α production, and supports findings that cytokine responses are a primary mechanism used to control poxviruses during zoonotic infection (Wang et al., 2008a). While DR signaling (Benedict, 2003; Benedict et al., 2003) as well as TLR signaling (Hoebe et al., 2003; Tabeta et al., 2004) contribute to the replication levels of WT MCMV in

mice, we found no evidence that either is involved in initiating MCMV-associated programmed necrosis during infection. We speculate that this antiviral death pathway is a cell intrinsic response to viral infection that responds to the initial events following entry into cells.

While we have identified RIP3 as the executioner of MCMV-induced programmed necrosis, the cellular processes leading to activation of this pathway by virus remain unidentified. UV-inactivated mutant virus does not induce cell death (Brune et al., 2001), and preliminary evaluation suggests that inhibition of viral DNA replication fails to protect from programmed necrosis. Thus, the RIP3-activating step likely originates from early events in virus-infected cells perhaps through cellular processes altered or usurped by viral infection. Alternatively, sensing of invading pathogens by PRRs initiate signals to contend with pathogens, and several of these sensor proteins are known to recruit RIP3 (Kaiser et al., 2008; Kumar et al., 2009; Meylan et al., 2004; Palm and Medzhitov, 2009; Saito and Gale, 2007). TLR3-TRIF contributes to the innate immune response to MCMV infection, though less significantly than TLR9 (Hoebe et al., 2003; Tabeta et al., 2004), and RIP3 binds to TRIF in a RHIM-dependent interaction (Kaiser and Offermann, 2005; Meylan et al., 2004), although the significance of this interaction remains unclear. The capacity of vIRA to suppress RHIM-dependent death signals relayed via TRIF (Upton et al., 2008) was not sustained here as TRIF-deficient peritoneal macrophages remained susceptible to killing by mutant virus and mice lacking TRIF were no more susceptible to mutant virus than WT mice. Thus suppression of programmed necrosis by vIRA during infection is unlikely to be tied to other characterized RHIM-dependent pathways dependent upon TRIF. Our results raise the possibility that another pathogen sensor pathway drives RIP3 activation, and the IFN-inducible, cytosolic DNA sensor DAI/ZBP1/DLM-1 (Takaoka et al., 2007) remains an attractive candidate to fulfill such a role, since it contains a RHIM and physically interacts with RIP3 as well as vIRA (Rebsamen et al., 2009). Defining the cellular

processes required for induction of RIP3-dependent death during MCMV infections remains a significant future line of investigation.

Cytomegaloviruses encode an array of cell death suppressors to counter apoptotic cell death pathways that may dominate in different cell and tissue settings (McCormick, 2008). MCMV encodes three genes that target core components of the apoptotic machinery: viral mitochondrial inhibitor or apoptosis, vMIA (Goldmacher et al., 1999; McCormick et al., 2005), viral inhibitor of Bak oligomerization, vIBO (Cam et al., 2009), and viral inhibitor of caspase-8 activation, vICA (Skaletskaya et al., 2001). Together, these functions antagonize caspase-dependent cell death pathways that would otherwise compromise viral replication (Cicin-Sain et al., 2008; Menard et al., 2003). vMIA and vIBO function at the level of the mitochondria to suppress amplification of pro-apoptotic signals induced by extrinsic and intrinsic stimuli (Cam et al., 2009; Goldmacher et al., 1999; McCormick et al., 2005). vICA inhibits caspase-8 activation and prevents DR-induced apoptosis (McCormick et al., 2005; Skaletskaya et al., 2001), and plays a critical role supporting viral replication in macrophages (Menard et al., 2003; McCormick et al., manuscript in revision). vICA suppression of apoptosis is critical *in vivo*, where the defect is restored by expression of FADD-DN (Cicin-Sain et al., 2008). The pro-necrotic activity of RIP3 is inactivated by caspase-8 processing (Feng et al., 2007), suggesting that, in instances of infection by pathogens encoding caspase-8 inhibitors such as vICA, a virally encoded inhibitor of programmed necrosis, like vIRA, prevents the induction of necrosis. A recombinant viral mutant lacking the Bax inhibitor, vMIA, replicates comparable to WT in visceral organs of infected animals, but is attenuated for leukocyte-dependent dissemination of virus to the salivary gland (Manzur et al., 2009). Mutants lacking the caspase-8 inhibitor vICA are attenuated *in vivo* following systemic inoculation, and are severely attenuated for dissemination to salivary glands (Cicin-Sain et al., 2005; Cicin-Sain et al., 2008). These results have supported

the importance of modulating host apoptotic pathways in MCMV pathogenesis. It is interesting to note that the attenuation of vIRA mutants *in vivo* is tied to suppression of RIP3 activation and is as critical to viral pathogenesis as the suppression of Bax activation or caspase-8 activation, by vMIA or vICA, respectively.

D) CONCLUSIONS

The identification of vIRA as an inhibitor of RIP3-dependent programmed necrosis in a natural biological setting extends the role of RIP3 as a vital player in host antiviral defense, and underscores the critical role of vIRA RHIM-dependent activities in suppression of programmed necrosis in MCMV pathogenesis. This study also begins to illustrate the balance of necrotic and apoptotic pathways in host defense against viruses, supporting the growing evidence that viruses exploit multiple innate immune processes to influence a wide range of alternative immune effector activities.

E) MATERIALS AND METHODS

Reagents. CHX, Bafilomycin A₁, and dimethyl sulfoxide (DMSO) were obtained from Sigma Aldrich. Nec-1 and z-VAD-fmk were purchased from Calbiochem and Enzo Life Sciences, respectively. Recombinant mouse TNF α was from PeproTech and anti-TNF α antibody was from R&D Systems. The following antibodies were used for IB analysis: mouse anti- β -actin (clone AC-74; Sigma), mouse anti-RIP1 (clone 38; BD Biosciences), rabbit anti-RIP3 (Imgenex), rabbit anti-cleaved caspase-3 (Cell Signaling Technology), rabbit anti-LC3B (Cell Signaling Technology), mouse anti-FLAG (M2 clone) peroxidase conjugate (Sigma Aldrich), mouse anti-c-Myc (clone 9E10, Sigma Aldrich), rabbit anti-c-Myc peroxidase conjugate (Sigma Aldrich), anti-mouse IgG-HRP (Vector Laboratories), anti-rabbit IgG-HRP (Vector Laboratories), anti-MCMV M45/vIRA (gift from David Lembo, University of Turin), and anti-MCMV IE1 (gift from Stipan Jonjic, University of Rijeka). Immunoprecipitations were performed with rabbit anti-c-Myc agarose conjugate (Sigma Aldrich) or goat anti-RIP3 (clone C-16; Santa Cruz Biotechnology) and Protein A/G agarose (Santa Cruz Biotechnology).

BAC mutagenesis and recombinant viruses. Plasmid pSIM6 encoding lambda red recombination functions (Datta et al., 2006) was introduced into bacteria carrying a bacterial artificial chromosome (BAC) harboring the MCMV K181(Perth) strain genome (Redwood et al., 2005). Recombineering for K181-BAC mutagenesis and diagnostics was performed essentially as previously described (Tandon and Mocarski, 2008), and is outlined in Supplemental Materials. The supernatant of NIH3T3 cells transfected with WT and mutant K181-BAC DNA was collected and M45mutRHIM viruses were identified by replication on NIH3T3 cells (ATCC number CRL-1658) and purified as previously described (Redwood et al., 2005). WT and mutant viruses were propagated and titered by plaque assay on NIH3T3 cells as previously described (Saederup et al.,

2001). Medium from infected cultures was clarified by centrifugation at 2500 g and virus collected by sedimentation at 17,000 g and stored at -80°C until use. Single step growth curves and viral yield assays were performed by infecting cell lines in 6 well plates at the indicated MOI in a volume of 0.5 ml for 2 hours at 37°C with periodic rocking. Following adsorption, inoculums were removed, cells washed three times with PBS, and refed with complete media. Samples were harvested at the indicated times, and virus growth assessed by plaque assay.

Mice, infections, and organ harvests. C57BL/6, BALB/c, TRIF mutant (Strain - C57BL/6J-Ticam1^{Lps2}) (Hoebe et al., 2003), and NSG mutant (NOD.cg-Prkdc^{scid}Il2rg^{tm1Wjl}/Sz) (Shultz et al., 2005) mice were obtained from Jackson Laboratory. RIP3^{-/-} mice (Newton et al., 2004) were provided by Francis Chan (University of Massachusetts) with permission from Vishva Dixit (Genentech). 8- to 12-week-old mice were inoculated with 10⁶ pfu into a rear footpad or by intraperitoneal injection as previously described (Saederup et al., 1999). Upon sacrifice, organs were removed using aseptic technique, placed in 1 ml complete DMEM and frozen at -80°C. Organs to be titered were thawed, disrupted by sonication and viral growth assessed by plaque assay. Resident peritoneal macrophages were collected from euthanized animals by DMEM lavage, resuspended in DMEM containing 10% FBS and seeded at a density of 5 X 10⁴ cells per a well in a 96 well plate 18 h prior to infection. For virulence studies, animals losing over 20% body weight or displaying severe signs of CMV-disease (ruffled fur, hunched posture, dehydration, diminished responsiveness) were scored and euthanized. Mice were bred and maintained by Emory University Division of Animal Resources in accordance with Institutional Guidelines, and all procedures were approved by the Emory University Institutional Animal Care and Use Committee.

Cell culture and embryonic fibroblast isolation. NIH3T3 fibroblasts, 3T3-SA (ATCC number CCL-92), SVEC4-10 (ATCC CRL-2181), HEK293T, L929, and MEFs were all maintained in DMEM containing 4.5 g/mL glucose, 10% FBS (Atlanta Biologicals), 2 mM L-glutamine, 100 U/mL penicillin, and 100 U/mL streptomycin (Invitrogen). SV40T transformed RIP1^{-/-} and control WT MEFs (Wong et al., 2009) were kindly provided by John Silke (LaTrobe University) with permission from Michelle Kelliher (University of Massachusetts). Murine embryonic fibroblasts were isolated from timed pregnancies at day E14.5-16.5, as previously described (Pollock and Virgin, 1995).

Immunoblot and Immunoprecipitations. Immunoprecipitation were performed essentially as described previously (Kaiser and Offermann, 2005), with minor modifications. Clarified cell lysates were incubated overnight with 25 µl of anti-c-Myc agarose conjugate slurry or 1 µg of goat-anti-RIP3 antibody and 25 µl of Protein A/G slurry. Immunoprecipitates were washed 4-6 time prior to analysis. Cell lysates and immunoprecipitated samples were separated on Criterion gels (Bio-Rad), transferred to Immobilon PVDF membranes (Millipore), and subjected to IB analysis as previously described (Kaiser and Offermann, 2005). Detection of c-myc- and RIP3- immunoprecipitates were performed with mouse anti-c-myc (clone 9E10) or rabbit anti-RIP3 antibodies, respectively.

Plasmids, Transfections, and Transductions. Transfections were performed using Lipofectamine 2000 (Invitrogen) and DNA at a 1:1 ratio diluted in Opti-MEM (Invitrogen). Carboxyl-terminal Flag-epitope tagged WT and *mut*RHIM M45 were generated by subcloning the respective ORF into pCMV-TAG4A (Stratagene). pCMV10-3xFLAG-RIP3 and pcDNA3-6myc-RIP1 (Kaiser and Offermann, 2005) have been previously described. Flag-RIP3, Flag-RIP3-KD (Kaiser et al., 2008), and Flag-RIP3-mRHIM (Kaiser and Offermann, 2005), as well as M45-myc, and

M45*mut*RHIM-myc (Upton et al., 2008) were subcloned into the pQCXIH (Clontech) retroviral construct. The pLKO.1-based RIP3-A (TRCN0000022535), RIP3-B (TRCN0000022538), RIP1-A (TRCN0000022467), and RIP1-B (TRCN0000022464) shRNA constructs were obtained from Open Biosystems. The pLKO.1-Scramble control shRNA vector (Sarbasov et al., 2005), as well as lentiviral and retroviral production, infection, and selection have all been described (Kaiser et al., 2008).

Cell Viability Assays. Cells (5000 cells/well) were seeded into 96-well plates. 16-18 hours post-seeding, media was replaced with 50 μ l of viral inoculum containing 10 pfu/cell (MOI=10.0). Nec-1 at the indicated concentration was added 1 h prior to infection, and maintained for the duration of the assay. Inoculums were removed 2 h post infection, and replaced with 50 μ l of complete media. Alternatively, cells were treated with the indicated concentrations of TNF α , CHX, zVAD-fmk and/or Nec-1. The Nec-1 vehicle, DMSO, was held constant for all cells. Viability was determined 18 h post infection/treatment. Unless otherwise indicated, the viable cells per a well was determined indirectly by measuring the intracellular levels of ATP as a marker for cell survival using the Cell Titer-Glo Luminescent Cell Viability Assay kit (Promega) according to the manufacturer's instructions. 96-well plate assays were allowed to reach RT prior to adding 50 μ L of reagent to each well and then shaken for 10 minutes. Released protease activity was measured using the CytoTox-Fluor Assay kit (Promega) according to the manufacturer's instructions. Briefly, 50 μ l of assay reagent was added to each sample well and incubated at room temperature for 2 h. Luminescence or fluorescence was measured on a Synergy HT Multi-Detection Microplate Reader (Bio-Tek).

Microscopy. 3T3-SA cells were infected with WT or M45*mut*RHIM viruses (MOI of 10) for the indicated time in 6- or 12-well dishes, and bright field images were acquired on an

AxioCam MRC5 camera attached to a Zeiss Axio Imager A1 and processed with AxioVision Release 4.5 software. Samples for EM were prepared by infecting 3T3-SA cells with WT or M45mutRHIM viruses (MOI of 10) for 18 h. Monolayer cells were fixed in 2.5% glutaraldehyde in 0.1 M cacodylate buffer (pH 7.2) for 2 h at 4°C. Cells then were washed with the same buffer and postfixed with buffered 1.0% osmium tetroxide at room temperature for 1 h. Following several washes with 0.1 M cacodylate buffer, cells were dehydrated with ethanol, infiltrated, and embedded in Eponate 12 resin (Ted Pella Inc.). Ultrathin sections (60 to 70 nm) of monolayer cells were cut and counterstained using uranyl acetate and lead citrate. The examination of ultrathin sections was carried out on a Hitachi H-7500 transmission electron microscope.

BAC mutagenesis and recombinant viruses. The MCMV-K181 bacterial artificial chromosome, pARK25 (Redwood et al., 2005), and pSIM6, a plasmid encoding λ -RED recombination functions (a gift from Tim Barnett, Emory Children's Center), were introduced into DH10B by electroporation. Recombineering was performed essentially as previously described (Tandon et al., 2008). Briefly, multiple clones of pARK25/pSIM6 containing bacteria were grown to OD₆₀₀ of 0.4 to 0.6, and recombination functions induced by incubation at 42°C. Bacteria were then rendered electrocompetent by multiple washes in ice-cold water. The kanamycin (Kan) resistance and levensucrase (SacB) genes and associated regulatory elements were PCR amplified from pTBE100 (another generous gift from Tim Barnett, Emory Children's Center) with 50nt overhangs corresponding to MCMV genomic sequence within the M45 ORF (primers; JUp045, 5'-GGGGAGCCTTCGGGGTGGGTGGGGGGCACAGCGTGCCTACGTCAGGATCAATTCGAGCTCGGTACCCGG-3' and JUp046, 5'-GGCGATGCTCATAGCATTATGGTTTCCGATCTGTATTCCAGAGACTCCATATCCCGGAAAAGTGCCACC-3'). PCR reactions were treated with DpnI to digest template DNA and the amplicons gel purified, then used to electroporate induced bacteria. Kanamycin-resistant, sucrose-sensitive clones were confirmed and analyzed for

recombineered insertion and genomic integrity by RFLP analysis. Kan/SacB insertion deletes 4nt of MCMV sequence and introduces 2.9kb within the M45 open reading frame. Specific M45 mutations were introduced by a second round of recombineering with PCR amplicons encoding M45*mut*RHIM (Upton et al., 2008) (primers; JUp097, 5'-CTCGTCGAGTTCGCGTGACATGGATC GCCAGCCCAAAGTC-3' and JUp098, 5'-TTGGCGACGAGTCCGCCGTCAGCGATAATTCACGG AAGGGG-3'). Colonies were screened for sucrose resistance and kanamycin sensitivity, and positive clones were further confirmed by RFLP and functional analyses. M45*mut*RHIM and M45*mut*RHIM* were each generated from independently isolated parental WT K181 bacmid clones. BAC DNA was isolated using Midi-prep columns (Qiagen), and cut with HindIII, EcoRI, or BamHI (New England Biolabs). Viruses were generated as described in Materials and Methods.

Time-lapse Microphotography. 3T3-SA cells were seeded on a 35mm glass bottom culture dish (MatTek Corp.) and infected 18 h later. At 4 h post infection, cells were placed in a heated chamber with CO₂ perfusion. Live cell analysis of cells was performed with a Perkin Elmer Ultraview RS mounted on a Zeiss Axiovert 200m using a 10X objective.

Immunofluorescence Analysis. At 6 h post infection with either MCMV WT or MCMV M45*mut*RHIM virus, 3T3-SA cells grown on coverslips were processed as described for immunofluorescence analysis (Kaiser et al., 2008). The anti-MCMV IE1 Ab (diluted 1/2000 in blocking buffer) was used as the primary Ab and AlexaFluor 488 (diluted 1/5000) was used as a secondary antibody.

F) FIGURES AND LEGENDS

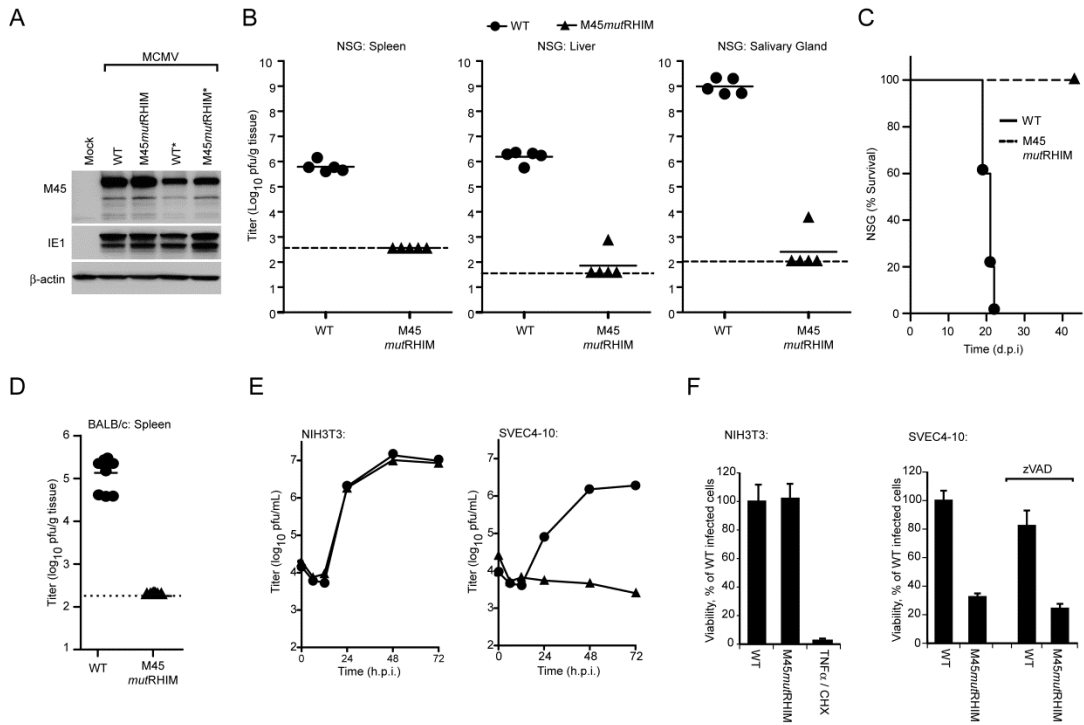


Figure 2.1. Role of MCMV M45 RHIM interactions in suppression of virus-induced death. (A)

IB analysis of vIRA expression from recombinant viruses to detect vIRA (M45), IE1, and β -actin.

NIH3T3 fibroblasts were either mock- or virus-infected at a multiplicity of infection (MOI) of 10 with bacmid-derived K181 (WT) or vIRA mutant virus (M45mutRHIM). An asterisk (*) designates a second independent WT or mutant virus isolate.

(B) Replication levels and pathogenesis of WT and M45mutRHIM virus in severely immunodeficient NSG mice. At 16 d post inoculation (10^6 pfu into footpads), spleen (left panel), liver (middle panel), and salivary glands (right panel) were harvested from euthanized mice and viral titers determined by plaque assay. Each symbol represents one animal, solid horizontal lines represent the mean for each group, and dashed lines indicate the limit of detection in each assay. (C) Kaplan-Meier survival plot of NSG mice

(Fig. 2.1 continued) monitored for 42 days post infection with WT and M45*mut*RHIM virus (10^6 pfu into footpads). (D) Replication levels of WT and M45*mut*RHIM virus in spleen at 3 d post inoculation (10^6 pfu into peritoneal cavity) of BALB/c mice. (E) Replication levels of WT and M45*mut*RHIM virus in infected NIH3T3 fibroblasts (left panel) and SVEC4-10 endothelial cells (right panel) (MOI=10). Viral titers were determined by plaque assay at the indicated times post infection. (F) Viability of NIH3T3 fibroblasts (left panel) or SVEC4-10 cells (right panel) following infection with WT and M45*mut*RHIM virus. Where noted, zVAD-fmk (50 μ M) was included throughout infection. Cell viability was determined by measuring intracellular ATP levels with a Cell Titer-Glo Luminescent Cell Viability Assay kit. Treatment with TNF α (25 ng/mL) and cycloheximide (CHX; 5 μ g/mL) was used to induce apoptosis in uninfected NIH3T3 cells as a control. Error bars indicate standard deviation (SD) of the mean. See also the related Figure 2.S1.

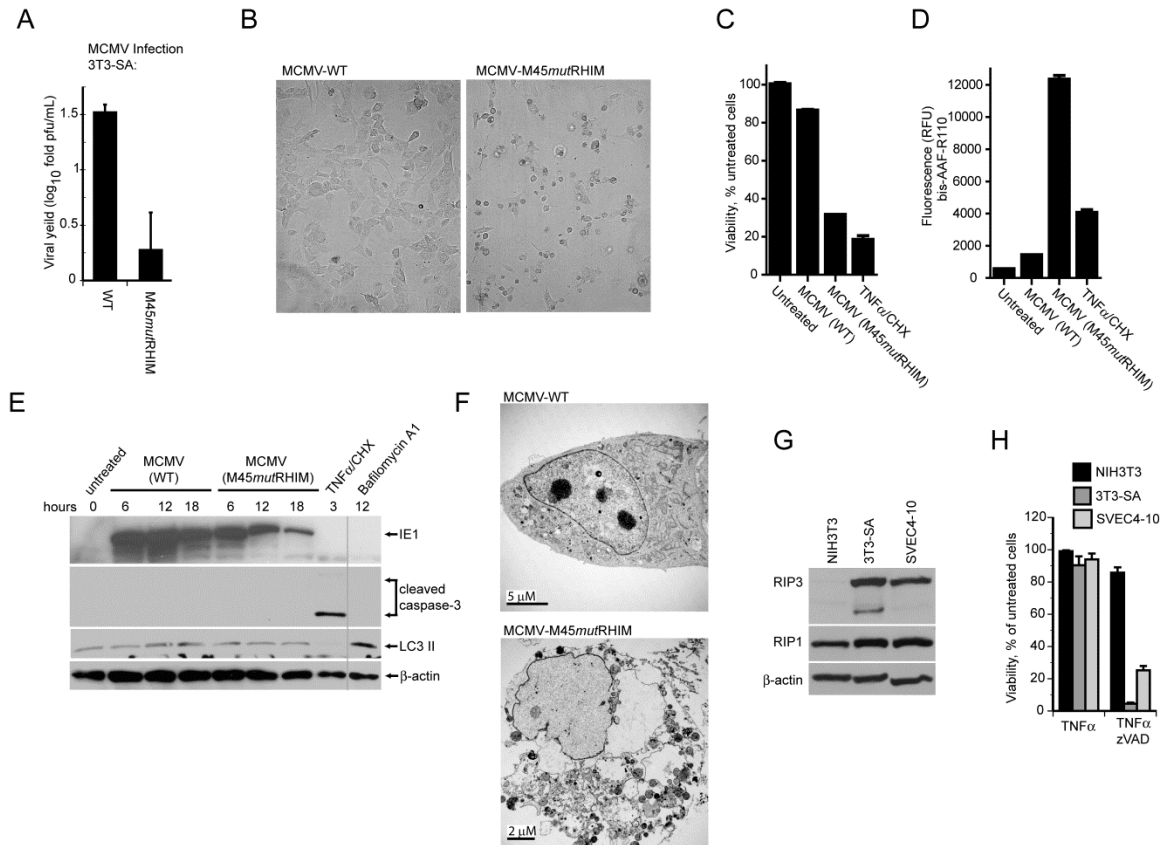


Figure 2.2. Cells sensitive to MCMV-associated programmed necrosis express high levels of

RIP3. (A) Viral yields determined by plaque assay at 72 hpi in 3T3-SA cells following infection with WT or M45mutRHIM virus (MOI=10). (B) Bright field micrographs of 3T3-SA cells infected for 18 h with either WT (left panel) or M45mutRHIM (right panel) virus. Magnification, 10X. (C) Viability of 3T3-SA cells assessed by intracellular ATP levels following infection with WT or M45mutRHIM virus. (D) Release of protease to the medium assessed in 3T3-SA cells using a CytoTox-Fluor kit. (E) IB of 3T3-SA cells infected with WT or M45mutRHIM virus (MOI=10) for the indicated times followed by detection of IE1, caspase-3, LC3 II and β -actin. Vertical line shows where lanes from the original gel were brought adjacent. In C - E, uninfected cells were treated to induce apoptosis (TNF α /CHX) as described in Figure 1F or with Bafilomycin A₁ (250 nM) to induce LC3 II, or left untreated. (F) Transmission electron micrographs of 3T3-SA cells at 18 hpi

(Figure 2.2 continued) with WT (top panel) or M45*mut*RHIM (bottom panel) virus. Size bars are indicated. (G) IB analysis of NIH3T3, 3T3-SA, and SVEC4-10 cells to detect RIP1, RIP3, and β -actin. (H) Viability of NIH3T3, 3T3-SA, and SVEC4-10 cells treated for 18 h with TNF α (25 ng/mL) in the absence or presence of zVAD-fmk (25 μ M). See also the related Figure S2.

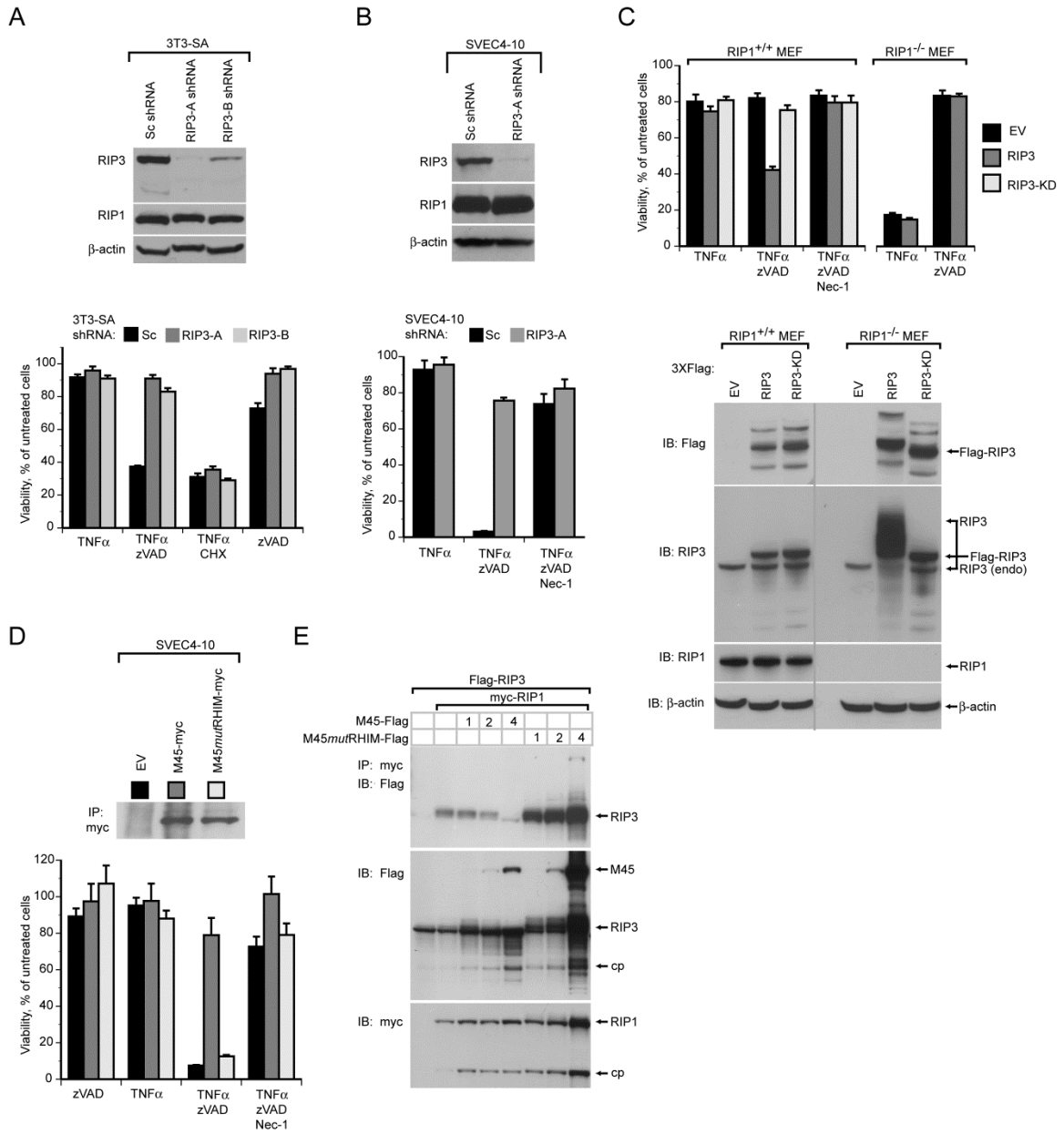


Figure 2.3. MCMV RHIM-dependent suppression of RIP3-mediated necrosis. (A) IB analysis (top panel) to detect RIP3, RIP1, and β -actin, and viability (lower panel) of 3T3-SA fibroblasts expressing a scramble control (Sc) or one of two RIP3-specific shRNAs (RIP3-A and RIP3-B) and treated to induce necroptosis as described in Figure 2H or to induce apoptosis as described in

(Figure 2.3 continued) Figure 2.1F. (B) IB analysis (top panel) to detect RIP1, RIP3, and β -actin and viability (bottom panel) of SVEC4-10 cells expressing Sc or RIP3-A shRNA. Cells were treated to induce necroptosis as described in Figure 2H in the absence or presence of Nec-1 (30 μ M).

(C) Viability (top panel) and IB analysis to detect RIP1, RIP3, β -actin and Flag-epitope tagged proteins (lower panel) in RIP1^{+/+} and RIP1^{-/-} MEFs transduced with empty vector (EV), Flag-tagged RIP3 (RIP3), or Flag-tagged kinase-deficient RIP3 (RIP3-KD) retroviral constructs. Transduced cells were treated as described in (B). The vertical line shows where lanes from the original gel were brought adjacent. (D) IB of myc-tagged proteins following IP with anti-myc conjugated agarose (top panel) of SVEC4-10 cells transduced with EV, M45-myc, or M45*mut*RHIM-myc retroviral constructs and viability (bottom panel) of these cells after treatment as described in (B). (E) IB of 293T cells transfected with Flag-tagged RIP3, myc-tagged RIP1 and 1, 2, or 4 μ g of either M45-Flag or M45*mut*RHIM-Flag expression plasmids after IP with anti-myc agarose beads. In all samples, the amount of transfected DNA was held constant with addition of control plasmid DNA. IB detection was with anti-Flag or anti-c-Myc (9E10) antibody. Major protein species are identified, with “cp” indicating a processed form of RIP1 or RIP3. Error bars indicate SD of the mean.

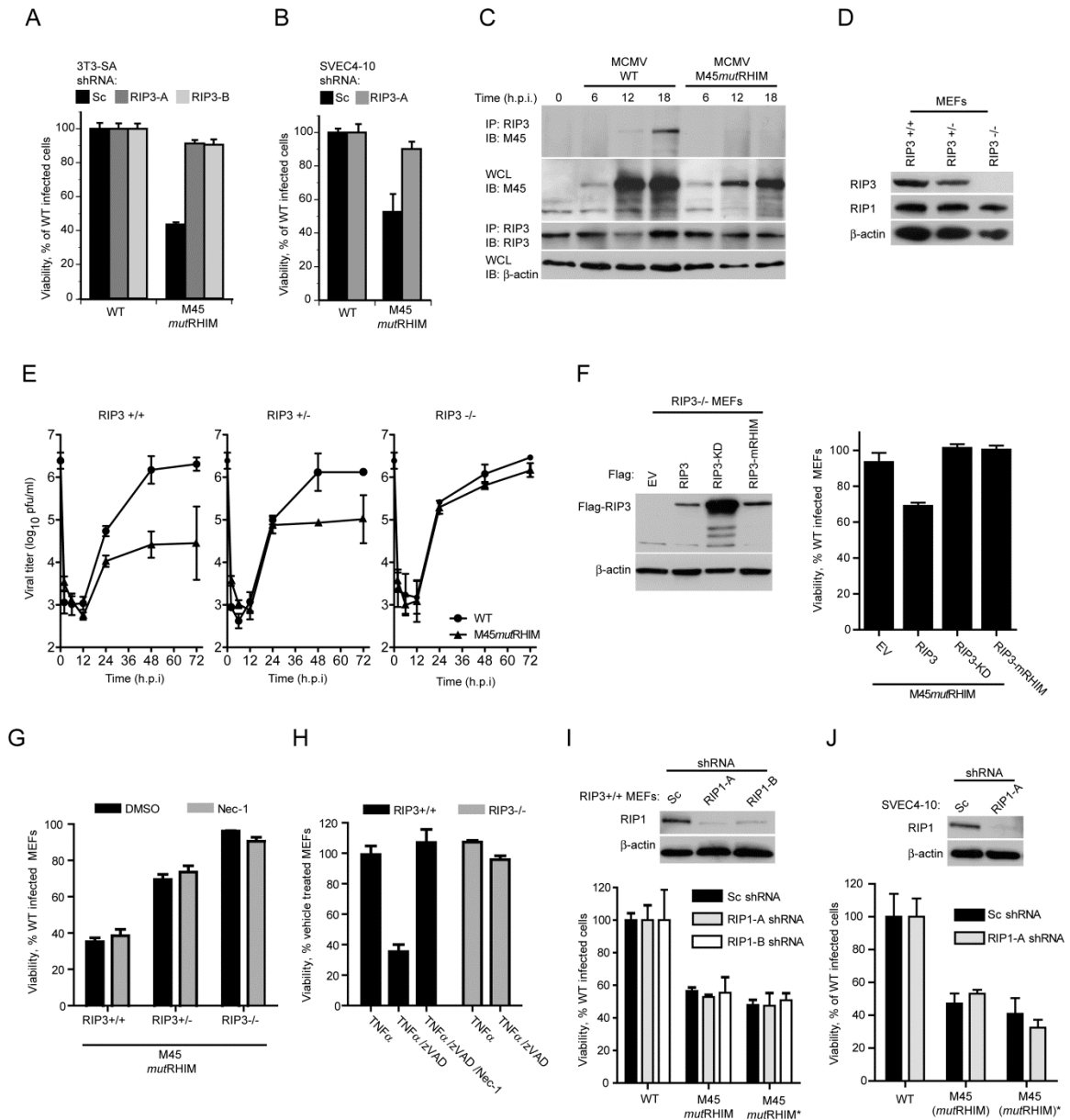


Figure 2.4. RIP3 is required, and RIP1 is dispensable for MCMV-associated programmed necrosis. (A) Viability of 3T3-SA cells expressing Sc, RIP3-A or RIP3-B shRNAs determined 18 hpi with WT or M45 *mutRHIM* virus (MOI of 10). (B) Viability of SVEC4-10 cells using a subset of conditions described in (A). (C) IB of 3T3-SA cells infected with WT or M45 *mutRHIM* virus (MOI of 5), harvested at indicated times for IP of RIP3 followed by detection of vIRA (M45) and RIP3. (D) Western blot analysis of RIP3 and RIP1 in MEFs from RIP3 +/+, RIP3 +/-, and RIP3 -/- mice. (E) Viral titers in MEFs from RIP3 +/+, RIP3 +/-, and RIP3 -/- mice infected with WT or M45 *mutRHIM* virus. (F) Western blot analysis of Flag-RIP3 and β -actin in RIP3 -/- MEFs transfected with EV, RIP3, RIP3-KD, or RIP3-miRHIM. (G) Viability of MEFs from RIP3 +/+, RIP3 +/-, and RIP3 -/- mice treated with DMSO or Nec-1 and infected with M45 *mutRHIM* virus. (H) Viability of MEFs from RIP3 +/+, RIP3 -/- mice treated with TNF α , TNF α /zVAD, or TNF α /zVAD/Nec-1. (I) Viability of RIP3 +/- MEFs transfected with Sc shRNA, RIP1-A shRNA, or RIP1-B shRNA and infected with M45 *mutRHIM* virus. (J) Viability of SVEC4-10 cells transfected with Sc shRNA or RIP1-A shRNA and infected with M45 *mutRHIM* virus.

(Figure 2.4 continued) IB using ~5% of cell lysate to detect vIRA (M45) and β -actin. (D) IB of RIP3^{+/+}, RIP3^{+/-}, and RIP3^{-/-} MEFs to detect RIP3, RIP1, and β -actin. (E) Replication of WT and M45mutRHIM viruses (MOI of 5) on RIP3^{+/+} (left panel), RIP3^{+/-} (middle panel), and RIP3^{-/-} (right panel) MEFs over a 72 h time course. Viral titers were determined by plaque assay with the first (0 h) time point representing the amount of virus in the inoculum. (F) IB analysis for FLAG-tagged proteins as well as β -actin (left panel) in RIP3^{-/-} MEFs expressing FLAG-tagged RIP3, RIP3-KD, or RIP3-mRHIM and viability of reconstituted cells (right panel) infected with M45mutRHIM and WT virus. (G) Viability of RIP3^{+/+}, RIP3^{+/-}, and RIP3^{-/-} MEFs infected with WT or M45mutRHIM virus in the presence or absence of Nec-1 (30 μ M). (H) Viability of RIP3^{+/+} and RIP3^{-/-} MEFs treated to induce necroptosis as described in Figure 2H in the presence or absence of Nec-1 (30 μ M). (I) IB analysis for RIP1 as well as β -actin (top panel) and viability (bottom panel) of WT (RIP3^{+/+}) MEFs stably expressing Sc, RIP1-A or RIP1-B shRNAs. Cell viability was determined for cells infected with WT or either of two independent isolates of M45mutRHIM virus. (J) IB analysis (top panel) and viability (bottom panel) of SVEC4-10 cells using a subset of conditions applied in (I). Error bars indicate SD of the mean. See also the related Figure 2.S3.

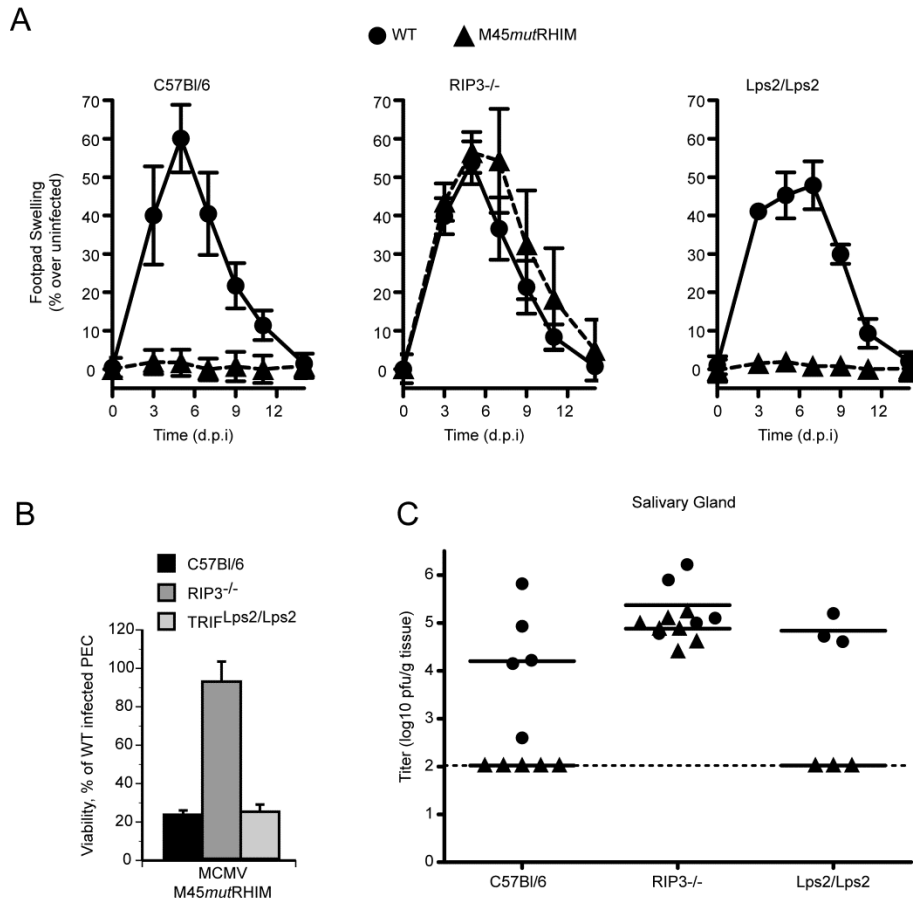


Figure 2.5. M45mutRHIM attenuation *in vivo* is specifically normalized in RIP3-deficient mice.

(A) Swelling induced by WT or M45mutRHIM virus infection of C57BL/6 (RIP3+/+), RIP3^{-/-}, and TRIF-deficient (Lps2/Lps2) mice. Groups of five (C57BL/6 and RIP3^{-/-}) or three (Lps2/Lps2) mice were inoculated (10^6 pfu) in footpads, and thickness was measured with a digital caliper (Saederup et al., 2001), and mean values were plotted at the indicated times over a 14 day time course. Error bars indicate standard error of the mean. (B) Viability of explanted, cultured RIP3^{-/-}, Lps2/Lps2, or C57BL/6 (WT) PECs at 18 hpi with either WT or M45mutRHIM. Error bars indicate SD of the mean. (C) Salivary glands were harvested from euthanized mice (described in A) and titers determined by plaque assay. Each symbol represents one mouse, and solid

(Figure 2.4 continued) horizontal lines represent the mean for each group. Dotted line is the limit of detection in this assay.

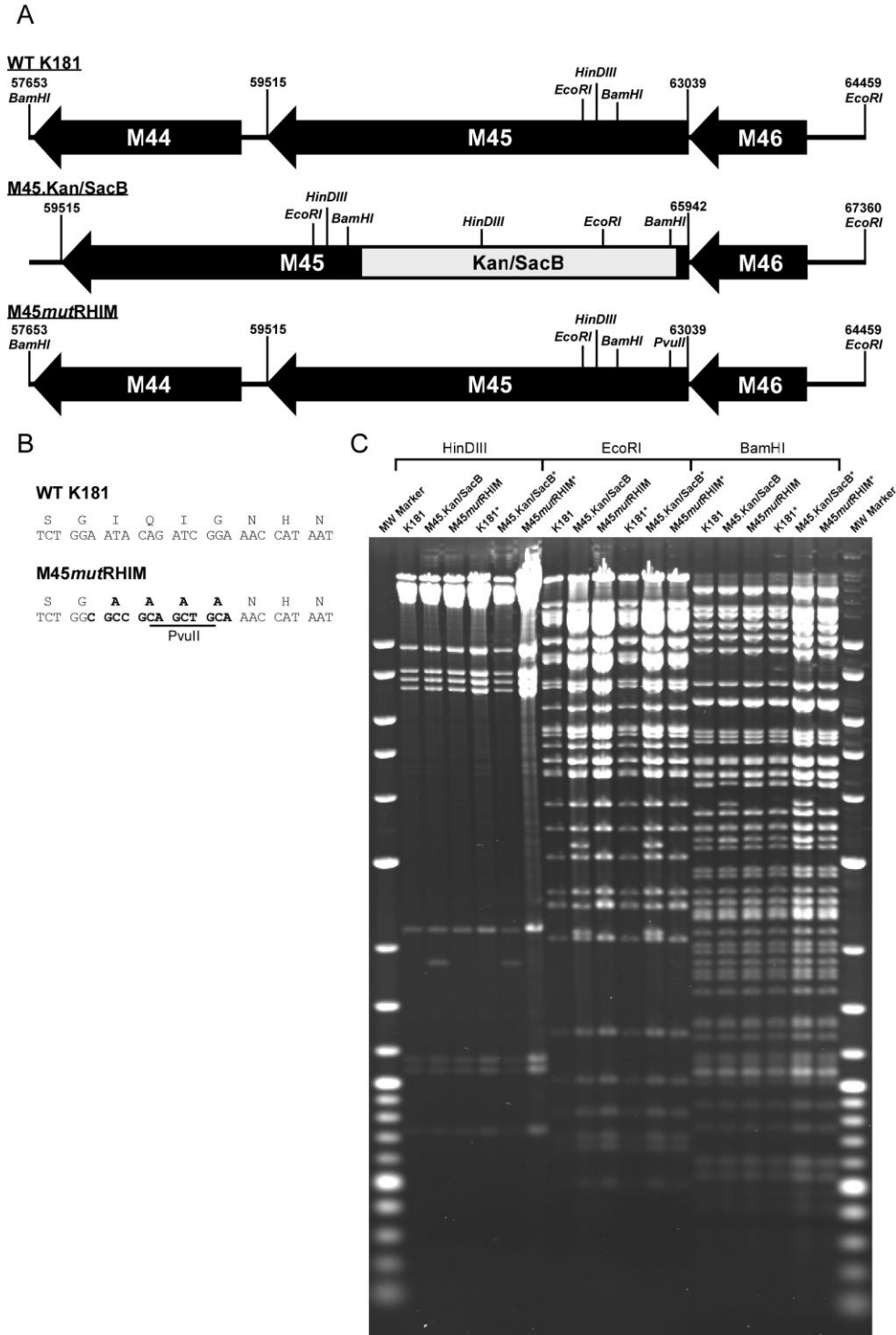


Figure 2S1. Relates to Figure 2.1. Generation of mutant MCMV viruses. (A) Schematic representation of MCMV region encoding M45 (vIRA) and surrounding genes from bp 57653 to 64459 based on the K181 sequence (Accession# AM886412.1). The M45 ORF is encoded on the

(Figure 2S1 continued) complementary strand from bp 63039 to 59515. Restriction enzyme sites shown were used for mutagenesis and/or diagnostics. Black arrows represent annotated ORFs. (B) Partial nucleotide and amino acid sequences of parental WT and mutant M45. Bold letters represent nucleotide changes. Underlined sequence represents introduced restriction enzyme site for mutant diagnostics. (C) Parental WT and mutant BAC DNAs were isolated from bacteria and subjected to restriction enzyme digest with indicated enzyme. WT and WT* are independently isolated parental WT K181-MCMV bacmids individually used to derive M45sB/K or M45sB/K*, and M45mutRHIM or M45mutRHIM*, respectively. MW Marker, 2-Log Ladder (New England Biolabs).

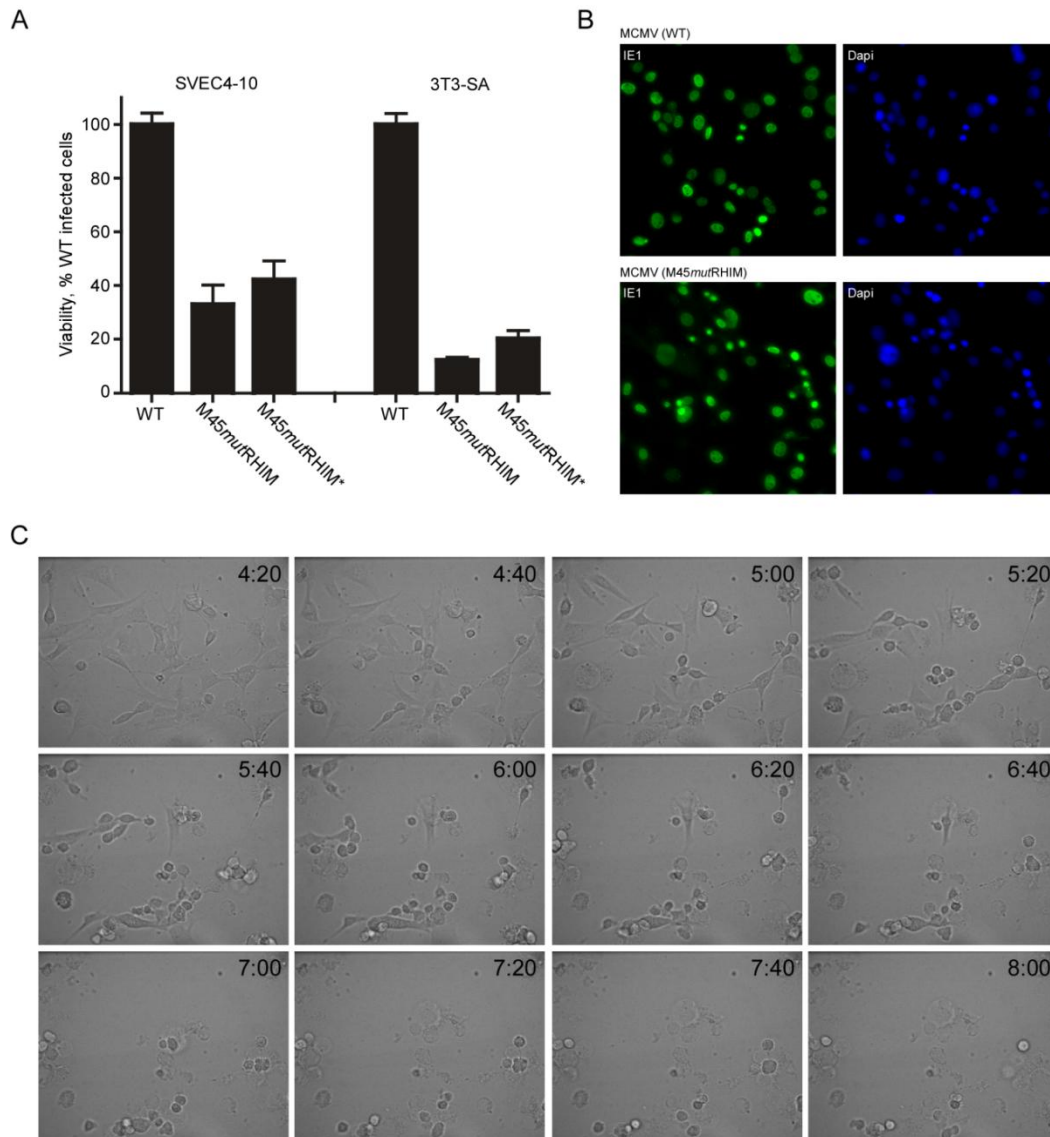


Figure 2.S2. Relates to Figure 2.2. Cell death induced by M45mutRHIM. (A) SVEC4-10 or 3T3-SA cells were infected with the indicated virus, where the asterisk indicates an independent isolate of M45mutRHIM. Viability was assessed by measuring intracellular ATP levels at 18 hpi. (B) 3T3-SA cells are highly permissive to parental WT and M45mutRHIM virus. Microphotographs of IE1 positive cells at 6 h post infection with the indicated virus. (C) 3T3-SA cells were infected with M45mutRHIM. The time (h:mm) post infection an image was captured is shown in the right corner of each image. For all panels, cells were infected at an MOI of 10.

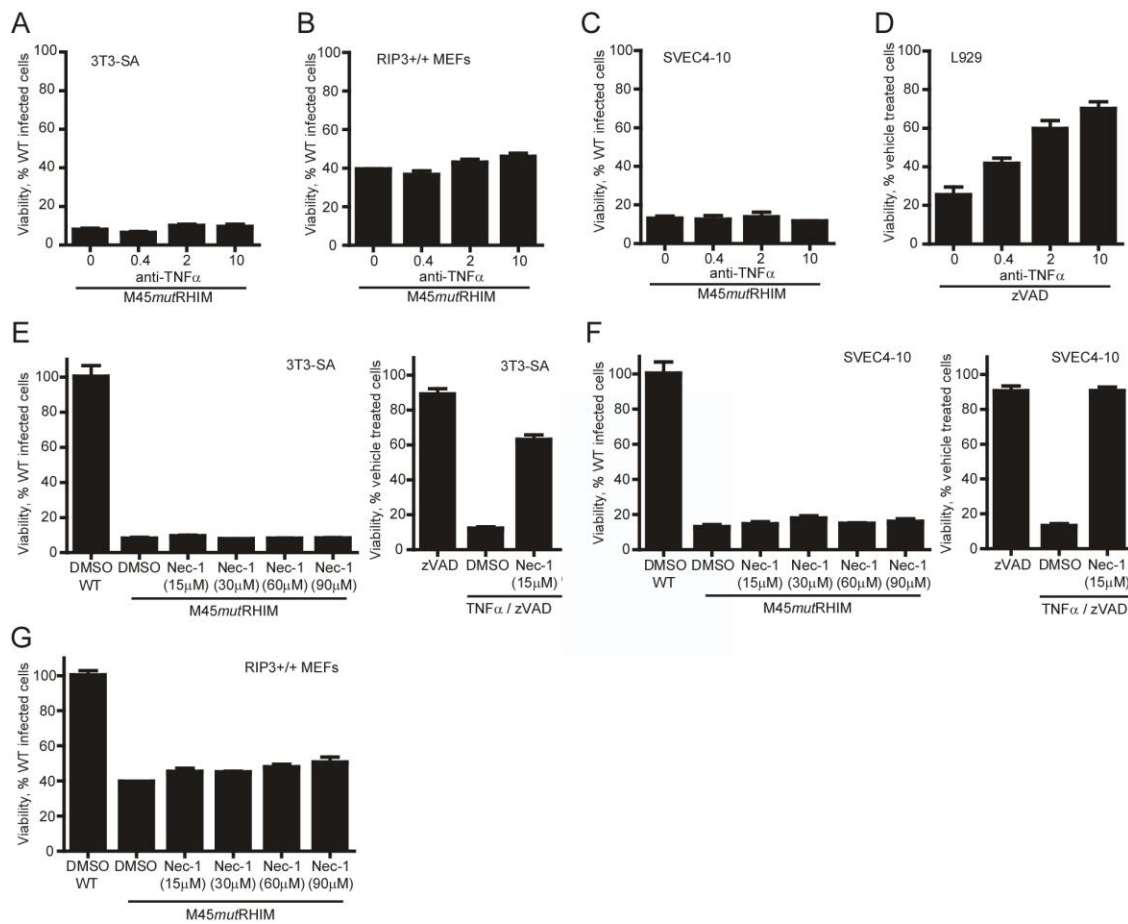


Figure S3. Relates to Figure 4. Nec-1 does not block virus-induced necrosis. (A-D) Anti-TNF α neutralizing antibody blocks DR-induced necroptosis induced by zVAD-fmk but not MCMV-associated programmed necrosis. 3T3-SA (A), SVEC4-10 (B), RIP3^{+/+} MEFs (C) were infected with parental WT or M45mutRHIM virus (MOI of 10) for 18 h. L929 (D) cells were treated with zVAD-fmk (25 mM) for 18 h. Cells were pretreated with the indicated concentration of mouse anti-TNF α antibody at the indicated concentration. Antibody levels were maintained until cell viability was determined. (E-G) Necrostatin-1 blocks TNF α -induced necroptosis but not MCMV-associated programmed necrosis. 3T3-SA (E) or SVEC4-10 (F) cells were infected (left panels) with parental WT or M45mutRHIM virus (MOI of 10) for 18 h in the absence or presence

(Figure 2.S3 continued) increasing concentrations of Nec-1, or treated (right panels) with TNF α (25 ng/ml) and zVAD-fmk (25 mM) for 18 h in the presence or absence of Nec-1. (G) RIP3 $^{+/+}$ MEFs were infected with parental WT or M45*mut*RHIM virus (MOI of 10) for 18 h in the absence or presence increasing concentrations of Nec-1. The concentration of the Nec-1 vehicle, DMSO, was identical for all samples assayed. Cell viability was determined by measuring ATP levels.

Chapter 3. RIP3 mediates the embryonic lethality of caspase-8-deficient mice³

Kaiser WJ[†], Upton JW, Long AB, Livingston-Rosanoff D, Daley LP, Hakem R, Caspary T, Mocarski ES. (2011) RIP3 mediates the embryonic lethality of caspase-8-deficient mice. **Nature**. 471(7338): 368-72.

[†]corresponding author

A. INTRODUCTION AND SUMMARY

Apoptosis and necroptosis are complementary pathways controlled by common signaling adaptors, kinases and proteases; among these, caspase-8 (Casp8) is critical for death receptor (DR)-induced apoptosis. This caspase has also been implicated in nonapoptotic pathways that regulate Fas-associated via death domain (FADD)-dependent signaling and other less defined biological processes as diverse as innate immune signaling and myeloid or lymphoid differentiation patterns (Strasser et al., 2009). Casp8 suppresses RIP3/RIP1 kinase complex-dependent (Cho et al., 2009; He et al., 2009; Zhang et al., 2009) necroptosis (Holler et al., 2000) that follows DR-activation as well as a RIP3-dependent, RIP1-independent necrotic pathway that has emerged as a host defense mechanism against murine cytomegalovirus (MCMV) (Upton et al., 2010). Disruption of *Casp8* expression leads to embryonic lethality in mice between E10.5 and E11.5 (Varfolomeev et al., 1998). Thus, Casp8 may naturally hold alternative RIP3-dependent death pathways in check in addition to its role promoting apoptosis. We find that RIP3 is responsible for the midgestational death of Casp8-deficient embryos. Remarkably, *Casp8*^{-/-}/*Rip3*^{-/-} double mutant mice are viable and mature into fertile adults with a full immune complement of myeloid and lymphoid cell types. These mice appear immunocompetent but develop lymphadenopathy by four months of age marked by accumulation of abnormal T cells in

³ This chapter derives from a published paper entitled “RIP3 mediates the embryonic lethality of caspase-8-deficient mice” (Kaiser et al. 2011). Sections of this chapter have been reproduced in whole, or in part, with permission from the publisher.

the periphery, a phenotype reminiscent of mice with Fas-deficiency (*lpr/lpr*). Casp8 contributes to homeostatic control in the adult immune system; however, RIP3 and Casp8 are together completely dispensable for mammalian development.

B) RESULTS AND DISCUSSION

To determine whether Casp8 can hold RIP3 kinase-dependent death (Chan et al., 2003; Cho et al., 2009; He et al., 2009; Holler et al., 2000; Zhang et al., 2009) in check, we employed murine L929 cells, a system that requires continued Casp8 expression for cell survival (Yu et al., 2004). Inhibition of Casp8 with either siRNA (Figure 3.S1a) or zVAD-fmk (Figure 3.S1c) induced death, as expected from prior studies (Yu et al., 2004). When treated with RIP3-specific shRNA, however, L929 cells were protected from death (Figure. 3.S1a), consistent with this being a RIP3-dependent necrotic death pathway. The MCMV M45 gene-encoded viral inhibitor of RIP activation (vIRA) blocks RIP3-dependent necrotic death (Upton et al., 2010). In keeping with the importance of a RIP3/RIP1 complex in necroptosis (Cho et al., 2009; He et al., 2009; Zhang et al., 2009), vIRA blocked death whereas a tetra-alanine RHIM substitution mutant, *M45mutRHIM* (Upton et al., 2010) failed to suppress death induced by either Casp8 siRNA or zVAD (Figures. 3.S1b and d). Necrostatin-1 was employed to demonstrate that RIP1 kinase activity was necessary for necroptosis (Figure 3.S1c). The specific viral inhibitor of Casp8 activation (vICA) encoded by the MCMV M36 gene (McCormick et al., 2003) also induced this death pathway (Figure 3.S1e and f). These data demonstrate that L929 cells succumb to RIP3-dependent necrotic death when Casp8 is inactive or eliminated.

Disruption of *Casp8* expression leads to embryonic lethality in mice between E10.5 and E11.5, coincident with embryonic vascular, cardiac and hematopoietic defects (Kang et al., 2004; Kang et al., 2008; Sakamaki et al., 2002; Varfolomeev et al., 1998); however, the molecular mechanisms behind these defects remain poorly defined (Kang et al., 2004; Kang et al., 2008; Sakamaki et al., 2002; Varfolomeev et al., 1998). To evaluate the potential contribution of RIP3

to embryonic lethality, we examined wild-type and *Casp8*^{-/-} embryos as well as extra-embryonic tissues for *Rip3* expression. Based on *in situ* hybridization, *Rip3* transcript levels increased and tissue distribution broadened as embryonic development proceeded from E9.5 to E12.5 in both genotypes, indicating *Rip3* transcript is not regulated by *Casp8* (Figure 3.1a and data not shown). At E9.5, *Rip3* was prominent in the apical ectodermal ridge (AER) of the hind-limb bud and the tail bud, and expanded to include the fore-limb bud AER, midline of the spinal cord, branchial arches and intersomitic regions by E10.5 through E12.5 (Figure 3.1a, and data not shown), a signal that was absent from RIP3-deficient E10.5 embryos (Figure 3.1b). Additionally, RIP3 was readily detected by immunoblot (IB) in E10.5 embryo and yolk sac cell lysates (data not shown). Mice homozygous for disruption of exons 3 and 4 in *Casp8* (Salmena et al., 2003) died by E11.5 and presented with heart defects, hyperemia in the abdominal region, and undulation of the neural tube (Figure 3.1c and Figure 3.2a) consistent with prior studies that used alternative targeting strategies to disrupt *Casp8* (Kang et al., 2004; Sakamaki et al., 2002; Varfolomeev et al., 1998).

The yolk sac is the initial site of hematopoiesis prior to the transfer of function to intraembryonic sites. The most dramatic impact of *Casp8* disruption, either in embryonic tissues or in the yolk sac, is the disruption of endothelial cell organization leading to circulatory failure in the yolk sac, the likely culprit behind embryonic lethality (Kang et al., 2004; Sakamaki et al., 2002). When we employed PECAM-specific antibody to localize endothelial cells in *Casp8*-deficient embryos (E10.5), we observed the expected contrast between an organized yolk sac vascular pattern in control mice and a disrupted pattern in *Casp8*-deficient mice (Fig. 1d). These observations affirmed the disruption of vascular development in *Casp8* null embryos. RIP3 was also detected in the yolk sac endothelium of both *Casp8*^{+/-}*Rip3*^{+/-} and *Casp8*^{-/-}*Rip3*^{+/-} embryos at this time (Figure 3.S2b); thus, RIP3 was present in the cell populations most widely implicated in

embryonic death of *Casp8*-deficient mice independent of *Casp8* expression. *Casp8* deficiency is also known to compromise primitive hematopoietic progenitor cell (HPC) development (Varfolomeev et al., 1998), a process dependent upon CD41⁺ cells populating yolk sac blood islands and fetal sites (Mitjavila-Garcia et al., 2002). RIP3 was detected in CD41⁺ cells in the yolk sac blood islands of embryos (Fig. 3.1e and Figure 3.S2c). The striking CD41⁺ cell fragmentation in the yolk sac blood islands of *Casp8*^{-/-}*Rip3*^{+/-} embryos at E10.5 further implicates this kinase in processes leading to embryonic death.

To establish the role of the RIP3 kinase in embryonic lethality of *Casp8*-deficient mice, we generated double knock out (DKO) *Casp8*^{-/-}*Rip3*^{-/-} embryos by a *Casp8*^{+/-}*Rip3*^{+/-} intercross. In contrast to *Casp8*^{-/-}*Rip3*^{+/-} embryos, which were developmentally arrested at ~E11.0, DKO embryos were indistinguishable from *Casp8*^{+/-}*Rip3*^{-/-} or *Casp8*^{+/-}*Rip3*^{+/-} embryos at E12.5 and later times, had a functioning heart and organized yolk sac endothelial architecture, and, remarkably, exhibited HPC colony formation at levels comparable to wild-type mice (Figure 1f and g, Figure 3.S2d and data not shown). The apparent normalization of the *Casp8*-deficient phenotype by removal of RIP3 suggested that this kinase was responsible for the ~E11.0 embryonic block, so we permitted the intercross pregnancies to complete gestation. PCR analysis performed on tissues from weanling mice confirmed deletion of *Casp8* exons 3-4 as well as deletion of *Rip3* in both alleles (Figure 3.S3a). We detected RIP1, Casp8 and RIP3 in spleen and thymus from wild-type mice examined by IB (Figure 3.2a). *Casp8*^{+/+}*Rip3*^{-/-}, *Casp8*^{+/-}*Rip3*^{-/-}, and DKO mice all lacked RIP3 but retained unaltered RIP1 levels in tissues. Casp8 was absent from DKO mice but present in other intercross progeny with predicted Mendelian frequencies (Figure 3.2b). As expected, Casp8-deficient, RIP3-expressing progeny were not seen. Furthermore, when bred, adult DKO mice gave birth to viable mice that survived through adulthood and appeared similar to *Casp8*^{+/-}*Rip3*^{-/-} mice bred in parallel (Figure 3.S3b). Prior studies showed that conditional deletion of *Casp8* in

epidermis promoted perinatal lethality characterized by chronic inflammation (Kovalenko et al., 2009; Lee et al., 2009). DKO mice did not exhibit any evidence of skin inflammation when followed for more than six months, indicating that RIP3 must have played a proinflammatory role in the absence of epithelial Casp8 in prior studies. These results further indicate that embryonic lethality as well as a range of vascular degeneration and neural tube defects, together with hematopoietic abnormalities and chronic inflammation seen in mice lacking Casp8 are all RIP3-dependent.

To verify the functional elimination of *Casp8* in cells derived from DKO animals, we evaluated susceptibility to inducers of DR-mediated apoptosis. Although *Casp8* plays an essential role in macrophage differentiation (Kang et al., 2004), DKO mice produced CD11b⁺F4/80⁺ bone marrow-derived mononuclear (BMDM) cells just as readily as controls, and these cells lacked detectable RIP3 or Casp8 (Figure 3.3a and b). Thus, the requirement for Casp8 during macrophage differentiation is suppressed by RIP3-deficiency. Macrophages prepared from wild-type, *Casp8*^{+/+}*Rip3*^{-/-} and *Casp8*^{+/-}*Rip3*^{-/-} mice died when exposed to reagents promoting Fas activation whereas DKO cells were completely resistant, consistent with the established role of this caspase in DR-induced apoptosis. In the presence of the caspase inhibitor zVAD-fmk, Fas activation promoted RIP3-dependent necroptosis in RIP3-containing BMDM cells (Figure 3.3c). Furthermore, cells expressing RIP3 were susceptible to necroptosis, whereas *Rip3* knock-out and DKO mice remained resistant to this death pathway. Thus, DKO cells were insensitive to either extrinsic DR-induced apoptosis or RIP3-dependent necroptosis, consistent with their genotype. Previously, conditional knock-out of *Casp8* in the liver revealed its essential role in TNF or Fas-induced fatal hepatitis (Kang et al., 2004; Kaufmann et al., 2009). DKO mice were resistant to anti-Fas-antibody treatment, survived for over 48 hours (Fig. 3d) and showed normal liver architecture (Figure 3.3e), although they exhibited slightly elevated levels of the

liver-associated transaminases ALT (alanine aminotransferase) and AST (aspartate aminotransferase) (data not shown). In contrast, *Casp8^{+/-}Rip3^{-/-}* littermate control mice developed hepatitis (Figure 3.3d and 3e). DKO mice were also resistant to administration of LPS in combination with the liver-specific transcriptional inhibitor D-(+) galactosamine (GalN), which induces a TNF-dependent fatal liver hepatitis in both wild-type (Kaufmann et al., 2009) and *Casp8^{+/-}RIP3^{-/-}* mice (Figure 3.S4). This resistance was comparable to the negative control TRIF-deficient mice (Hoebe et al., 2003) (Figure 3.S4).

Although RIP3 is dispensable for myeloid and lymphoid development (Newton et al., 2004), *Casp8* is essential for generation of both myeloid and lymphoid lineages (Beisner et al., 2005; Kang et al., 2004; Salmena and Hakem, 2005; Salmena et al., 2003). To determine whether this essential role of *Casp8* was due to dysregulation of RIP3, we evaluated the characteristics of leukocytes from the thymus, bone marrow, spleen, and lymph node (LN) of DKO mice, littermate *Casp8^{+/-}Rip3^{-/-}* and wild-type mice (Figure 3.4a) by FACS analysis, detecting the presence of myeloid and lymphoid populations in all three genotypes based on forward (size) and side (granularity) light scatter properties (data not shown) in combination with surface markers. We observed inflammatory monocytes (CD11b⁺Ly6C^{hi}) and polymorphonuclear leukocytes (CD11b⁺Ly6C^{int}) in the bone marrow and spleen (Figure 3.4a) of wild-type and DKO mice. Based on CD11c and F4/80 expression, dendritic cells and macrophages, respectively, populated the same tissues of DKO and *Casp8^{+/-}Rip3^{-/-}* littermate controls (data not shown). Thus, myeloid cell populations continued to be generated in the absence of RIP3 and *Casp8*, consistent with the successful derivation of BMDM cells from DKO mice (see Figure 3.3). NK (CD49b⁺CD3⁻), NKT (CD49b⁺CD3⁺) and B (CD19⁺) lymphocytes, including predominant IgD⁺ as well as less prevalent IgD⁻ B cells (data not shown) were present in all tissues examined (Figure 3.4a).

Defects in the Fas (CD95)-death receptor pathway promote the accumulation and expansion of lymphocytes and the development of autoimmune lymphoproliferative syndromes (ALPS) (Bidere et al., 2006). Caspase-8 is downstream of Fas, and similarly DKO mice exhibited pronounced splenomegaly and lymphadenopathy over the first few months of age (Figure 3.S5a, 5b, and 5c). Adult DKO mouse spleens ranged from three to seven times the size of *Casp8^{+/-}Rip3^{-/-}* littermate controls (Figure 3.4b and Figure 3.S5b and 5c) and contained more lymphoid cells in splenic white pulp (data not shown). Histological examination revealed lymphocytic infiltrates in the salivary glands, pancreas, and lamina propria of both stomach and small intestine (data not shown). Consistent with size, DKO mice had significantly greater numbers of leukocytes in secondary lymphoid tissues such as spleen (Figure 3.S5d) that appeared to result from abnormally high levels of CD3⁺ T cells and to a lesser degree CD19⁺ B cells (Figure 3.S5e). Whereas these characteristics are consistent with the known role of Casp8 in DR-associated hematopoietic homeostasis (Bidere et al., 2006), they contrast the characteristics of mice with Casp8 deficient T cells, where there are fewer T cells than B cells in secondary lymphoid tissues (Salmena and Hakem, 2005; Salmena et al., 2003). Thus, there was a dramatic accumulation of T cells that contributed to lymphadenopathy and splenomegaly as DKO mice aged.

Casp8 deficient T cells exhibit defects in the response to antigens and mitogens (Ch'en et al., 2008; Salmena et al., 2003). To compare T cell activation in DKO and *Casp8^{+/-}Rip3^{-/-}* littermate controls, we evaluated the sensitivity of bulk splenocytes from mock and MCMV-infected mice, to anti-CD3 and anti-CD28 treatment. In contrast to prior observations on Casp8-deficient T cells (Ch'en et al., 2008; Salmena et al., 2003), this treatment induced a response in mock-infected DKO cells and this response was enhanced at 7 days post MCMV infection. In fact, the CD8 T cells from DKO mice responded with an increased frequency in bifunctional INF γ ⁺TNF⁺ cells (Figure 3.S4c). Furthermore, DKO mice survived a dose of virus that is lethal to

immunocompromised *scid/scid* mice and controlled viral replication levels for 30 days similar to *Casp8^{-/-}Rip3^{-/-}* littermate controls (data not shown). Although more characterization is required to fully understand the quality of the immune response in DKO mice, T cell receptor-dependent activation of naïve and enhanced activation of antigen-exposed T cells is clearly retained despite the combined disruption of *Casp8* and *Rip3*.

Fas-deficient (*lpr/lpr*) mice are marked by the accumulation in the periphery of the CD3⁺ T cells that are B220⁺ but lack CD4 and CD8; these cells have been ascribed to a failure of apoptosis (Laouar and Ezine, 1994). DKO mice had normal CD4 and CD8 T cell populations in the thymus (Figure 3.S5f), but contained this signature B220⁺ T cell population in secondary lymphoid organs (Fig. 4d and Figure 3.S5g). Interestingly, conditional deletion of *Casp8* in T cells, while resulting in lymphadenopathy did not result in the emergence of this signature phenotype (Salmena and Hakem, 2005), suggesting that RIP3-dependent necroptosis eliminates T cells where *Casp8* is absent or nonfunctional. Thus, Fas DR-induced death pathways is essential for immune homeostasis and in the absence of both *Casp8* and RIP3, excess unusual T cells likely accumulate due to a failure of both apoptosis and necroptosis.

The data presented here point to RIP3 as the vital target of *Casp8* during mammalian development, with *Casp8* functioning during embryogenesis to restrict RIP3 rather than to mediate apoptosis. We speculate that the RIP3-dependent pathway controlled by *Casp8* during embryogenesis, as well as later in life, is related to known necrotic pathways controlled by this kinase. Eliminating this RIP3-dependent embryonic death in combination with *Casp8*-deficiency results in the accumulation of abnormal T cells starting in the first few months of age but does not lead to defects at other developmental stages. *Casp8* may have other nonapoptotic roles such as influencing cell motility and proliferation; however one key role of *Casp8* is its essential

nonapoptotic function to control RIP3. FADD promotes Casp8 activation within the death-inducing signaling complex (DISC), a process subject to regulation by cFLIP. Deletion of FADD, cFLIP or Casp8 in all tissues causes a common pattern of vascular and hematopoietic defects associated with embryonic lethality in mice around E10.5 (Strasser et al., 2009), suggesting the coordinate control of RIP3 by these three players during development. The signals controlling activation of Casp8 and/or RIP3 during embryogenesis remain to be identified. Nevertheless, therapeutic strategies targeting DISC components aimed at apoptosis will need to take into account the likely triggering of RIP3-dependent pathways. Upon combined elimination of Casp8 and RIP3, defects in DR-dependent lymphocyte differentiation and homeostasis emerge. The discovery that Casp8 suppresses RIP3 pathways and is essential for maintenance of the vasculature, hematopoiesis, suppression of the innate immune system and T cell function points to the unexpected importance of these pathways in humans and other mammals. The observation here that Casp8 is a gatekeeper, suppressing RIP3 during development in addition to promoting apoptosis mediated via death receptors, promises to have broad implications in approaches to cancer therapy and regenerative medicine as well as during elaboration of the innate and adaptive phases of the immune response.

C) MATERIALS AND METHODS

Mice. *RIP3*^{-/-} mice have been described previously (Newton et al., 2004). TRIF mutant (Strain - C57BL/6J-Ticam1^{Lps2}) (Hoebe et al., 2003) mice were from Jackson Laboratory. *Casp8*^{+/-} mice were generated by crossing *Casp8*^{fl3-4/wt} (Salmena et al., 2003) with Rosa-CreER mice (Ventura et al., 2007). *Rip3*^{-/-} and *Casp8*^{+/-} were subsequently intercrossed. PCR genotyping of *Casp8*^{-/-} mice was performed with primers 5'-TTGAGAACAAGACCTGGGGACTG and 5'-GGATGTCCAGGAAAAGATTTGTGTC. PCR amplification allele produces a 750-bp band (wild-type *Casp8*), or a 200 bp band (*Casp*^{Δ3-4} allele produces). Genotyping of *Rip3*^{-/-} mice was performed with the primers 5'-CGCTTTAGAAGCC TTCAGGTTGAC, 5'-GCAGGCTCTGGTGACAAGATTCATGG, and 5'-CCAGAGGCCACTTGTGTAGCG. PCR produces a 700 bp band (wild-type *Rip3* allele) or a 450 bp band (*Rip3* deletion allele). Mice were bred and maintained by Emory University Division of Animal Resources where all procedures were approved by the Emory University Institutional Animal Care and Use Committee.

Cell culture, plasmids, transfections and transductions. L929 were maintained in DMEM containing 4.5 g/mL glucose, 10% FBS (Atlanta Biologicals), 2 mM L-glutamine, 100 U/mL penicillin and 100 U/mL streptomycin (Invitrogen). For BMDM culture, pooled bone marrow cells from flushed tibias and femurs of indicated animals were differentiated for 5 to 7 days in DMEM containing 20% serum and 20% filtered L929 medium containing macrophage colony-stimulating factor (M-CSF). Cells were harvested with PBS containing 0.5 mM EDTA, seeded at a density of 3 X 10⁴ cells per well in a 96-well plate, and then cultured at least 18 h in DMEM containing 10% FBS prior to stimulation. Transient transfections were performed using Lipofectamine 2000 according to the manufacturer's protocol (Invitrogen). Plasmid encoding an amino-terminal Flag-epitope tagged M36 was generated by inserting M36 amplified from K181

strain MCMV genomic DNA into pQCXIH (Clontech). The pLKO.1 based RIP3 (TRCN0000022535) shRNA (CCGGCCTCAGATTCCACATACTTTACTCGAGTAAAGTATGTGGAATCT GAGGTTTTT) construct were obtained from Open Biosystems. The pLKO.1-Scramble control shRNA (CCTAAGGTTAAGTCGCCCTCGCTCGAGCGAGG GCGACTTAACCTTAGG) vector (Sarbasov et al., 2005) and all other plasmids have been described (Kaiser and Offermann, 2005; Kaiser et al., 2008; Upton et al., 2010). Lentiviral and retroviral production, infection, and selection of transduced cells have all been described previously (Kaiser et al., 2008). Inhibition of Caspase-8 expression in L929 cells employed murine Caspase-8 SMARTpool (L043044-00-0005) Dharmacon siRNAs consisting of GUGAAUGGAACCUUGUAUA, GUCACGGACUUCAGACAAA, GAAGAUCGAGGAUUAUGAA, and AGAGUUGUCUUUAUGCUAU, in comparison to OnTarget Plus Non-Targeting Pool (D-001810-10) siRNA Control. L929 cells seeded on 96-well plates were transfected with 4 pmol of siRNA with Lipofectamine 2000 according to the manufacture's protocol.

Immunoblot and immunoprecipitations. Immunoblotting, preparation of protein extracts, and immunoprecipitations were as previously described (Kaiser and Offermann, 2005). The following antibodies were used in IB analyses: mouse anti- β -actin (clone AC-74; Sigma), mouse anti-RIP1 (clone 38; BD Biosciences), rabbit anti-RIP3 (Imgenex), rat anti-Caspase-8 (clone 1G12; Axxora), anti-mouse IgG-HRP (Vector Laboratories), anti-rabbit IgG-HRP (Vector Laboratories), and anti-rat IgG-HRP (Jackson Laboratories).

Cell viability assays. Viability of L929 cells (5000 cells/well) or BMDM (30,000 cells/well) seeded into 96-well plates was determined 96 h post transfection of siRNAs, 12 h post transfection of plasmids, or as indicated in the text. Where indicated, cells were stimulated in the presence of CHX (5 μ g/mL) (Sigma). Nec-1 and z-VAD-fmk were from Calbiochem and Enzo Life Sciences, respectively. Cell viability was determined indirectly by measuring the intracellular

levels of ATP using the Cell Titer-Glo Luminescent Cell Viability Assay kit (Promega) according to the manufacturer's instructions and was graphed relative to control cultures. Luminescence was measured on a Synergy HT Multi-Detection Microplate Reader (BioTek). To determine the number of surviving GFP positive cells, cells were transfected with pMaxGFP (Amara Biosystems) and analyzed at 48 h post-transfection on an LSRII (BD Biosciences) using FlowJo software (Tree Star).

***In situ* hybridization.** Whole-mount *in situ* hybridization was performed as described (Belo et al., 1997). Digoxigenin-labeled antisense RNA probes were transcribed from linearized RIP3 encoding plasmid (accession number BC029210, ATCC) according to the manufacturer's directions (Roche). For the hybridization results shown, the probe was synthesized from plasmid linearized with BamHI. A second RIP3 *in situ* hybridization probe revealed a similar pattern of RIP3 expression (data not shown).

Flow cytometry. Single cell suspensions were prepared from spleen, lymph nodes and thymus by mechanical disruption through a metal strainer. Bone marrow cells were isolated by flushing femurs with RPMI supplemented with 10% FBS, penicillin, streptomycin and 50 μ M β -mercaptoethanol. Red blood cells were lysed using ammonium chloride solution (0.15 M NH_4Cl , 10 mM NaHCO_3 , and 1.0mM Na_2EDTA in H_2O , pH 7.4). Cells were resuspended in FACS staining buffer (PBS containing 0.2% BSA and 0.09% sodium azide), filtered through 40 μ m screens and viable cells were enumerated using trypan blue exclusion. In all instances 1×10^6 cells were prepared for flow cytometric analysis of surface antigens. Cells were incubated with 10% normal rat serum (Pel-Freez) and anti-mouse CD16/CD32 (2.4G2; BD Pharmingen) to reduce non-specific antibody interactions prior to incubating with lineage specific antibodies. For T cell stimulation with anti-CD3 and anti-CD28 (BD Biosciences), splenocytes were incubated for 5 h in

the presence of GolgiPlug (BD Biosciences) and subsequently evaluated for intracellular cytokine production using the Cytofix/Cytoperm kit (BD Biosciences) according to manufacturer's instructions and staining for intracellular cytokines IFN γ -FITC (clone XMG1.2 from BD) and TNF α -PE-Cy7 (clone MP6-XT22 from BD). The antibodies used were: Ly6C FITC (AL-21), B220 FITC (RA3-6B2), IgD PE (11-26c), CD19 PerCP-Cy5.5 (1D3), CD25 PerCP-Cy5.5 (PC61.5), CD11b APC-Cy7 (M1/70) and CD3 Pacific Blue (500A2), purchased from BD Biosciences; CD4 PE (GK1.5) and CD49b APC (DX5) purchased from eBioscience; CD62L PE-Cy7 (MEL-14) CD8 APC (53-6.7), and CD44 APC-Cy7 (IM7) purchased from BioLegend; and CD45 PE-Texas Red (30-F11) and F4/80 Pacific Orange (BM8) purchased from Invitrogen. Data were acquired using an LSRII flow cytometer (BD Biosciences) and analyzed with FlowJo software. All statistical analyses were unpaired Student's t tests using Prism (GraphPad Software).

Immunofluorescence microscopy. Yolk sacs were harvested and fixed for 2 h using 4% paraformaldehyde (Electron Microscopy Sciences) in PBS. Cells were permeabilized for 45 min in 0.25% Triton X-100 (Sigma) in PBS, blocked for 1 h in PBS containing 2% goat serum, and incubated 2 h at RT with rabbit polyclonal RIP3 antibody (Imgenex) along with PECAM Rat IgG2a (clone MEC 13.3; BD Biosciences) or FITC conjugated CD41 Rat IgG1a (clone MwReg30; BD Biosciences) diluted in blocking buffer. Yolk sacs were washed multiple times with PBS and then incubated for 1 h at RT with Alexa Fluor 488 (or 594) goat anti-rabbit/rat antibody and Alexa Fluor 594 (or 488) goat anti-rabbit/rat antibody (Invitrogen). 4',6-diamidino-2-phenylindole (DAPI, Sigma) was used as a nuclear (DNA) counter stain. Following multiple washes with PBS, cells were mounted with Gel Mount (Biomedica). Images were acquired on a Carl-Zeiss LSM 510 META confocal fluorescence microscope.

DR-induced hepatitis. Fatal hepatitis was induced by intraperitoneal injection of with 12.5 µg of anti-mouse Fas antibody (clone Jo2, BD Biosciences) or for LPS+GalN induced hepatitis, mice were injected intraperitoneally with 100 ng of ultrapure LPS K12 (InvivoGen) in the presence of 20 mg of the liver-specific transcriptional inhibitor D-(+)-galactosamine (GalN, SIGMA). The organs evaluated for histology were fixed in 10% neutral buffered formalin prior to paraffin embedding, processing and staining for H&E. Tissue processing and staining was performed by Emory University's Division of Animal Resources (DAR).

MCMV Infections. Mice were inoculated by i.p. (intraperitoneal) injection with 10^6 pfu salivary gland derived v70 strain of MCMV (a kind gift of C. Biron, Brown University, Providence, RI). Salivary gland viral stock was generated by sonicating submaxillary glands of 8 wk old BALB/c mice infected with 1×10^3 pfu of v70 strain of MCMV at 14 days post infection.

HPC progenitor assay. For yolk sac-derived clonogenic progenitor assays, single cell suspensions were prepared from E10.5/E11.5 yolk sacs in 2 ml of medium (M3434; StemCell Technologies). Cells were grown for 12 days at 37°C in 5% CO₂ in the absence or presence of 30 µM Nec-1. Colonies were scored by microscopic analysis.

D) FIGURES AND LEGENDS

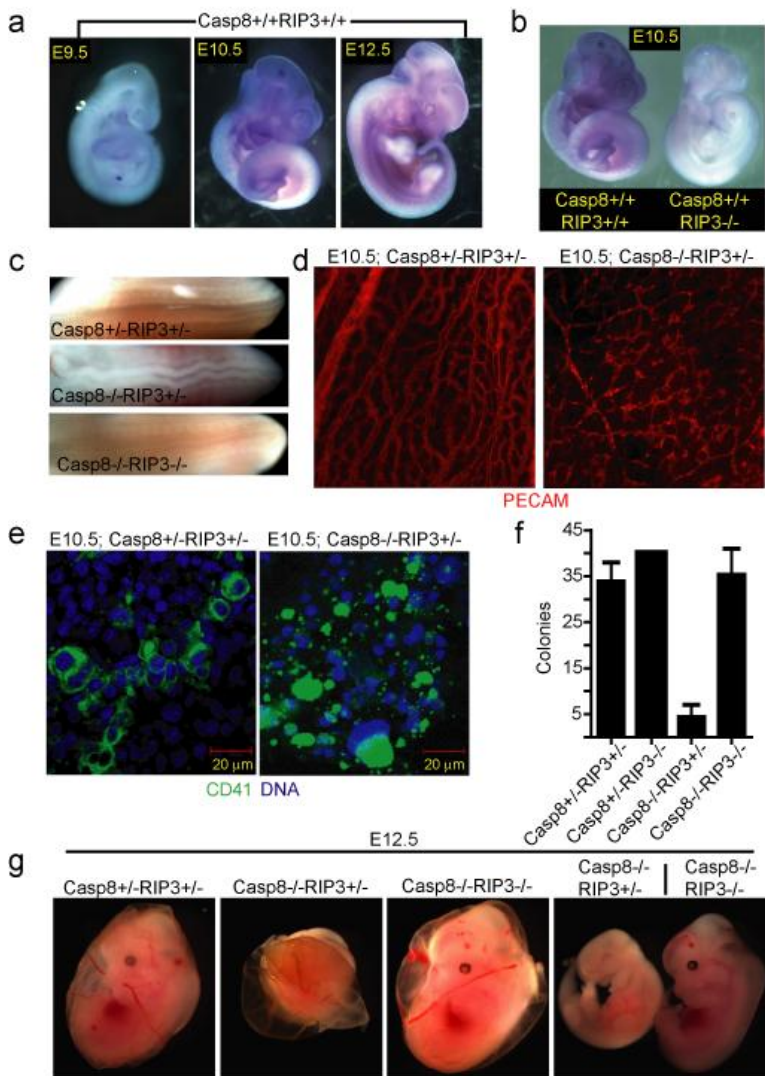


Figure 3.1. Embryonic expression of *Rip3*. (a) Whole-mount *Rip3* *in situ* hybridization of *Casp8*^{+/+}*Rip3*^{+/+} E9.5 (left panel), E10.5 (middle panel), and E12.5 (right panel) embryos. (b) Whole-mount *Rip3* *in situ* hybridization of *Casp8*^{+/+}*Rip3*^{+/+} and *Casp8*^{+/+}*Rip3*^{-/-} E10.5 embryos demonstrating specificity of the probe. (c) View of the neural tube of E11.5 embryos with the indicated genotype. (d) PECAM-1 (CD31) staining of a whole-mount E10.5 yolk sac from a representative *Casp8*^{+/-}*Rip3*^{+/-} (left panel) and *Casp8*^{-/-}*Rip3*^{+/-} (right panel) embryo (100X). (e)

(Figure 3.1 continued) CD41 (green) and nuclear DNA (blue) staining of a yolk sac from a E10.5 *Casp8^{+/-}Rip3^{+/-}* (left panel) and a *Casp8^{-/-}Rip3^{+/-}* (right panel) embryo. **(f)** Average number of colony-forming cells (CFC) following culture of disrupted E10.5 yolk sacs of the indicated genotype. Error bars, SD (n = 3). **(g)** Photographs of E12.5 embryos and yolk sacs with the indicated genotype. The right panel shows side by side embryos with yolk sacs removed.

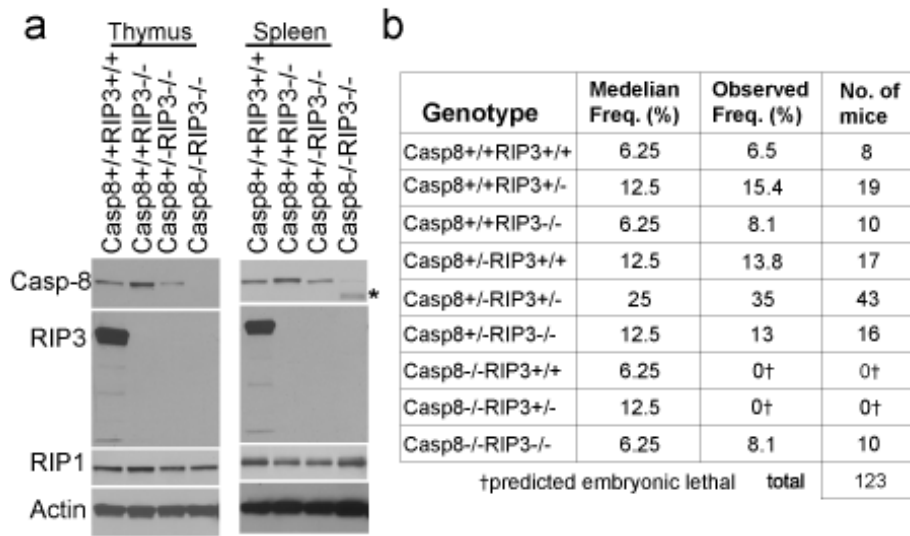


Figure 3.2. *Casp8^{-/-}Rip3^{-/-}* mice are viable. (a) IB of Casp8, RIP3, RIP1 and β -actin from thymus (left panel) and spleen (right panel). The asterisk denotes elevated heavy IgG heavy chain reactive with secondary antibody in DKO sample. (b) Epistatic analysis of mice born following *Casp8^{+/+}Rip3^{+/+}* intercross with predicted and observed frequencies.

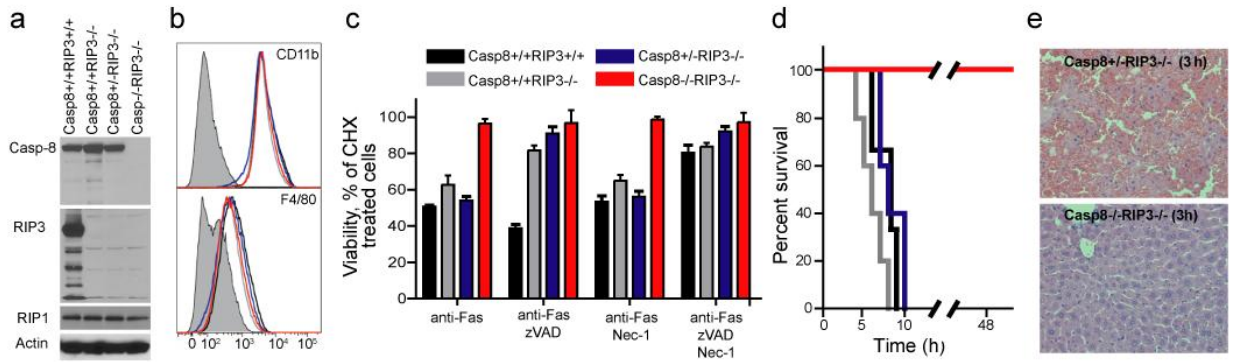


Figure 3.3. Sensitivity to DR-induced apoptosis, necroptosis and disease. (a) IB of Casp8, RIP3, RIP1 and β -actin in BMDM derived from mice with the indicated genotype. **(b)** Relative cell surface expression levels of CD11b (top panel) or F4/80 (bottom panel) shown by red line (DKO), black line (*Casp8^{+/+}Rip3^{+/+}*), grey line (*Casp8^{+/+}Rip3^{-/-}*), or blue line (*Casp8^{-/-}Rip3^{-/-}*) on BMDM stained cells. Isotype control is shown by shaded histogram. **(c)** Viability of BMDM cultured in CHX (5 μ g/mL) and treated with anti-Fas antibody for 18 h in the presence or absence of the caspase inhibitor zVAD-fmk (25 μ M) and/or Nec-1 (30 μ M). Cell viability was determined by measuring intracellular ATP levels with a Cell Titer-Glo Luminescent Cell Viability Assay kit. Error bars, SD. (n = 4). **(d)** Kaplan-Meier survival plot of 12 week old *Casp8^{+/+}Rip3^{+/+}* (n = 3), *Casp8^{+/+}Rip3^{-/-}* (n = 5), *Casp8^{-/-}Rip3^{-/-}* (n = 5), and DKO (n = 5) mice injected intraperitoneally with 12.5 μ g of anti-Fas Jo-2 antibody; n, numbers of mice analyzed. Legend genotypes and line color is the same as in (c). **(e)** Histology of liver sections from *Casp8^{+/+}Rip3^{-/-}* (left panel) and *Casp8^{-/-}Rip3^{-/-}* mice (right panel) 3 h following injection with Jo-2 antibody.

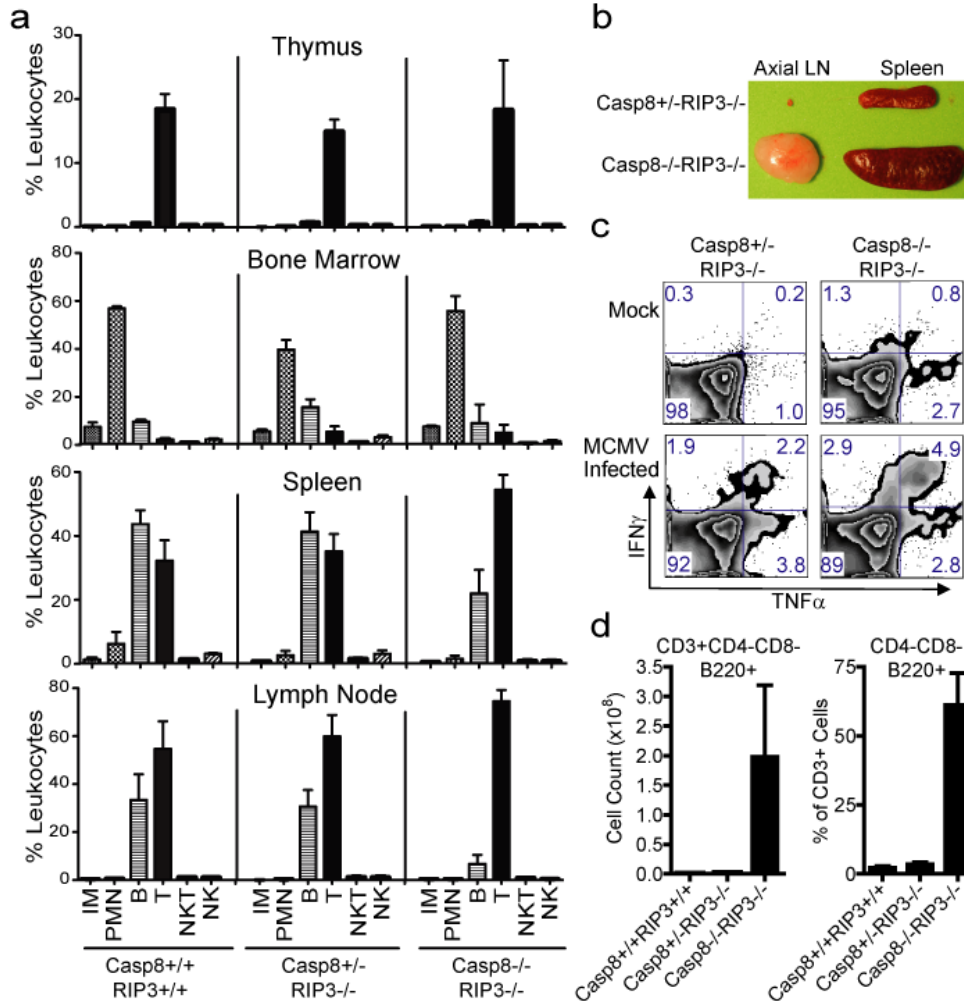


Figure 3.4. Immune compartment of 16-week-old DKO mice. (a) Live cells from thymus (top panels), bone marrow (second set of panels), spleen (third set of panels) and LN (bottom panels), gated based on forward and side scatter properties, and stained for surface expression of CD19, CD3, CD49b, Ly6C and CD11b to define non-overlapping leukocyte (CD45⁺) populations. The average and SD for three wild-type (left panels), four *Casp8^{+/-}RIP3^{-/-}* (middle panels) littermate control and three DKO (right panels) mice showing levels of inflammatory monocytes (IM), polymorphonuclear leukocytes (PMN), B cells, T cells, NK cells and NKT cells. **(b)** Photograph of the axial LN and spleen from representative mice of the indicated genotype. **(c)** Flow cytometric analysis of IFN γ and TNF α on T cells from naïve or MCMV-infected (7 days) mice

(Figure 3.4 continued) following stimulation with CD3/CD28 antibodies. CD8⁺ T cells from one representative animal per experimental group are shown. **(d)** B220 expression was assessed on CD4⁻CD8⁻ splenic T cells. Error bars, SD for three wild-type, four *Casp8*^{+/-}*RIP3*^{-/-} littermate control and three DKO mice.

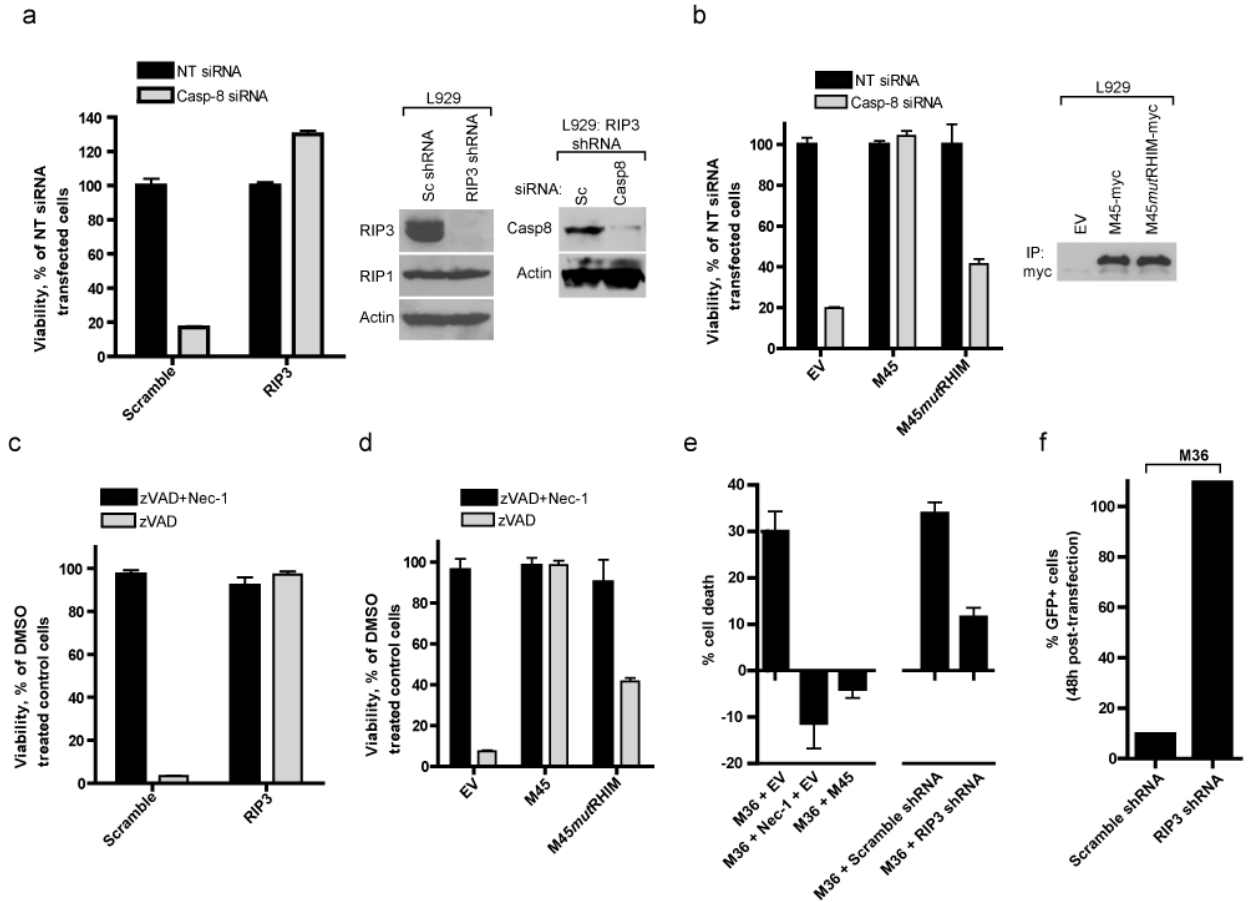


Figure 3.S1. Casp8 suppresses programmed necrosis. (a) Viability (left) and RIP3, RIP1, Casp8, and β -actin immunoblots (right) of L929 cells expressing a control scramble shRNA or RIP3-specific shRNA following transfection with non-targeting (NT) or Casp8-specific siRNA. Cell viability was determined 96 h post-transfection by measuring intracellular ATP levels (Cell Titer-Glo Luminescent Cell Viability Assay kit, Promega). **(b)** Viability (left) and M45 immunoblot (right) of L929 cells transduced with empty vector (EV), M45-myc, or M45mutRHIM-myc at 96 h post-transfection with NT or Casp8 siRNA. **(c)** Viability of L929 cells expressing a control scramble shRNA or RIP3-specific shRNA following treatment for 18 h with zVAD-fmk (25 μ M) in the absence or presence of the RIP1 kinase inhibitor Nec-1 (30 μ M). **(d)** Viability of L929 cells transduced with empty vector (EV), M45-myc, or M45mutRHIM-myc following treatment as

(Figure 3.S1 continued) described in c. **(e)** Percent cell death, calculated as the difference between the indicated treatment and the EV-transfected cell viability, in L929 cells expressing an EV or M45-myc (left), or control scramble shRNA or RIP3-specific shRNA (right), constructs at 96 h post-transfection with plasmid encoding M36 and cultured in the presence of Nec-1 (30 μ M) or vehicle DMSO for 12 h. Viability assays (a-e) represent the mean and SD from three independent measurements. **(f)** L929 cells carrying a control scramble shRNA or RIP3-specific shRNA following cotransfection with M36 or EV control plasmids together with a GFP expression plasmid. The percent GFP positive cells for a representative sample was calculated by comparing to control EV-transfected cells determined by flow cytometry at 48 h post-transfection.

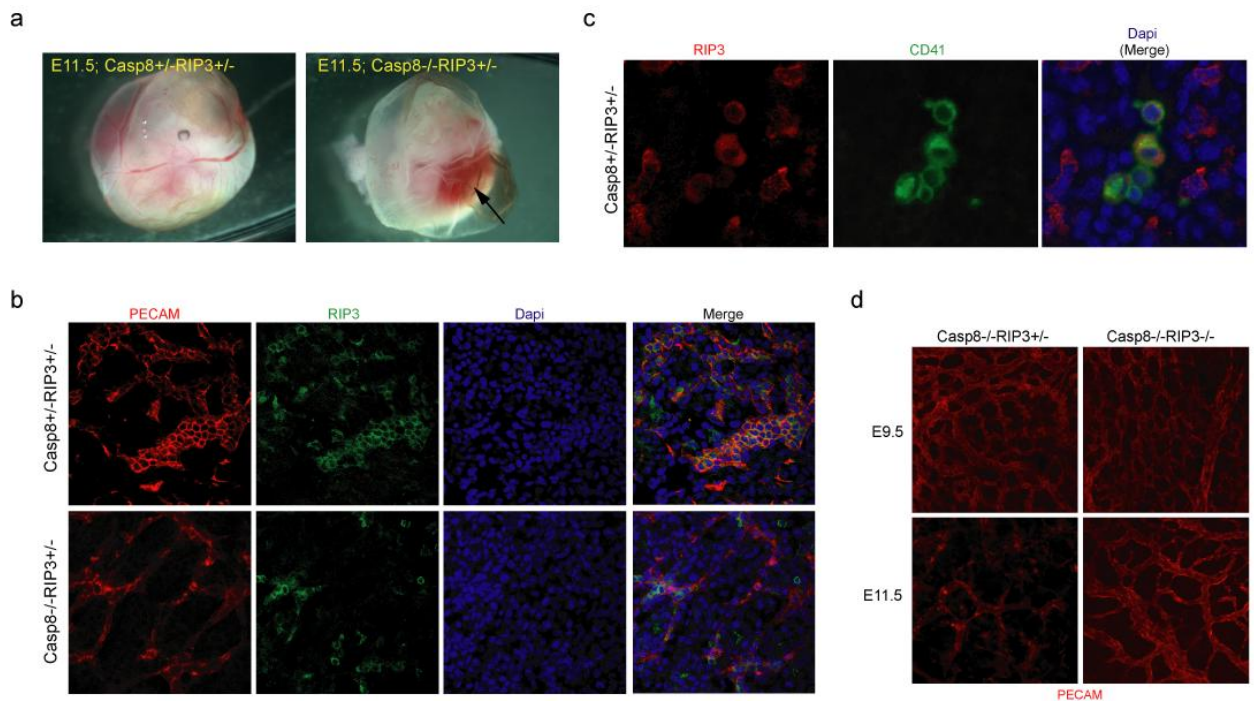
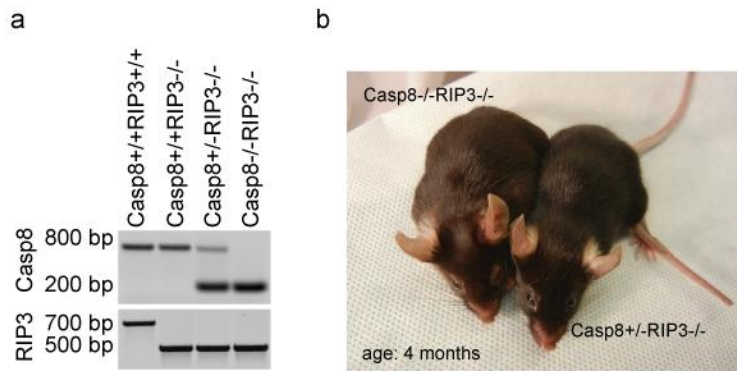


Figure 3.S2. Embryonic lethality and RIP3 detection in Casp8-deficient mice. (a)

Photomicrographs of E11.5 yolk sac and embryo with the indicated genotype, highlighting the region of hyperemia (arrow in right panel). **(b)** PECAM (red), RIP3 (green) and DAPI (blue) fluorescent staining of representative *Casp8*^{+/-}*Rip3*^{+/-} and *Casp8*^{-/-}*Rip3*^{+/-} E10.5 yolk sacs (400X original magnification). **(c)** RIP3 (red), CD41 (green) and DAPI (blue) fluorescent staining of representative *Casp8*^{+/-}*Rip3*^{+/-} yolk sacs (630X original magnification). **(d)** PECAM-1 (CD31) staining of a whole-mount E9.5 and E11.5 yolk sac from a representative *Casp8*^{-/-}*Rip3*^{+/-} (left panels) and *Casp8*^{-/-}*Rip3*^{-/-} (right panels) embryo (200X).



Supplementary Figure 3. *Casp8^{-/-}Rip3^{-/-}* mice are viable. (a) PCR confirmation of genotype on tail DNA from the indicated *Casp8^{+/+}Rip3^{+/+}* intercross progeny to detect wild-type (upper bands) and mutant (lower bands) *Casp8* and *Rip3* alleles. **(b)** Photograph of 4-month-old *Casp8^{-/-}Rip3^{-/-}* mouse bred from a DKO cross alongside a *Casp8^{+/-}Rip3^{-/-}* mice bred from an intercross.

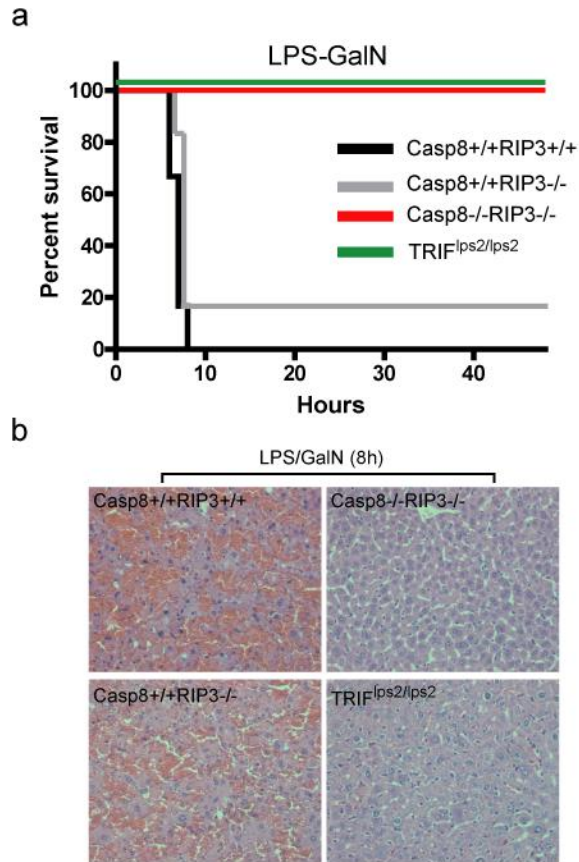


Figure 3.S4. Susceptibility to LPS+GalN induced hepatitis in *Casp8^{+/+}Rip3^{+/+}*, *Casp8^{+/+}Rip3^{-/-}*, *Casp8^{-/-}Rip3^{-/-}* and control TRIF-deficient (*lps2/lps2*) mice. (a) Kaplan-Meier survival plot of indicated strains of mice following intraperitoneal inoculation with LPS (100 ng) and GalN (20 mg). 6 animals per *Casp8^{+/+}Rip3^{+/+}* genotype and 5 animals per *Casp8^{-/-}Rip3^{-/-}*, *Casp8^{+/+}Rip3^{-/-}*, and TRIF^{*lps2/lps2*} genotype were analyzed. (b) Histology of liver sections from indicated strains of mice 8h following injection with LPS/GalN.

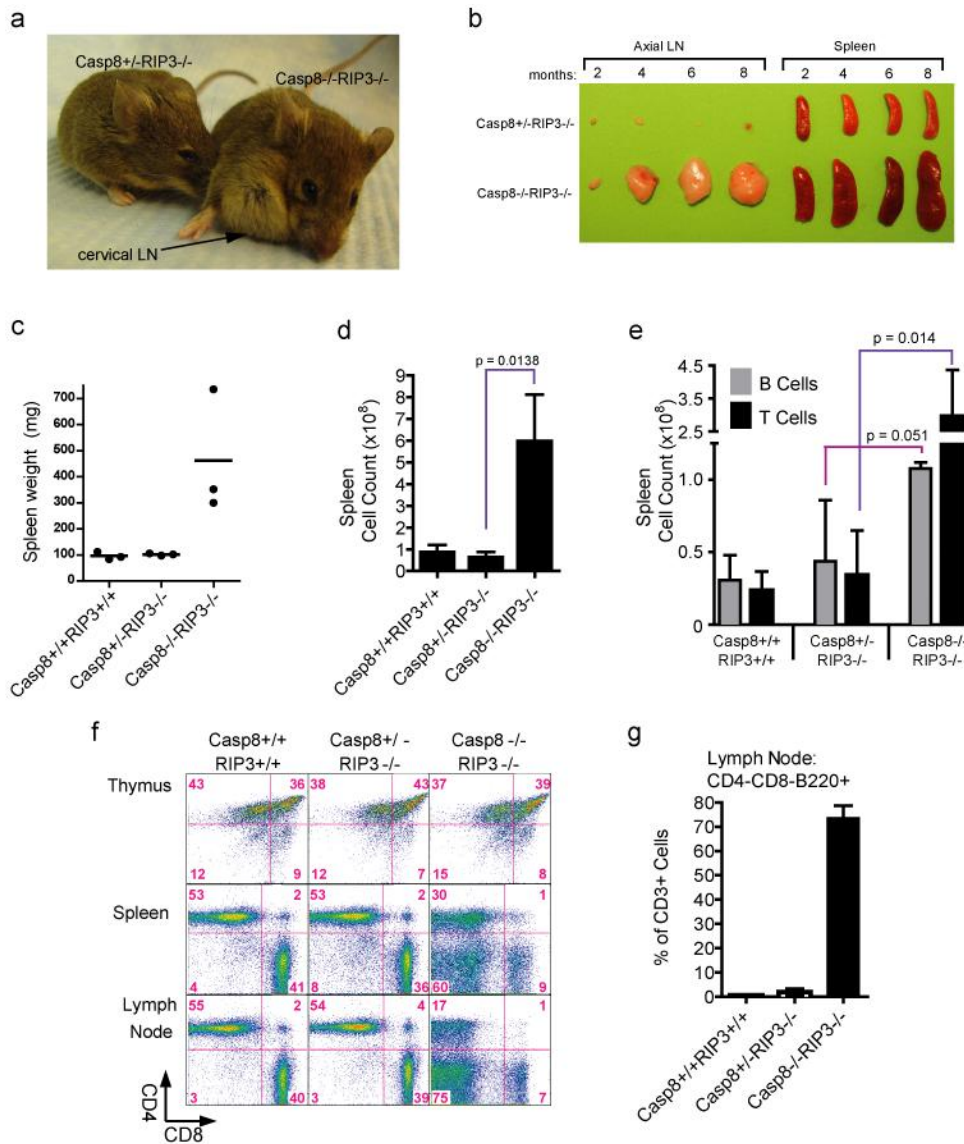


Figure 3.S5. DKO mice accumulate aberrant T-cells. **(a)** Photographs of six-month-old *Casp8*^{+/-}*Rip3*^{-/-} and *Casp8*^{-/-}*Rip3*^{-/-} mice. The arrow indicates enlarged cervical LN present in the DKO mouse. **(b)** Images of spleen and axial LNs from *Casp8*^{+/-}*Rip3*^{-/-} and *Casp8*^{-/-}*Rip3*^{-/-} mice of the indicated ages. **(c)** Graph of weights of spleen from mice of the indicated genotype. Horizontal lines represent the mean. **(d)** The numbers of cells and **(e)** numbers of B and T cells recovered from spleens from mice with the indicated genotype. Statistical analyses were performed

(Figure 3.S5 continued) applying a two-tailed unpaired Student's *t*-test. **(f)** CD4 vs. CD8 expression of CD3⁺ T cells in spleen (top panels), LN (middle panels) and thymus (bottom panels) identified as in C, in representative wild-type (left panels), *Casp8^{+/-}RIP3^{-/-}* (middle panels) and *Casp8^{-/-}RIP3^{-/-}* (right panels) mice. **(g)** Frequency (graph) and level of CD3⁺CD4⁻CD8⁻B220⁺ T cells from LN of mice. For (d), (e), and (g) the average and SD for three wild-type, four *Casp8^{+/-}RIP3^{-/-}* littermate control and three DKO mice are shown.

Chapter 4. DAI-RIP3 complex mediates virus-induced programmed necrosis⁴

Upton JU, Kaiser WJ, Mocarski ES. (2012) DAI/ZBP1/DLM-1 complexes with RIP3 to mediate virus-induced programmed necrosis that is targeted by murine cytomegalovirus vIRA. **Cell Host & Microbe**. 11(3): 290-297.

A) INTRODUCTION

Viral pathogens trigger host pattern recognition receptors (PRR) to initiate protective inflammatory and cell death responses. The activation of nuclear factor (NF)- κ B and interferon (IFN) response factor (IRF)3 leads to an IFN response that is subject to viral subversion (Bowie and Unterholzner, 2008; Rahman and McFadden, 2011; Versteeg and Garcia-Sastre, 2010). Apoptotic or necrotic programmed cell death may be triggered to cut short viral infection, and is subjected to pathogen-encoded suppression (Best, 2008; Galluzzi et al., 2008; Lamkanfi and Dixit, 2010). Apoptosis may be triggered through cell-intrinsic and cell-extrinsic signals and follows a caspase-dependent pathway long recognized for shaping embryonic development as well as for maintaining tissue homeostasis and defending against infection (Hengartner, 2000; Strasser et al., 2000). Recent insights have shown programmed necrotic cell death to be an important alternate pathway involved in host defense (Cho et al., 2009; Upton et al., 2010). The cellular protein kinase RIP3 plays a central role in transducing signals that drive programmed necrosis (Mocarski, 2012), whether induced through death receptor (DR) activation (Cho et al., 2009; He et al., 2009; Upton et al., 2010; Zhang et al., 2009), during embryonic development in the absence of caspase 8 (Kaiser et al., 2011; Oberst et al., 2011) or in the course of viral infection (Upton et al., 2010). DR-induced programmed necrosis, also called necroptosis,

⁴ This chapter derives from a published paper entitled “DAI/ZBP/DLM-1 complexes with RIP3 to mediate virus induced programmed necrosis that is targeted by murine cytomegalovirus” (Upton et. al. 2012). Sections of this chapter have been reproduced in whole, or in part, with permission from the publisher.

requires the formation of a RHIM-dependent RIP1-RIP3 complex (necrosome) as well as the protein kinase activity of both RIP1 and RIP3 (Cho et al., 2009; He et al., 2009; Upton et al., 2010; Zhang et al., 2009). Importantly, when DR activation fails to initiate apoptosis because caspase 8 activity is compromised, RIP3-dependent necrosis becomes the dominant programmed death pathway. Embryonic lethality in the face of caspase 8 or FADD deficiency also involves the release of a RIP1-RIP3 complex from caspase 8 regulation (Kaiser et al., 2011; Zhang et al., 2011b). Murine cytomegalovirus (MCMV)-induced programmed necrosis requires RIP3 kinase activity and RHIM-dependent interactions; however, neither RIP1 nor TRIF is required (Upton et al., 2010).

MCMV-encoded viral inhibitor of RIP activation (vIRA), the product of the M45 gene, is a potent cell death suppressor (Brune et al., 2001; Mack et al., 2008; Upton et al., 2008) that is expressed by the virus to prevent RIP3-dependent, RIP1-independent programmed necrosis during infection (Upton et al., 2010). vIRA specifically blocks RHIM-dependent interactions leading to apoptosis, programmed necrosis and NF- κ B activation. When transiently expressed, vIRA is sufficient to inhibit DR- or TRIF-dependent Toll-like receptor (TLR)3 induced apoptosis, necroptosis (Mack et al., 2008; Upton et al., 2008, 2010), and virus-induced programmed necrosis (Mack et al., 2008; Upton et al., 2008, 2010). vIRA also blocks NF- κ B activation and RIP3 auto-phosphorylation induced by overexpression of DAI (Rebsamen et al., 2009). Although vIRA was initially implicated as a cell tropism determinant (Brune et al., 2001), this cell death suppressor plays a crucial, natural role in preventing rapid RIP3-dependent necrosis over the initial 8 to 12 h of infection independent of cell type (Upton et al., 2008, 2010). Importantly, viruses lacking vIRA, or carrying a tetra-alanine RHIM substitution mutation are severely attenuated in immunocompetent as well as immunodeficient strains of mice (Lembo et al., 2004; Upton et al., 2010). The tetra-alanine RHIM mutant *M45mutRHIM* virus has provided key

insights as a tool to study necrosis, both as an isolated gene product and in the context of viral infection. The importance of programmed necrosis in host defense was effectively demonstrated by complete normalization of vIRA RHIM mutant virus replication and pathogenesis in RIP3-deficient mice (Upton et al., 2010). MCMV vIRA thereby illuminated a novel death RHIM-dependent pathway that functions alongside apoptosis in mammalian host defense (Mocarski, 2012).

Although DR-induced necroptosis relies on a RIP1-RIP3 signaling complex, virus-induced necrosis depends on RIP3 RHIM-dependent signaling that is independent of RIP1 and TRIF (Upton et al., 2008, 2010). Observations that RIP3 and DAI form a RHIM-dependent complex to mediate NF- κ B activation under overexpression conditions (Kaiser et al., 2008) raise the possibility that DAI and RIP3 mediate virus-induced necrosis if they interact under physiological conditions. RIP3, in particular, is not implicated in NF- κ B activation in natural settings (Newton et al., 2004). DAI is expressed constitutively in many mouse tissues (Fu et al., 1999), and because of its constitutive presence, was the first cellular DNA-binding protein implicated as a pathogen sensor triggering IFN β expression in response to cytosolic double stranded DNA (dsDNA) (Takaoka et al., 2007). Constitutive DAI in cultured cells responds to herpes simplex virus (HSV) infection (Furr et al., 2011; Takaoka et al., 2007) as well as human cytomegalovirus (CMV) infection (DeFilippis et al., 2010a; DeFilippis et al., 2010b). DAI, like many other PRR, is also known to be IFN-inducible (Fu et al., 1999) and, in response to HCMV infection, DAI is necessary to induce IFN β and augments its own expression (DeFilippis et al., 2010b). DAI contains two amino-terminal DNA binding motifs that coordinate DNA binding, driving oligomerization and activation of downstream signaling and IRF3-mediated gene expression (Takaoka et al., 2007; Wang et al., 2008c). Additionally, DAI contains three RHIM-like repeats, one or two of which bind RIP3 and/or RIP1 to activate NF- κ B (Kaiser et al., 2008; Rebsamen et al., 2009). Because

DAI-deficient mice produce IFN β in response to dsDNA, DAI has been considered “dispensable for both innate and adaptive immune responses to B-DNA and DNA vaccine” (Ishii et al., 2008), leaving the natural function of DAI to be resolved. Given the observed impact of RIP3-dependent necrosis during MCMV infection, together with the acknowledged potential for a RHIM-dependent complex between RIP3 and DAI (Kaiser et al., 2008), we unveiled the role of DAI as the RIP3 partner mediating virus-induced necrosis.

B) RESULTS

RIP3 levels differentially confer susceptibility to necroptosis and virus-induced

necrosis. Our previous investigation showed that RIP3 is a mediator of virus-induced programmed necrosis as well as the direct target of vIRA during infection (Upton et al., 2010). When used to investigate necroptosis or virus-induced necrosis, murine cell lines have scored as either sensitive (3T3-SA, SVEC4-10) or resistant (NIH3T3) depending on the level of RIP3 expressed (Upton et al., 2010; Zhang et al., 2009). Normal murine embryonic fibroblasts (MEFs) are sensitive, and RIP3^{-/-} MEFs are resistant to both pathways. Reintroduction of WT RIP3, but not RHIM-mutant (RIP3mRHIM) into RIP3^{-/-} MEFs was shown to be sufficient to sensitize these cells to virus-induced necrosis (Upton et al., 2010). To extend these findings to a naturally resistant cell type, NIH3T3 cells were stably transduced with retroviruses expressing FLAG-epitope tagged WT RIP3, RIP3mRHIM, or vector control (Figure 4.1A). Following selection, each stable cell line was assessed for sensitivity to programmed necrosis by infection with the vIRA deficient MCMV M45*mut*RHIM or treatment with TNF together with the caspase inhibitor, zVAD-fmk. NIH3T3 stable cells with elevated levels of either WT or mutant RIP3 remained insensitive to virus-induced necrosis (Figure 1B). In contrast, WT RIP3, but not RIP3mRHIM, sensitized NIH3T3 cells to TNF-induced necroptosis (Figure 4.1C). Thus, RIP3 levels are not the sole limiting determinant of virus-induced necrosis given that over-expression of this protein kinase does not sensitize NIH3T3 cells to this death pathway under conditions where they are sensitive to RIP1-RIP3 necroptosis. Necroptosis and virus-induced necrosis are both RIP3 RHIM-dependent processes where necroptosis requires RHIM-dependent association of RIP1 and RIP3 (Cho et al., 2009; He et al., 2009; Upton et al., 2010; Zhang et al., 2009). Virus-induced necrosis requires RHIM-dependent function of RIP3 independent of RIP1. In addition, a recently

elaborated TLR3-induced necroptosis involves RIP1 as well as RIP3 together with RHIM-dependent interactions mediated by TRIF (Feoktistova et al., 2011; He et al., 2011). Given the fact that neither RIP1 nor TRIF contribute to the viral death pathway (Upton et al., 2010), we turned attention to DAI, a constitutively expressed RHIM-containing adaptor implicated as a DNA sensor leading to NF- κ B as well as IRF3 activation (Kaiser et al., 2008; Rebsamen et al., 2009; Takaoka and Taniguchi, 2007; Takaoka et al., 2007).

IFN β and NF- κ B signaling in necroptosis and virus-induced necrosis. We found that constitutive levels of DAI expression correlate with sensitivity to virus-induced programmed necrosis. DAI was present in necrosis-sensitive 3T3-SA and SVEC4-10 cells, but was absent in necrosis-resistant NIH3T3 cells (Figure 1D-E). As expected (Upton et al., 2010), RIP3 levels were higher in necroptosis-susceptible cells and lower in NIH3T3 cells (Figure 4.1A), while RIP1 was present in all cell lines. Thus, both DAI and RIP3 were present in cells exhibiting sensitivity to virus-induced necrosis.

Previous work has shown that DAI is both constitutively expressed and IFN-inducible (Fu et al., 1999), necessary for herpesvirus-induced IFN β production (DeFilippis et al., 2010b; Furr et al., 2011; Takaoka et al., 2007), and able to activate NF- κ B when overexpressed (Kaiser et al., 2008). Given that infection may induce IFN β in a DAI-dependent manner, we evaluated whether NIH3T3 cells upregulate DAI following MCMV infection and compared these patterns to induction by IFN β treatment (Figure 4.S1A). Importantly, DAI remained undetectable throughout infection in NIH3T3 cells. IFN β treatment, as expected (Fu et al., 1999), induced this protein within 9 h. Levels of DAI in 3T3-SA or SVEC4-10 cells (data not shown) increased from 9 to 24 h after MCMV infection or IFN β treatment. Thus, NIH3T3 cells do not upregulate DAI during infection even though they respond to IFN β treatment. These results are consistent with

a role for DAI as an inducer of the IFN-response to herpesviruses (DeFilippis et al., 2010a; DeFilippis et al., 2010b; Furr et al., 2011; Takaoka et al., 2007) and indicate DAI is a constitutive component of the host cell machinery that governs the response to MCMV infection. The same level of IFN β mRNA is induced in SVEC4-10 cells by WT MCMV and vIRA-deficient MCMV Δ 45 (Brune et al., 2001) (Figure 4.S1B), indicating induction of IFN β is independent of vIRA as well as conditions where cell death is induced by vIRA-deficient virus (Brune et al., 2001; Upton et al., 2008, 2010). Furthermore, DAI protein is induced to comparable levels in WT and M45*mut*RHIM MCMV-infected MEFs (Figure 4.S1C). Despite the upregulation of IFN β and DAI expression during infection with parental or vIRA-mutant virus, treatment of SVEC4-10 cells with increasing concentrations of IFN β -neutralizing antibody does not influence virus-induced programmed necrosis (Figure 4.S1D), indicating type I IFNs induced by MCMV infection, whether via DAI or additional pathogen sensing pathways, are not involved in the virus-induced necrosis pathway.

In addition to IFN, DAI has been implicated as an inducer of NF- κ B activation (Kaiser et al., 2008; Takaoka et al., 2007). Canonical NF- κ B signaling is dispensable for MCMV infection, and the virus replicates slightly better in RelA-deficient fibroblasts compared to controls (Benedict et al., 2004). Moreover, NF- κ B signaling does not influence necroptotic cell death (Irrinki et al., 2011; Vanden Berghe et al., 2006). To evaluate any role for NF- κ B signaling in virus-induced necrosis, BMS-345541, a specific inhibitor of I κ B kinase (IKK) activity was employed (Burke et al., 2003). As expected, inhibition of IKK sensitized SVEC4-10 cells to TNF-induced apoptosis (Figure 4.S1E), indicating the drug dose used here was sufficient to inhibit NF- κ B (Katdare et al., 2007; Roue et al., 2007). However, BMS-345541 treatment failed to normalize the viability of SVEC4-10 cells infected with M45*mut*RHIM MCMV (Figure 4.S1F) as would be expected if NF- κ B signaling played a dominant role in this RIP3-dependent antiviral pathway

(Upton et al., 2010). Together, these results demonstrate neither IFN β nor NF- κ B signaling is a major factor in virus-induced necrotic cell death.

Introduction of DAI sensitizes resistant cells to virus-induced programmed necrosis. To determine whether DAI confers sensitivity to virus-induced programmed necrosis, NIH3T3 cells constitutively expressing FLAG-epitope-tagged WT DAI, as well as tetra-alanine substitution RHIM mutant DAI (DAImRHIM, previously called DAImRLR-A)(Kaiser et al., 2008) and empty vector control (Figure 4.2A) were derived. WT DAI rendered NIH3T3 cells susceptible to mutant virus-induced death (Figure 4.2B), whereas, DAImRHIM did not convey susceptibility. These results were consistent with a role for RHIM-dependent interaction between DAI and RIP3 (Kaiser et al., 2008; Rebsamen et al., 2009) and showed a requirement for DAI together with RIP3 to sensitize NIH3T3 cells to death. Nec-1, a potent RIP1 kinase inhibitor (Degterev et al., 2008), specifically blocks TNF-induced necroptosis, but fails to block virus-induced programmed necrosis (Upton et al., 2010). Additionally, virus-induced necrosis is caspase-independent and does not require the action of TNF (Upton et al., 2010). The necrotic death observed in DAI-expressing NIH3T3 cells was RIP1 kinase-independent based on resistance to Nec-1 (Figure 4.2B), caspase-independent based on resistance to zVAD-fmk, and independent of DR-ligation based on resistance to TNF-neutralizing antibodies (Figure S2). These criteria are consistent with characteristics of virus-induced necrosis as established previously (Upton et al., 2010).

Given that DAI was sufficient to sensitize NIH3T3 cells to death, we sought to establish the need for RIP3. To address the role of RIP3, specific lentivirus shRNAs were employed to knockdown expression (Figure 4.2C). RIP3 was needed to confer sensitivity to virus-induced death, demonstrating the need for endogenous RIP3 in addition to DAI (Figure 4.2D). Thus DAI and RIP3 together sensitize cells to virus-induced necrotic death. The failure of DAImRHIM to

sensitize NIH3T3 cells (Figure 4.2B) complements previous observations on RHIM mutant RIP3 (Upton et al., 2010), suggesting that a RHIM-dependent RIP3-DAI complex (Kaiser et al., 2008) is involved in the death pathway. The previous demonstration that a DAI-RIP3 complex mediates NF- κ B activation (Kaiser et al., 2008) that can be inhibited by vIRA (Rebsamen et al., 2009) reinforces the possibility that this complex can be regulated by vIRA.

DAI-RIP3 complex in virus-induced programmed necrosis. To demonstrate a role of a DAI-RIP3 complex in the execution of virus-induced necrosis, we investigated the interaction between RIP3 and DAI during viral infection. Cell extracts were prepared from 3T3-SA cells infected for 12 h with mutant MCMV. RIP3 co-immunoprecipitated DAI from these cells, consistent with a physical interaction (Figure 4.3A). Expression of RIP3 (using β -actin, as a loading control) was constant, whereas levels of DAI increased with time. Levels of the nonfunctional tetra-alanine mutant protein expressed by M45mutRHIM MCMV increased between 1 and 12 hpi. When WT MCMV infection was evaluated (where WT vIRA is expressed), no DAI-RIP3 interaction could be detected (Figure 4.S3A). Given the recognized importance of RIP3 RHIM interactions in virus-induced necrosis (Upton et al., 2010), as well as the known RHIM-dependent interaction between RIP3 and DAI (Kaiser et al., 2008; Rebsamen et al., 2009), these results implicate a RIP3-DAI complex mediating programmed necrosis.

To investigate the functional cooperation between endogenous DAI and RIP3, we first employed RNAi to reduce levels of DAI or RIP3 in necrosis sensitive cells. 3T3-SA cells transfected with DAI- or RIP3-specific siRNAs showed knockdown of the corresponding protein compared to non-targeting control (Figure 4.3B). As a specificity control, RIP1 levels were unchanged by either treatment. When infected with mutant virus, DAI knock-down 3T3-SA cells were protected from virus-induced necrosis at levels comparable to RIP3 knock-down cells

(Figure 4.3C). As expected, treatment with RIP1 kinase inhibitor Nec-1 had no influence. Thus, both RIP3 and DAI are necessary to execute virus-induced programmed necrosis. To further support these results, control (C57BL/6) *DAI*^{-/-} and *RIP3*^{-/-} MEFs were isolated (Figure 4.3D) and infected with mutant MCMV. In agreement our previous report (Upton et al., 2010), RIP3 knock-out MEFs were resistant to virus-induced necrosis, while control MEFs remained highly sensitive. Even though they retained a similar level of RIP3 protein, *DAI*^{-/-} MEFs were resistant to virus-induced necrosis, similar to *RIP3*^{-/-} (Figure 4.3E) or siRNA knockdown cells (Figure 4.3C). Furthermore, DAI knockdown in 3T3-SA cells as well as *DAI*^{-/-} MEFs remained sensitive to TNF-induced necroptosis (Figure 4.S3B-C), showing that DAI is dispensable for programmed necrosis mediated by RIP1-RIP3 complex formation. Likewise, the RIP3-dependent necroptotic event resulting in embryonic lethality of *Casp8*^{-/-} mice (Kaiser et al., 2011; Oberst et al., 2011) was not rescued loss of DAI (Figure 4.S3D), and *Casp8*^{-/-}*DAI*^{-/-} embryos were phenotypically indistinguishable from *Casp8*^{-/-} *DAI*^{+/-} or *Casp8*^{-/-} *DAI*^{+/+} embryos (data not shown). Taken together, these data indicate loss of DAI ameliorates RIP3-dependent virus-induced programmed necrosis without altering the response to programmed necrosis that depends on the RIP1-RIP3 necrosome.

To investigate the influence of DAI on WT or mutant virus growth, control or *DAI*^{-/-} MEFs were infected and assessed for virus replication. Parental MCMV replicated to comparable high titers in all MEF lines tested, whereas mutant virus was attenuated in control cells (Figure 4.3F, left), where RIP3 and DAI were both detected (Figure 4.3D). However, mutant virus replication was normalized in *DAI*^{-/-} MEFs (Figure 4.3F, right), reminiscent of normalized mutant virus growth in *RIP3*^{-/-} MEFs (Upton et al., 2010). Together, these results provide compelling evidence that RIP3 and DAI are both necessary to execute virus-induced programmed necrosis, and that the RHIM-dependent association of RIP3 and DAI is the natural target of MCMV vIRA.

vIRA mutant virus inflammation and replication in DAI-deficient mice. To address the contribution of DAI to virus-induced death directly in a natural setting, we infected *DAI*^{-/-} and control (C57BL/6) mice by footpad (FP) inoculation and evaluated inflammatory events dependent on expression of the MCMV-encoded CC chemokine, MCK2 (Saederup et al., 2001), a strategy previously used to characterize inflammation in *RIP3*^{-/-} mice (Upton et al., 2010). As in *RIP3*^{-/-} mice, virus infection induced swelling in *DAI*^{-/-} mice at levels similar to parental virus, peaking with a similar pattern to controls (Figure 4.4A). In contrast, mutant virus infection failed to elicit detectable swelling in C57BL/6 mice, a result expected due to attenuated replication (Upton et al., 2010). Consistent with a role for virus replication and MCK-2 in this inflammatory pattern (Saederup et al., 2001), swelling correlated with detection of infected cells in footpads of inoculated mice (data not shown). Thus, in the absence of DAI, mutant virus infection patterns exhibited inflammatory characteristics of WT MCMV infection. These results indicate that DAI is dispensable for the MCK2-enhanced inflammatory response to MCMV infection and strongly support a role for DAI in host cell functions modulated by vIRA in suppression of cell death during natural infection. Interestingly, dissemination to the salivary glands (SGs) of *DAI*^{-/-} mice 14 days postinfection with parental MCMV was consistently higher than control mice (Figure 4.S4A) regardless of inoculation route, while mutant virus was comparably inefficient in reaching this organ.

To more directly assess the role of DAI in M45mutRHIM virus replication patterns, control, *DAI*^{-/-}, and *RIP3*^{-/-} mice were inoculated via the intraperitoneal route. Mutant and parental virus titers were comparable in spleen (Figure 4.4B) and liver (Figure 4.4C) of *DAI*^{-/-} mice throughout the duration of acute infection, while mutant virus was not detected in any organ at any time in control animals. Mutant virus growth was normalized in spleen and liver during acute infection of *RIP3*^{-/-} animals, as was dissemination to, and growth within, the SGs (Figure

4.4B-D, right panels), consistent with previous findings (Upton et al., 2010). Mutant virus was detected in SGs of *DAI*^{-/-} mice (Figure 4.4D), albeit at levels lower than parental virus in control or *RIP3*^{-/-} mice. Thus, DAI-deficiency permits mutant virus growth and dissemination *in vivo*. As was observed following inoculation of footpads, parental virus titers in spleen and liver were elevated in *DAI*^{-/-} mice compared to C57BL/6 mice and compared to mutant virus in *DAI*^{-/-} mice (Figure 4.4B-C). Mutant virus failed to replicate in highly susceptible IFN α/β receptor (*IFNAR*^{-/-}) knockout mice (Figure 4.4B), indicating that the host defense pathway controlling type I IFN is irrelevant to virus-induced necrosis. Taken together, DAI emerges as a target of vIRA RHIM-mediated suppression independent of the type I IFN pathway. Thus, the specific cell-intrinsic death program mediated by DAI and RIP3 dominates MCMV infection in the absence of vIRA. Together, these results provide compelling evidence that virus-induced necrosis *in vivo* is dependent upon DAI, establishing a natural function for DAI in mammalian host defense as well as a natural target of viral escape.

C) DISCUSSION

Recognition of invading pathogens is a critical part of the host defense, leading to cellular responses that range from the induction of cytokines to cell death. In this work, we implicate the constitutively expressed, cytosolic dsDNA sensor DAI in the host response to MCMV infection, showing that DAI partners with RIP3 to induce RHIM-dependent programmed necrosis that is naturally suppressed by vIRA function. These data also provide the first direct evidence of a crucial role for DAI *in vivo*, and implicates DAI as a DNA sensor in addition to its role as a signaling component in virus-induced necrosis. Cytosolic dsDNA activates a multiple of PRR, such as RNAPolIII (Ablasser et al., 2009; Chiu et al., 2009), IFI16 (Unterholzner et al., 2010), LRRFIP1 (Yang et al., 2010), DDX41 (Zhang et al., 2011d), and Ku70 (Zhang et al., 2011c) that activate IFNs, as well as AIM2, which can activate the inflammasome (Ablasser et al., 2009; Fernandes-Alnemri et al., 2009). Multiple lines of evidence have stressed that DAI is redundant as an IFN-inducing DNA sensor (Lippmann et al., 2008; Wang et al., 2008c), and are supported by findings that DAI is dispensable for innate or adaptive responses to dsDNA or DNA vaccination (Ishii et al., 2008). Here, M45*mut*RHIM MCMV, which is avirulent for normal or immunocompromised animals (Upton et al., 2010), replicates in DAI-deficient animals. As we have previously demonstrated that RIP3-dependent, virally-induced programmed necrosis underlies the attenuation of mutant virus, the results presented here clearly implicate DAI as the second player in this pathway. Thus, although inflammatory and cells death pathways are controlled by DAI, it is the regulation of cell death that is most critical, contributing to host defense in a way that has recently emerged in evaluation of caspase 8 as well as RIP3 (Mocarski, 2012).

vIRA is one of several cell death suppressors encoded by MCMV that balance the host response to infection. Studies on viral mutants eliminating single inhibitors have proved informative. The rapid programmed necrosis that characterizes vIRA mutant virus-infected cells is likely to be revealed because this mutant retains the activity of at least two additional classes of cell death suppressors: viral inhibitor of caspase 8 activation (vICA) (Cicin-Sain et al., 2008; McCormick et al., 2003; Menard et al., 2003; Skaletskaya et al., 2001) and mitochondrial inhibitors of cell death targeting Bax and Bak, referred to as viral mitochondrial inhibitor of apoptosis (vMIA) and viral inhibitor of Bak oligomerization (vIBO) (Cam et al., 2010; McCormick et al., 2005; McCormick et al., 2003). Here, vICA, in particular, is likely to sensitize virus-infected cells to programmed necrosis through inhibition of caspase 8 activity (Kaiser et al., 2011). The phenotype of viral mutants lacking individual cell death suppressors has been instrumental in revealing previously unrecognized host response pathways of cell death (reviewed in (Brune, 2011; McCormick, 2008). The role caspase 8 in negatively regulating necroptosis (Kaiser et al., 2011; Oberst et al., 2011) highlights the intricate redundancies and cross-talk between these cell death pathways; in many cases, when caspase 8 activity is absent or suppressed, necrotic pathways emerge, and must be controlled. Therefore, understanding the function of additional MCMV cell death suppressors, such as vICA, vMIA, and vIBO, in setting the stage for vIRA-inhibited programmed necrosis will provide crucial insight into the cellular environment necessary for the execution of programmed necrosis in response to virus or other inducers. As recently emerged from studies on caspase 8 and FADD (Kaiser et al., 2011; Oberst et al., 2011; Zhang et al., 2011b), extrinsic cell death pathways are dispensable for mammalian development, and may have evolved specifically as components of host defense. Vaccinia virus B13R encodes a caspase inhibitor that predisposes infected cells to TNF-induced necroptosis (Li and Beg, 2000). It seems that virus-encoded inhibitors of caspase 8 activation such as vICA (Skaletskaya et

al., 2001) very likely contributed to the adaptation of programmed necrosis as a means of host defense and this triggered the evolutionary co-adaptation of viral suppressors like vIRA that evade necrosis (Mocarski, 2012). Thus, understanding how pathogens simultaneously influence these interconnected pathways will yield critical insight into the initiation and execution of host cell death defenses.

The most important RHIM of DAI (also known as RLR-A or RHIM-A) (Kaiser et al., 2008; Rebsamen et al., 2009) is required to direct interactions between DAI and RIP3, as well as for transduction of necrotic death signals (Figure 2). However, two additional RHIM-like repeats (RLR-B/RHIM2 and RLR-C (Kaiser et al., 2008; Rebsamen et al., 2009) are present in this adaptor, raising the possibility that additional protein-protein interactions regulate DAI activities. One current model suggests ligand recognition and binding induces DAI oligomerization, which may drive signal transduction (Wang et al., 2008c), in the way reminiscent of RIP1 and RIP3 oligomerization in necroptosis (Zhang et al., 2011a). Although our results demonstrate one RHIM of DAI is critical for virus-induced programmed necrosis, homotypic DAI RHIM-RHIM interactions, or oligomerization with additional RHIM-containing proteins, mediated by one or more of these additional RHIMs could play a role. The contribution of additional potential signaling players is of great interest and recent work showing the contribution of the “Ripoptosome” to necroptosis (Feoktistova et al., 2011; Tenev et al., 2011), implies a DAI-RIP3 complex could engage the same players, or coordinate an analogous signaling platform, to execute virus-induced programmed necrosis. Additional studies will be necessary to delineate the contribution of the other potential DAI protein-protein interaction motifs, including RHIMs and Z-DNA binding domains, to DAI function during MCMV infection.

Multiple cell-type specific pathways likely contribute to RIP3 activation, and additional host mechanisms probably play a role in RIP3-dependent necrosis *in vivo*. Such a scenario is not

unprecedented, as TNF-induced necroptosis has recently been shown to utilize multiple pathways leading to death, depending on cell type and context (Zhang et al., 2011a). Despite restoring replication, *DAI*^{-/-} mice failed to completely normalize efficient dissemination of M45mutRHIM following intraperitoneal IP (Figure 4D) or FP (Figure 4SA) injection compared to *RIP3*^{-/-} animals. DAI-deficient mice retain both RIP3 and RIP1, suggesting that this behavior may reflect a contribution of necroptosis to host defense. This would also explain differences between DAI- and RIP3-deficient mice. It is worth noting that parental virus reached titers 10-fold higher in *DAI*^{-/-} animals compared to controls, consistent with the importance of this adaptor in host defense. In addition to a role in cell death, DAI influences the host IFN response against herpesviruses (DeFilippis et al., 2010a; DeFilippis et al., 2010b; Furr et al., 2011; Takaoka et al., 2007), and it is likely that elimination of DAI, while normalizing M45mutRHIM virus replication by failure to initiate virus-induced programmed necrosis, also dysregulates some additional aspect of innate or adaptive host defense pathways necessary for efficient control of MCMV. Further characterization of DAI function during MCMV infection *in vivo*, as well as virus induced signaling events leading to RIP3-dependent necrosis, will be important future endeavors.

In summary, we have identified DAI as a critical mediator of RIP3-dependent anti-viral necrosis, providing the first evidence DAI participates in an intrinsic host cell death pathway. DAI expression is detected in settings where virus-induced necrosis occurs, and expression of DAI sensitizes resistant cells to this RIP3 RHIM-dependent pathway. A RIP3-DAI complex is detected during mutant virus infection, providing compelling evidence that modulation of this complex is critical for viral pathogenesis. Indeed, like RIP3 (Upton et al., 2010), loss of DAI permits vIRA-deficient viral replication *in vivo*, providing formal proof DAI participates in RIP3-dependent anti-viral necrosis, as well as the first indication of DAI function *in vivo*. Inclusion of this PRR in the

pathway of RIP3-dependent, MCMV-induced programmed necrosis adds to our current understanding of pathogen sensing and the intrinsic host responses elicited by these pathways.

D) METHODS

Reagents and Viruses. BAC-derived parental WT K181 and M45 *mut* RHIM viruses were previously described (Upton et al., 2010). Dimethyl sulfoxide (DMSO, Sigma-Aldrich) and necrostatin (Nec-1, Calbiochem) were used as described (Upton et al., 2010). Growth curves were performed as previously described (Upton et al., 2010).

Plasmids, Transfections and Transductions. FLAG-tagged WT and *mut* RLR-A DAI (Kaiser et al., 2008) were cloned into the pQCXIH retroviral vector (Clontech). FLAG-tagged WT and mRHIM RIP3 retroviral constructs were previously described (Upton et al., 2010). The pLKO.1-based scramble RIP3-A (TRCN0000022535) and RIP3-B (TRCN0000022538) shRNA constructs were from Open Biosystems, The pLKO.1-scramble control has been described (Sarbasov et al., 2005), and retro- and lentiviral production, infection and selection were previously described (Kaiser et al., 2008). siRNA transfections were performed using 200 pg of non-targeting, DAI, and RIP3 ON-TARGET *plus* SMARTpool siRNAs (Dharmacon) with Lipofectamine RNAiMAXX (Invitrogen) according to the manufacturer's recommendations, and assays performed 48 h post transfection.

Mice, Infections, and Organ Harvests. C57BL/6 mice were from Jackson Laboratories. *RIP3*^{-/-} mice (*Ripk3*^{tm1Vmd}) were from Genentech (Newton et al., 2004), and *DAI*^{-/-} mice (*Zbp1*^{tm1Aki}) (Ishii et al., 2008) were from Shizuo Akira (Osaka University). Infections and organ titers were performed as previously described (Upton et al., 2010). Mice were maintained by Emory University Division of Animal Resources, and all procedures approved by the Emory University Institutional Animal Care and Use Committee.

Cell culture and Embryonic Fibroblast Isolation. NIH3T3 fibroblasts (ATCC CRL-1658), 3T3-SA (ATCC CCL-92), and SVEC4-10 (ATCC CRL-2181) were maintained as previously described

(Upton et al., 2010). MEFs were isolated and maintained as previously described (Upton et al., 2010).

Cell Viability Assays. Viability assays were performed as previously described (Upton et al., 2010) using Cell Titer-Glo Luminescent Cell Viability Assay kit (Promega) according to the manufacturer's instructions. Luminescence was measured on a Synergy HT Multi-Detection microplate reader (Bio-Tek). Values are plotted as % of vehicle treated or WT infected cells assessed in parallel with experimental samples.

IP and IB. IP and IB analyses were performed using established methods, as previously described (Upton et al., 2010). Antibodies used : mouse anti- β -actin (clone AC-74; Sigma), mouse anti-RIP1 (clone 38; BD Biosciences), anti-DAI (Karayel et al., 2009) a gift from Tillman Burckstummer and Giulio Superti-Furga, CeMM), anti-MCMV M45 (Lembo et al., 2004)(a gift from David Lembo, University of Turin), rabbit anti-RIP3 (Imgenex), mouse anti-Flag (M2 clone) horseradish peroxidase (HRP) conjugate (Sigma-Aldrich), anti-mouse and anti-rabbit IgG-HRP (Vector Laboratories). IP were performed with goat anti-RIP3 (clone C-16; Santa Cruz Biotechnology) and protein A/G agarose (Santa Cruz Biotechnology).

Viruses. Bacmid-derived parental virus WT MCMV-GFP (strain Smith-ATCC) and MCMV Δ 45 (Brune et al., 2003) were propagated and used for infections as previously described (Upton et al., 2008).

Quantitative RT-PCR analysis. RT-PCR was performed as previously described (Kaiser et al., 2008). Briefly, Total RNA isolated using the RNeasy Mini Kit (Qiagen) was reverse transcribed using the High Capacity cDNA Reverse Transcription Kit (Applied Biosystems) with oligo d(T)₈₋₁₆ primer (Invitrogen) followed by RNase H (Invitrogen) treatment. Analysis was done using an aliquot of the reverse transcription reaction on the 7500 Fast Real Time PCR System with

IFN β (O'Donnell et al., 2005) and *β -actin* (Hida et al., 2000) primers and SYBR Green Master Mix (Applied Biosystems). Data are presented as relative expression levels normalized to *β -actin*.

E) FIGURES AND LEGENDS

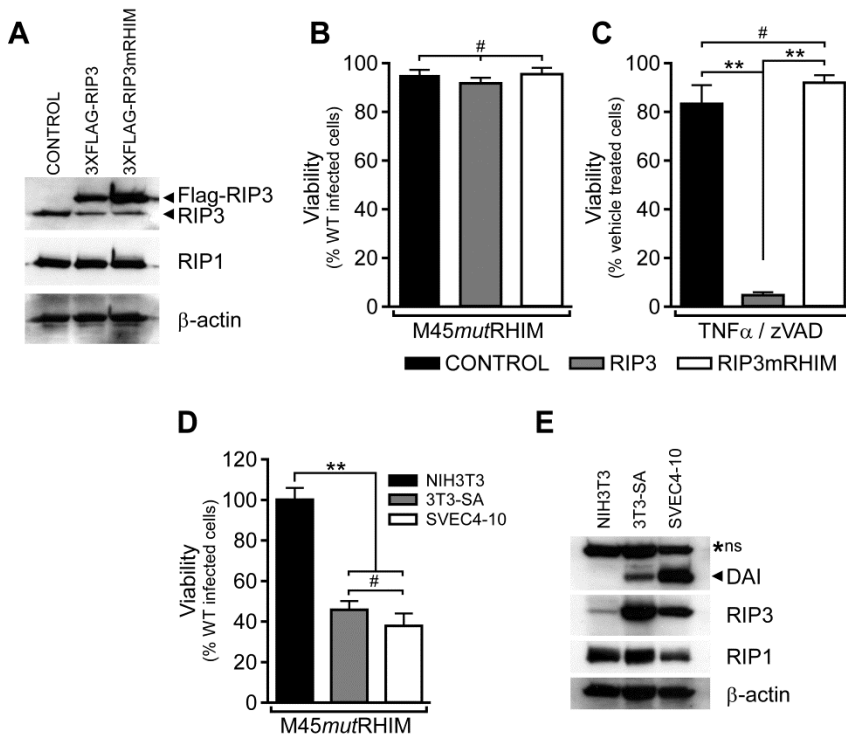


Figure 4.1. RIP3 levels differentially confer susceptibility to necroptosis and virus-induced programmed necrosis. (A) Immunoblot (IB) analysis to detect RIP3, RIP1 and β -actin from NIH3T3 cells stably transduced with retroviruses encoding 3XFLAG-tagged RIP3, RIP3mRHIM, or control. (B) Viability of RIP3-expressing NIH3T3 stable cell lines infected with M45mutRHIM MCMV at a multiplicity of infection (MOI) of 10. (n=4) (C) Viability of RIP3-expressing NIH3T3 stable cell lines following treatment with TNF (25 ng/ml) and zVAD-fmk (50 μ M) to induce necroptosis (n=3-4). (D) Viability of NIH3T3, 3T3-SA and SVEC4-10 cell lines infected with M45mutRHIM MCMV at a multiplicity of infection (MOI) of 10. (n=3-7) (E) IB analysis of uninfected NIH3T3, 3T3-SA, and SVEC4-10 cells to detect DAI, RIP3, RIP1, and β -actin. A non-specific (*ns) band characteristic for this antibody (Karayel et al., 2009) was detected in all lanes. Error bars indicate standard deviation (SD) of the mean. **p<0.001, by one way analysis of

(Figure 4.1 continued) variation (ANOVA) with Bonferroni's Multiple Comparison Test. #not significant ($p > 0.05$). See also related Figure 4.S1.

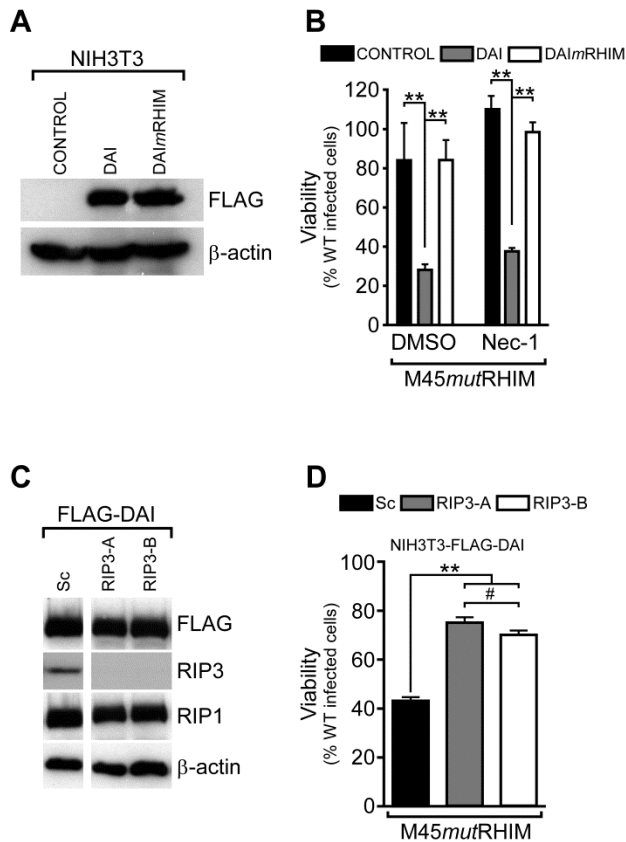


Figure 4.2. Increased DAI expression sensitizes resistant cells to virus-induced necrosis. (A) IB analysis to detect FLAG and β -actin of NIH3T3 stable cells expressing FLAG-tagged WT DAI, FLAG-tagged DAI^{mut}RHIM, or control. (B) Viability of DAI-expressing NIH3T3 stable cell lines infected with M45mutRHIM MCMV (MOI of 10) and treated with DMSO or Nec-1 (30 μ M). (n=4) (C) IB analysis to detect FLAG, RIP3, RIP1 and β -actin in stable NIH3T3 cell lines expressing FLAG-tagged WT DAI together with either a scramble control (Sc) or one of two RIP3-specific shRNAs (RIP3-A or RIP3-B). (D) Viability of DAI-expressing, RIP3 knockdown NIH3T3 stable cell lines following infection with M45mutRHIM MCMV (MOI of 10). (n=3) Error bars, SD. **p<0.001, by one way analysis of variation (ANOVA) with Bonferroni's Multiple Comparison Test. #not significant (p>0.05). See also related Figure 4.S2.

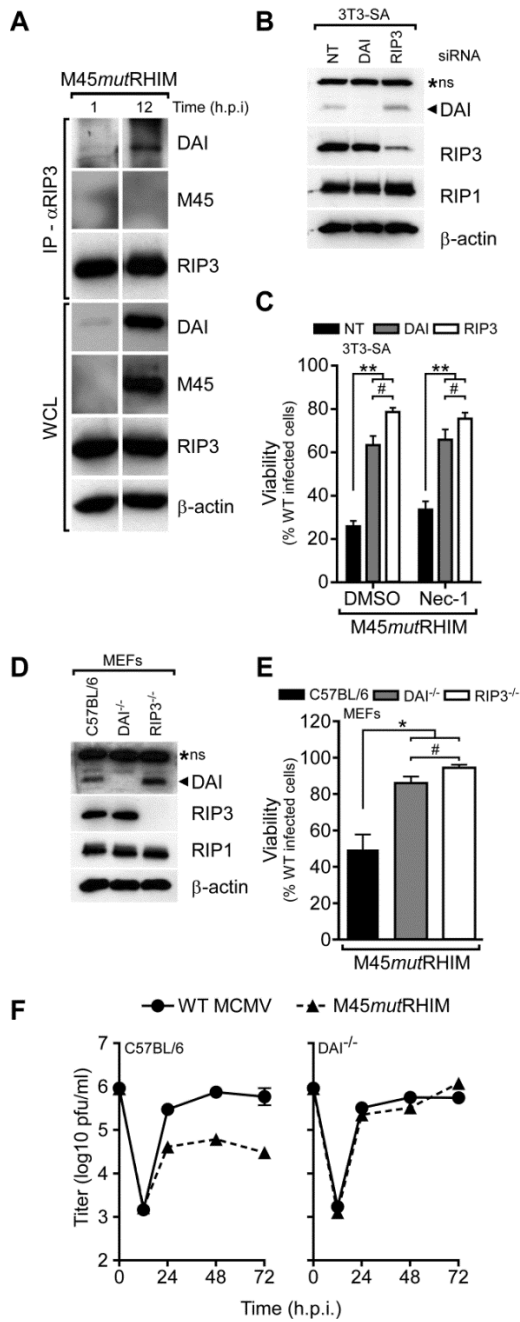


Figure 4.3. DAI and RIP3 cooperate in virus-induced necrosis. (A) RIP3 and DAI interaction in the absence of vIRA. IB of immunoprecipitations (IP) and whole cell lysates (WCL; 5% total) showing DAI, M45, RIP3 and β -actin in 3T3-SA cells infected with M45mutRHIM MCMV (MOI=5) harvested at the indicated times (h.p.i.). (B) IB analysis to detect DAI, RIP3, RIP1 and β -actin in

(Figure 4.3 continued) 3T3-SA cells transfected with non-targeting (NT) control, DAI, or RIP3 siRNAs (C) Viability of 3T3-SA cells transfected with the indicated siRNA and infected with M45mutRHIM (MOI of 10) and treated with DMSO control or Nec-1 inhibitor (30 μ M). (n=4) (D) IB analysis to detect DAI, RIP3, RIP1, and β -actin in C57BL/6 control, *DAI*^{-/-}, and *RIP3*^{-/-} murine embryonic fibroblasts (MEFs) (E) Viability of C57BL/6 control, *DAI*^{-/-}, and *RIP3*^{-/-} MEFs infected with M45mutRHIM MCMV (MOI=10)(n=3). (F) Single-step replication of WT and M45mutRHIM MCMV (MOI of 5) on control C57BL/6 (left) and *DAI*^{-/-} (right) MEFs. Viral titers determined by plaque assay with the first (0 h) time point representing amount of virus in the inoculum. Error bars, SD. *p<0.01, **p<0.001, by one way analysis of variation (ANOVA) with Bonferroni's Multiple Comparison Test. #not significant (p>0.05). See also related Figure 4.S3.

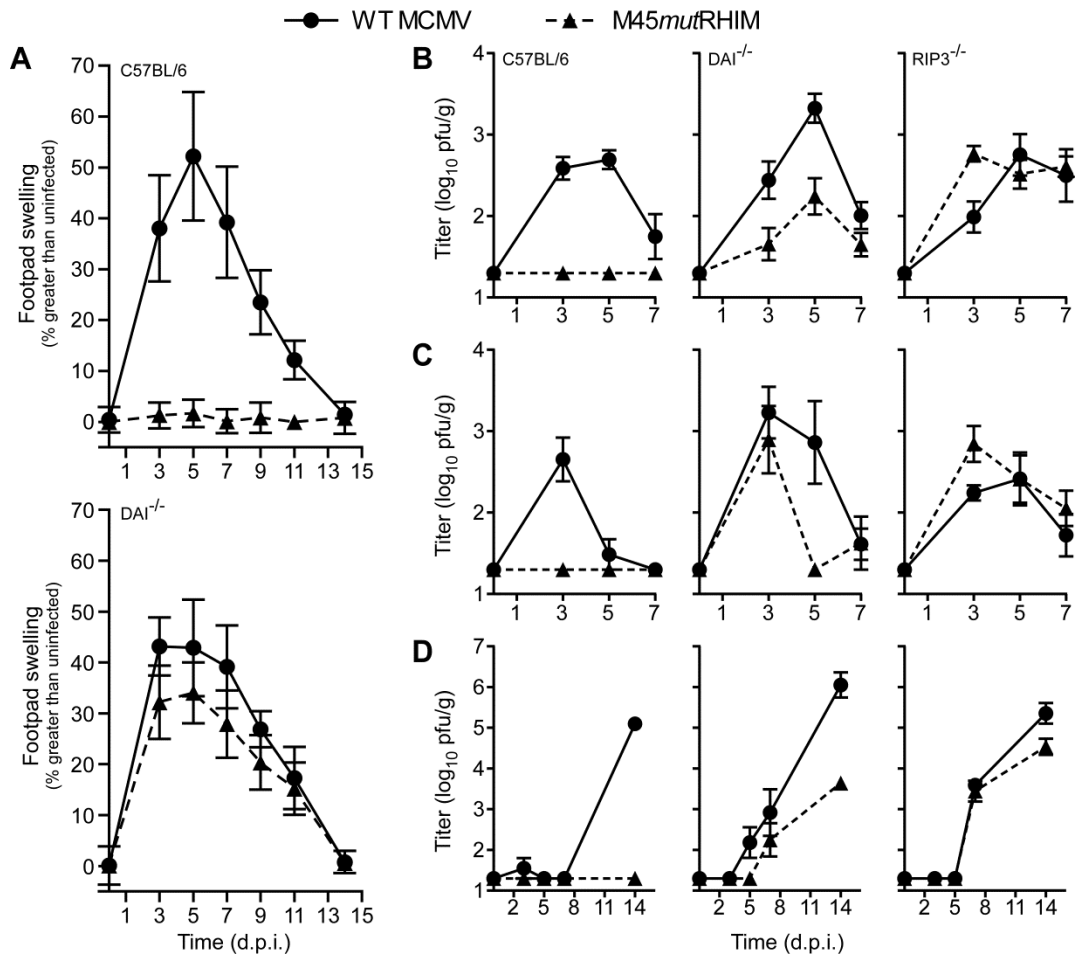


Figure 4.4. M45mutRHIM virus attenuation *in vivo* is reversed in DAI^{-/-} mice . (A) Footpad swelling induced by parental WT or M45mutRHIM MCMV infection. Footpad thickness of C57BL/6 control (top) and DAI^{-/-} (bottom) mice inoculated with 10⁶ pfu was measured with a digital caliper, and mean values plotted at the indicated times over a 14 day time course (n=7-9 animals/group). (B-D) Viral titers from spleen (B), liver (C), and SGs (D) of control (C57BL/6), RIP3^{-/-}, and DAI^{-/-} mice infected via intraperitoneal inoculation with 10⁶ pfu of indicated virus and harvested at the indicated time (n= 5-10 animals/group). Error bars, SEM. See also related Figure 4.S4.

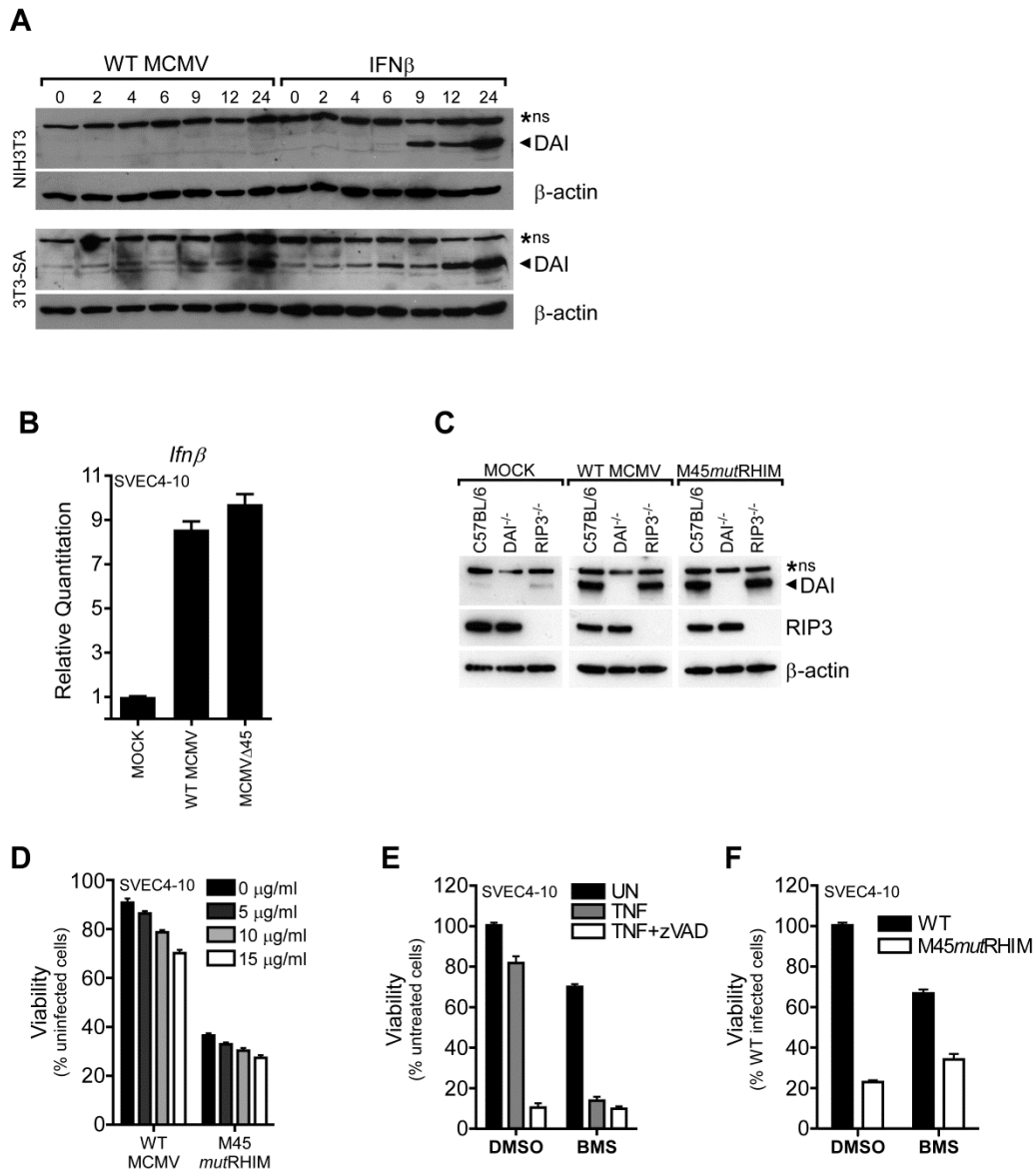


Figure 4.S1, related to Figure 4.1: IFN β , but not MCMV infection induces DAI expression in NIH3T3 cells. (A) NIH3T3 and 3T3-SA cells were infected with WT MCMV (MOI=5.0) or treated with recombinant mouse IFN β (100U/ml; Millipore). Cells were harvested at indicated times post infection or treatment and lysates subjected to SDS-PAGE and immunoblotting for DAI or β -Actin. (B) IFN β gene induction in SVEC4-10 cells infected 6 h with WT MCMV-GFP or MCMV Δ 45 (MOI=10.0), or mock infected. (C) IB analysis to detect DAI, RIP3, and β -actin in C57BL/6 control,

(Figure 4.S1 continued) *DAI*^{-/-}, and *RIP3*^{-/-} MEFs mock infected, or infected 12 h with WT or M45mutRHIM MCMV (MOI=5). (D) Viability of SVEC4-10 cells infected 18 h with WT or M45mutRHIM MCMV (MOI=10) in the absence or presence of indicated amount of rat anti-mouse Interferon-β neutralizing antibody (PBL Interferon Source). (E) Viability of SVEC4-10 cells 18 h following addition of recombinant murine TNF (25 ng/ml; Peprotech) with or without zVAD-fmk (50μM; Enzo Life Sciences) and treated with BMS-345541 (10μM) or DMSO. Cells were preincubated with BMS or DMSO for 1 h prior to addition of death stimuli. (F) Viability of SVEC4-10 cells infected 18 h with WT or M45mutRHIM MCMV (MOI=10) and treated with BMS-345541 (BMS, 10μM; Sigma) or DMSO. Cells were pretreated for 1 h prior to infection.

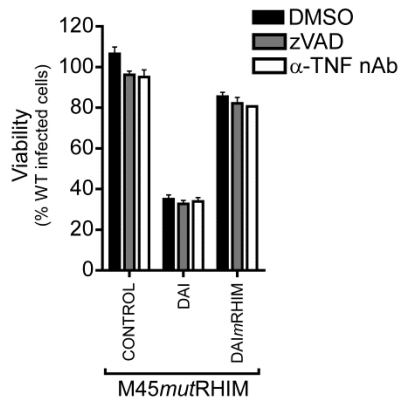


Figure 4.S2, related to Figure 4.2: Infection induced, DAI-mediated cell death displays characteristics of MCMV-induced programmed necrosis. Viability of DAI-expressing NIH3T3 stable cell lines infected 18 h with M45mutRHIM MCMV (MOI=10.0) and treated with DMSO, zVAD-fmk (50μM), or neutralizing anti-TNF antibodies (10μg/ml; R&D Systems).

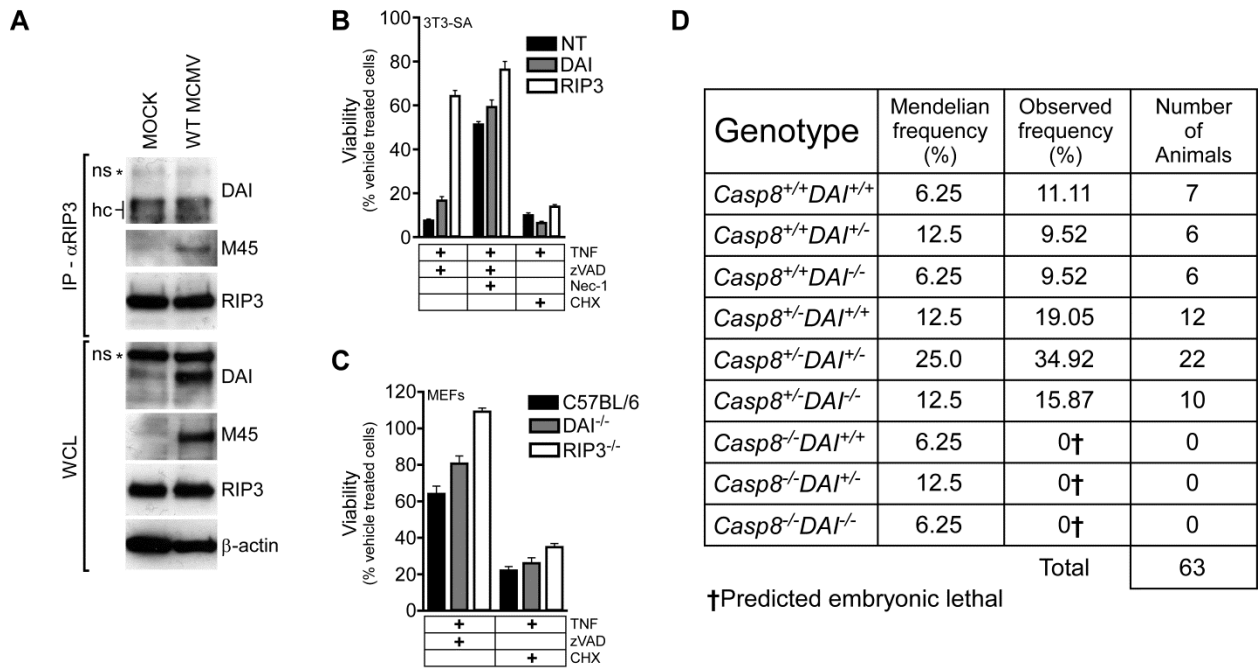


Figure 4.S3, related to Figure 4.3: Loss of DAI does not influence DR-induced necroptosis or apoptosis. (A) IB of immunoprecipitations (IP) and whole cell lysates (WCL; 5% total) showing DAI, M45, RIP3 and β -actin in 3T3-SA cells mock treated or infected 12 h with WT MCMV (MOI=5). (B) Viability of 3T3-SA cells transfected with non-targeting control (NT), DAI, or RIP3 specific siRNA, and treated 12 h with recombinant murine TNF (25ng/ml) and zVAD-fmk (50 μ M), with or without Nec-1 (30 μ M) or cyclohexamide (5 μ g/ml; Sigma). (C) Viability of control (C57BL/6), *DAI^{-/-}*, and *RIP3^{-/-}* MEFs treated 12 h with recombinant murine TNF (25ng/ml) and zVAD-fmk (50 μ M) or cyclohexamide (5 μ g/ml). (D) Epistatic analysis of mice following *Casp8^{+/+}DAI^{+/-}* intercross, with predicted and observed frequencies of live births.

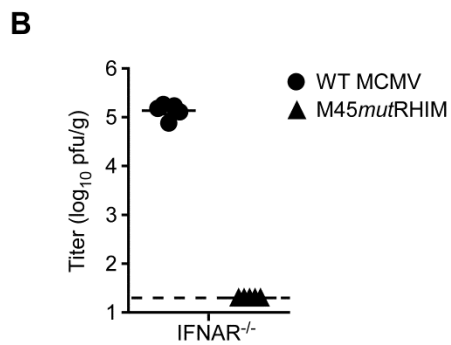
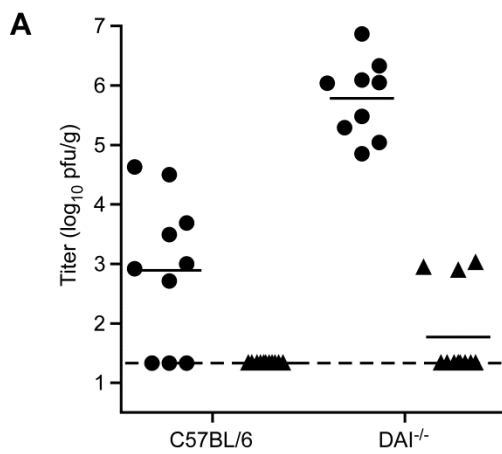


Figure 4.S4, Related to Figure 4.4: M45mutRHIM disseminates poorly to SGs of $DAI^{-/-}$ mice, and remains attenuated in $IFNAR^{-/-}$ animals. A) SG titers from control and $DAI^{-/-}$ animals 14 d.p.i. with parental WT (circles) or M45mutRHIM (triangles) MCMV by footpad inoculation (from Figure 4A). B) Spleen titers from $IFNAR^{-/-}$ mice 5 days post intraperitoneal inoculation with parental WT (circles) or M45mutRHIM (triangles) MCMV.

Chapter 5: Toll-like Receptor 3 induces RIP1-independent necrosis via a TRIF-RIP3 complex

A) INTRODUCTION

Pathogen sensors recognize pathogen-associated molecular patterns (PAMPs) during viral or microbial infection, initiating well-recognized host defense pathways by triggering the production of immunomodulatory cytokines, chemokines and interferons that restrict infection. Besides sculpting inflammatory responses these factors facilitate antigen presentation in the adaptive immune response to infection. Host-encoded pattern recognition receptors (PRRs) also dictate cell fate decisions. The regulated cell death pathways apoptosis, pyroptosis and necrosis eliminate infected cells and contribute to control of microbial and viral infections in the host (Lamkanfi and Dixit, 2010). These cell death pathways are themselves targeted by pathogen-encoded cell death suppressors that modulate effectiveness and contribute to virulence (Lamkanfi and Dixit, 2010). Toll-like receptors (TLRs) were the first PRRs to be recognized (Kumar et al., 2011) and include sensors of pathogen-associated peptidoglycan (TLR2), double-stranded (ds)RNA (TLR3), lipopolysaccharide (LPS) (TLR4), flagellin (TLR5), unmethylated CpG DNA motifs (TLR9), as well as other PAMPs (Kumar et al., 2011). TLRs recruit Toll/IL-1R (TIR) domain-containing adapters that transduce signals and activate gene expression via transcription factors, including NF- κ B and IRF3/IRF7, and activate type I interferon. The responses evoked via TLRs mediate both inflammation and innate host defense (Kumar et al., 2011). Only TLR3 and TLR4 employ the adapter TRIF. TLR4 and all other TLRs signal via MyD88. Although the mechanism through which TLRs activate cytokines and interferons is clear (Kumar et al., 2011), the interface with cell fate decisions remains to be established.

Viral infection of mammalian cells triggers apoptosis or necrosis via death receptors (Cho et al., 2009; He et al., 2009; Zhang et al., 2009) or other infection-associated signals

(Mocarski et al., 2011; Upton et al., 2010, 2012). Apoptosis depends on a caspase-dependent proteolytic cascade that dismantles cells in an orderly fashion while maintaining membrane integrity (Hengartner, 2000; Strasser et al., 2000), whereas programmed necrosis leads to cell leakage using mechanisms that are still being defined. Death receptor-induced programmed necrosis, also called necroptosis (Vandenabeele et al., 2010b), depends on an association of the receptor interacting protein kinase (RIP)1 acting together with RIP3 (Cho et al., 2009; He et al., 2009; Holler et al., 2000; Mocarski et al., 2011; Zhang et al., 2009); whereas, virus-induced programmed necrosis depends on the interaction of the DNA sensor DAI and RIP3 (Upton et al., 2012). Furthermore, TLR3 and TLR4 can induce necrotic death via TRIF (He et al., 2011), although the relationship of RIP1, RIP3 and TRIF in this process has not been resolved. Through these diverse studies, RIP3 has emerged as the key, common mediator of programmed necrosis (Mocarski et al., 2011), potentially acting via adaptors such as MLKL to mediate downstream impacts (Sun L Fau - Wang et al., 2012; Zhao et al., 2012). The entwined nature of these distinct death processes has been most extensively studied in the context of TNFR1 (Cho et al., 2009; He et al., 2009; Holler et al., 2000; Mocarski et al., 2011; Zhang et al., 2009). Death receptor activation drives the assembly of a cytosolic caspase-8 (Casp8) signaling platform (called Complex IIB) that includes RIP1, Casp8, Fas-associated via death domain (FADD) and cellular FLICE/Casp8 inhibitory protein (cFLIP). This complex maintains control over Casp8-dependent apoptosis as well as RIP3-dependent necroptosis. A comparable, but death receptor-independent signaling platform (called a Ripoptosome) forms downstream of TLR3 activation (Feoktistova et al., 2011). In either case, the complex regulates homodimerization and autocleavage that drives the proapoptotic potential of Casp8 as well as the basal level of Casp8 activity necessary to prevent RIP3-dependent death. This relationship became very clear when the midgestational death of Casp8-deficient mice was reversed by the elimination of RIP3

(Kaiser et al., 2011; Oberst et al., 2011). In the face of either Casp8 or FADD compromise, RIP1 and RIP3 oligomerize via a RIP homotypic interaction motif (RHIM) to drive necroptosis (Cho et al., 2009; He et al., 2009; Holler et al., 2000; Vandenabeele et al., 2010b; Zhang et al., 2009). Thus, the complex prevents programmed necrosis, possibly by cleaving RIP1 and RIP3 directly, separating the kinase and RHIM domains (Chan et al., 2003; Feng et al., 2007; Lin et al., 1999; Lu et al., 2011), or by targeting some downstream component in the pathway. The long form of cFLIP (cFLIP_L), an NF- κ B inducible noncatalytic paralog of Casp8, is best known for its ability to blunt apoptosis by preventing homodimerization and autocleavage-mediated maturation of Casp8 (Thome and Tschopp, 2001). Recently, cFLIP_L has been directly implicated in maintaining basal Casp8 catalytic activity that prevents the unleashing of necrosis (Dillon et al., 2012; Oberst et al., 2011).

Toll-like receptor 3 (TLR3) regulates Casp8 signaling via the adapter protein TRIF (Kaiser and Offermann, 2005) and signals through the Ripoptosome (Feoktistova et al., 2011). TLR3-signaling may result in any of three distinct cellular outcomes that are mediated by TRIF via a C-terminal RHIM domain-dependent interaction with RIP1 and RIP3 (Kaiser and Offermann, 2005; Meylan et al., 2004): (1) activation of NF- κ B (Meylan et al., 2004; Vivarelli et al., 2004), partly through binding to RIP1; (2) initiation of apoptosis (Kaiser and Offermann, 2005); and, (3) initiation of programmed necrosis when Casp8 activity is compromised (He et al., 2011; Kalai et al., 2002). These outcomes are all analogous to TNFR1-signaling (Mocarski et al., 2011) where RIP1, which interacts with FADD via a death domain, employs a RHIM-dependent interaction to recruit RIP3 and execute necroptosis. In this process, the kinase activities of both RIP1 and RIP3 contribute to execution of necrotic death. RIP1 and RIP3 compete for RHIM-dependent binding to the TLR3/TLR4 adapter TRIF, with RIP3 outcompeting RIP1 (Meylan et al., 2004). Although, little is known about the hierarchy of RHIM-interactions dictating cell fate decisions following

TLR3 or TLR4 engagement, a precedent has recently emerged from studies of the RHIM-containing cytosolic DNA-sensor protein DAI. Necrotic death in response to murine cytomegalovirus (MCMV) infection depends on a complex between DAI and RIP3, completely independent of RIP1 (Upton et al., 2010, 2012). MCMV, similar to other large DNA viruses, deploys an array of cell death suppressors, including M36-encoded viral inhibitor of Casp8 activation (vICA). vICA impairs the full maturation of Casp8 as well as basal Casp8 catalytic activity necessary to prevent necrotic cell death (Kaiser et al., 2011). MCMV has evolved a dedicated suppressor that counteracts necrotic death, the viral inhibitor of RIP activation (vIRA) (Mocarski et al., 2011; Upton et al., 2010), a competitor of RHIM-dependent interactions (Rebsamen et al., 2009; Upton et al., 2008).

In this study, we demonstrate that macrophage survival following TLR-engagement requires caspase activity to suppress RIP3-dependent necrosis. TLRs rely on either MyD88 or TRIF for signal transduction. Those using the adaptor protein MyD88, trigger RIP1-RIP3 activation indirectly by inducing intermediate TNF that drives necroptosis via TNFR1, while TLR3 and TLR4 drive RIP3 activation directly via the adapter protein TRIF. In this manner, competing, RHIM-dependent cell death and survival signals radiate from TRIF via RIP3 as well as Casp8. In a manner parallel to TNFR1 and other death receptors, the presence of a virally encoded Casp8 inhibitor or when Casp8 is otherwise compromised, necrotic death becomes unveiled in response to TLR3 or TLR4 activation. Furthermore, TRIF-RIP3 is analogous to virus-induced necrosis mediated by DAI-RIP3 given that both of these pathways trigger necrotic cell death via a pathogen sensor independent of RIP1 kinase. Thus, the host defense arsenal employs programmed necrosis as a trap door that may be initiated by RIP1, DAI or TRIF when caspase 8 activity is compromised. RHIM-dependent oligomerization of RIP3 emerges as the common feature of necrotic death.

B) RESULTS

Macrophage survival following TLR stimulation requires caspase activity. When BMDM were stimulated in the presence of the pan-caspase inhibitor zVAD-fmk, cell death was uniformly induced by all TLR agonists tested, including Pam3CysK (TLR2), poly(I:C) (TLR3), LPS (TLR4), flagellin (TLR5), and CpG DNA (TLR9) as shown in Figure 5.1A. This pattern raised a concern that TNF, a cytokine that is produced following TLR activation (Kumar et al., 2011) and that is known to mediate both apoptotic and necrotic cell death pathways via activation of TNFR1 (Vandenabeele et al., 2010b), might be indirectly responsible for TLR-induced death. To determine whether TNF contributed to death in this setting, we evaluated the same series of agonists in TNF-deficient BMDM. These mutant cells did not die in response to TLR2, TLR5 or TLR9 agonists, indicating that TNF autocrine or paracrine signaling was required for cell death in these settings (Figure 5.1A). The activity of two TLR agonists, poly(I:C) and LPS, was independent of TNF, and correlated with the known reliance of these two TLRs on the adapter protein TRIF. TLR3-induced death was completely unaffected by elimination of TNF, consistent with the use of TRIF for signal transduction (Kumar et al., 2011); whereas, stimulation of TLR4, which is able to use MyD88 as well as TRIF, resulted in a partial dependence on TNF. The kinetics depended on the class of TLR, such that TLR3 and TLR4 agonists induced cell death rapidly, within 4 to 6 h (Figure 5.1B), consistent with a direct impact. In contrast, death induced by TLR2, 5, and 9 became apparent only 12 to 18 h after stimulation (Figure 5.1A). From these data, it appears that MyD88-dependent TLRs signal via an two-stage process involving activation of TNF as an intermediary. Thus, each of the TLRs tested have the biological potential to initiate necrotic death when caspases are inhibited, reinforcing the contribution of programmed

necrosis as a (Vandenabeele et al., 2010b) trap door that opens during infection with viruses encoding caspase inhibitors (Mocarski et al., 2011). The evidence points to a TRIF-dependent, TNF independent pathway that on we investigated further.

We found that TRIF-deficient ($TRIF^{Lps2/Lps2}$) BMDM did not support death induced by either LPS or poly(I:C) in the presence of zVAD-fmk (Figure 1C). To further investigate TRIF signaling, we examined IFN-primed L929 cells, which are sensitive to poly(I:C) induced death (Hitomi et al., 2008). As expected, under these conditions, L929 cells died rapidly (Fig 5.1D). Expression of a dominant negative TIR-only truncation (TRIF-TIR-M) (Yamamoto et al., 2002) suppressed cell death (Figure 5.1D), indicating the role of TLR3 rather than other dsRNA sensors. TRIF-specific signaling via TLR3 or TLR4 requires endocytosis and endosomal acidification (Kawai and Akira, 2011; Kumar et al., 2011). Consistent with a requirement of endosomal acidification, the inhibitor Bafilomycin A₁ completely prevented cell death (Figure 5.1D). Furthermore, addition of TNF-neutralizing antibody failed to block death when used at concentrations that effectively suppressed TNF-dependent necroptosis (Upton et al., 2010). TNF alone was not effective (Figure 5.1E), again consistent with poly(I:C) being a potent TNF-independent inducer of cell death. Similar to L929 cells, IFN β primed WT and TNF KO MEFs were susceptible to TLR3-induced necrosis; whereas, TRIF-deficient MEFs were resistant to death (Figure 5.1F). Thus, similar to BMDM, both L929 and MEF cells support TLR3-induced, TRIF-dependent cell death that is TNF-independent.

We next focused on the mechanism through which TRIF signals. NIH3T3 fibroblasts are susceptible to death receptor-induced apoptosis but not necrosis; whereas, 3T3-SA fibroblasts support both pathways due to adequate levels of RIP3 to support necrosis (Upton et al., 2010; Zhang et al., 2009). As expected (Kaiser and Offermann, 2005), overexpression of TRIF in

NIH3T3 fibroblasts led to cell death that was reversed by addition of caspase inhibitor zVAD-fmk (Figure 5.2A), consistent with the induction of apoptosis. When TRIF was overexpressed in 3T3-SA murine fibroblasts, caspase inhibition with zVAD-fmk triggered necrotic death. Thus, TRIF has the capacity to transduce signals for either caspase-dependent apoptosis or programmed necrosis. Consistent with known signaling properties of TRIF, cell death was dependent on RHIM signaling, as overexpression of a mutant RHIM construct (TRIF-mutRHIM) failed to induce cell death (Figure 5.2B) and virally encoded RHIM antagonist (vIRA), known to prevent RHIM-dependent interactions and disrupt cellular RHIM-dependent signal transduction (Rebsamen et al., 2009; Upton et al., 2008), abrogated cell death induction. To reinforce the RHIM-dependence of this pathway, BMDM were infected with WT or vIRA mutant (M45mutRHIM) MCMV for 12 h and then stimulated with either LPS or poly(I:C) in the presence of zVAD-fmk. WT, but not mutant virus blocked TLR3 or TLR4-induced death, indicating that RHIM-dependent signaling was crucial for TRIF-mediated programmed necrosis (Figure 5.2C).

To further define the pathway controlled via TRIF signaling, we evaluated the contribution of RIP1 and RIP3 kinases in death pathways. A TRIF-RIP3 complex was detected (Figure 5.3A) following stimulation with poly(I:C) in the absence or presence of caspase inhibitor. Interestingly, RIP3 rapidly migrated to the detergent insoluble fraction (Figure 3B), in a pattern that was reminiscent of oligomerization. This interaction appeared to cause similar post-translational modification affecting RIP1 solubility as occurs in death receptor signaling (Gentle et al., 2011). Within an hour of TLR3 stimulation, both RIP1 and RIP3 migrated more slowly, consistent with the type of phosphorylation-induced changes that accompany necroptosis. Thus, both RIP1 and RIP3 become engaged following TLR3 activation in ways that have been previously shown to occur to RIP1 following death receptor activation (He et al., 2011; Kaiser and Offermann, 2005; Meylan et al., 2004).

Based on these data, we focused on the contribution of RIP3 to TLR-signaling. RIP3 is known to be dispensable for activation of NF- κ B by either TLR3 (Figure 5.4A) or TLR4 (Newton et al., 2004). RIP3-deficient BMDM were resistant to death induced by TLR3 or TLR4, indicating that caspase activity suppresses RIP3-dependent necrosis to maintain cell survival in this setting (Figure 5.4B). Because TRIF activates both NF- κ B and IRF3, resulting in IFN β production (Kaiser and Offermann, 2005; Kawai and Akira, 2007), we examined a C-terminal truncation of TRIF (TRIF-C), containing only the RHIM domain, which can interact with RIP1 and RIP3 kinases but is deficient in triggering IRF3 activation (Kaiser, 2005 #60). Expression of TRIF-C, but not TRIF-C-mutRHIM induced similar levels of necrosis as full-length TRIF, indicating cell death signaling was RHIM-dependent but independent of the N-terminal TRAF-binding regions and TIR that are crucial for activation of NF- κ B and IRF3, respectively (Meylan et al., 2004). Consistent with this result, expression of TRIF-C retained the ability to mediate necrosis even in the presence of the dominant negative I κ B α super repressor (I κ B α -SR) (Van Antwerp et al., 1996) (data not shown). Therefore, neither NF- κ B- nor IRF3-activated gene expression contribute to TRIF-induced necrosis. This pattern is similar to that shown for virus-induced necrosis mediated by the pathogen sensor DAI (Upton et al., 2012). Next, we stimulated L929 cells expressing either RIP3 shRNA or a control scramble (Sc) shRNA with poly(I:C) in the presence of zVAD-fmk. Cells where RIP3 expression was depleted were resistant to TLR3-induced necrosis (Figure 5.4C and D). Furthermore, RIP3 was crucial for necrosis induced by transient TRIF overexpression such that TRIF-C expression in RIP3 shRNA-expressing 3T3-SA cells resisted necrosis (Figure 5.4E). Similar to BMDM lacking RIP3, RIP3 KO MEFs did not die under these conditions (Figure 5.4F). Importantly, reconstitution studies in RIP3 KO MEFs revealed that the kinase domain and RHIM of RIP3 as well as the RHIM of TRIF are all essential for TLR3-induced necrosis (Figure 5.4G).

This requirement for the RIP3 kinase domain suggested that kinase activity may mediate

necrosis. To evaluate the contribution of RIP3 kinase activity more directly, we utilized two recently identified potent and selective RIP3 kinase inhibitors, GSK'843 and GSK'872, that, importantly, have no impact on RIP1 kinase (P. G., C. S., R. M. and J. B., manuscript in preparation). First, we confirmed the ability of these inhibitors to prevent necroptosis in 3T3-SA cells (Vandenabeele et al., 2010b) by showing both compounds suppressed TNF-induced death in a dose dependent fashion (Figure 5.5A), confirming the importance of RIP3 in this pathway. Second, the RIP3 inhibitors also prevented virus-induced necrosis, which is dependent on a DAI-RIP3 complex but independent of RIP1 (Upton et al., 2012) (Figure 5.5B). Finally, and most relevant here, both RIP3 kinase inhibitors also protected cells from TLR3-induced necrosis induced by poly(I:C) in the presence of zVAD-fmk (Figure 5.5C). These data reinforce the specificity of these inhibitors for RIP3 kinase and show that this activity contributes directly to TLR3-induced necrosis as it does in RIP1-RIP3 necroptosis as well as DAI-RIP3 virus-induced necrosis.

We next determined whether RIP1 kinase activity played any role in TLR3-induced necrosis by employing the RIP1 kinase inhibitor Nec-1 (Degterev et al., 2008)(Figure 5.4A). 3T3-SA and SVEC4-10 cells were susceptible to TLR3-induced necrosis in the presence of Nec-1 (Figure 5.5C and D) at a concentration of drug that effectively blocked TNF-induced necroptosis (Upton et al., 2010). Furthermore, shRNA-mediated RIP1 suppression in SVEC4-10 did not alter sensitivity to TLR3-induced necrosis (Figure 5.5D). Consistent with these knock-down experiments, RIP1-deficient MRFs were as sensitive as WT MEFs to TLR3-induced necrosis (Figure 5.5E). Even though RIP1 behaves as if it is engaging the other RHIM adaptors, this protein kinase is dispensable for TRIF-signaling dependent programmed necrosis. Thus, in contrast to the death receptor-induced necroptosis, but similar to DAI/RIP3 virus-induced necrosis, TLR3-induced necrosis proceeds independent of RIP1.

TRIF dependent necrosis required the inclusion of the broad caspase inhibitor zVAD-fmk. To directly evaluate the contribution of Casp8, we employed the virus-encoded Casp8-specific inhibitor, vICA to sensitize cells to TNF-induced necroptosis (Kaiser et al., 2011). When coexpressed with TRIF, this inhibitor blocked cell death in NIH3T3 cells and induced cell death in 3T3-SA cells. These results show that sustained Casp8 catalytic activity regulates the susceptibility to necrotic cell death (Figure 5.6A and data not shown). In contrast, cells resisted death when either RIP3 levels were reduced using RIP3 shRNA or following coexpression of the RHIM antagonist vIRA (Figure 5.6A). Cells deficient in Casp8 died following TLR-stimulation, even in the absence of caspase inhibitor zVAD-fmk indicating that Casp8 is likely the physiologic target of zVAD-fmk which confers sensitivity to necrotic death when proteolytic activity is antagonized (Figure 5.6B). Casp8/RIP3 DKO fibroblasts were resistant to poly(I:C) induced necrosis indicating that the loss of Casp8 triggered RIP3-dependent necrosis (data not shown). Thus, TLR3-signaling requires Casp8 to suppress a RIP3-dependent pathway that was independent of RIP1.

FADD or Casp8-deficient mice die during midgestation (E10.5-E11.5) due to aberrant RIP1 (Zhang et al., 2011b) (data not shown) and RIP3 activity (Kaiser et al., 2011; Oberst et al., 2011). Casp8-null mice develop normally in the absence of either RIP1 or RIP3; however, the signals driving midgestational demise is unclear and may be due to activation of RIP1 or RIP3 via a RHIM-containing adapter protein. To test a possible contribution of TRIF to the Casp8-null phenotype, we crossed Casp8 KO and TRIF^(Lps2/Lps2) mice. Casp8/TRIF double-mutant mice were not viable (Figure 5.6C) and died at E10.5 similar to Casp8 mutant embryos (data not shown). Thus, the RHIM containing proteins RIP1 and RIP3 but not DAI (Upton et al., 2012) or TRIF (this study) mediate RIP1/RIP3-dependent developmental defects caused by Casp8-deficiency.

C) DISCUSSION

The sentinel role of macrophages in innate immunity depends on pathogen sensing (via TLRs, and other PRRs) to detect foreign signatures on proteins, carbohydrates, lipids, and, in the case of viruses, nucleic acids. Once triggered, macrophages respond both directly and indirectly to facilitate elimination of pathogens. Two distinct programmed cell death pathways, apoptosis and necrosis, play alternate evolutionarily ancient roles that are differentially regulated by Casp8 following death receptor activation. A similar pattern emerges from TLR stimulation, such that both MyD88- and TRIF-dependent pathways drive pro-survival caspase levels in macrophages, that, when compromised, unleashes RIP3 kinase-dependent necrosis. Thereby, cell fate is dictated via pathogen recognition using the machinery that has been most closely associated with death receptors. Together, death receptor and pathogen sensing provides macrophages with the capacity to respond to broad range of infection-associated signals, executing dual roles as professional phagocytes and innate immune sentinels in host defense. Expanded capacity to trigger cell death certainly fits with the distribution of these cells in all tissues as well as their rapid recruitment from bone marrow via the bloodstream during infection or inflammation. Macrophages express the broadest complement of PRRs of any cell type and sense both foreign and host-derived molecular signatures to trigger activation of inflammatory transcription as well as cell death. Two general patterns emerged from our studies: (1) MyD88-dependent TLRs initiate the production of TNF as a result of NF- κ B activation, with TNF then mediating conventional RIP1-RIP3 kinase-dependent necroptosis. In contrast, TLR3 and TLR4, act through a novel TRIF-RIP3 complex to initiate RIP3 kinase-dependent necrosis. The TRIF-RIP3 pathway is distinct from the MyD88-death receptor axis in that it proceeds independent of NF- κ B and TNF, does not require RIP1 and follows a more rapid

time course. Thus, macrophages, a cell type exquisitely sensitive to Casp8 function for development and activation, rely on this caspase to promote apoptosis and suppress necrosis.

TLR3 and TLR4 make use of the adapter protein TRIF to trigger NF- κ B activation as well as cell death pathways (He et al., 2011; Kaiser and Offermann, 2005; Meylan et al., 2004). TRIF-dependent TLR signaling has many parallels to death receptor signaling: (1) RIP1 controls NF- κ B activation in a RIP3-independent manner; (2) basal Casp8 activity suppresses programmed necrosis and autoactivation of Casp8 drives apoptosis; and, (3) a compromise in Casp8 activity unleashes RIP3 kinase-dependent programmed necrosis. A central role of Casp8 in both death receptor and TLR necrotic signaling can be recognized through the importance of basal catalytic activity that prevents the activation of RIP3 kinase-dependent death. The most dramatic manifestation of this control is the contribution that RIP3 makes in midgestation death of Casp8-deficient mice (Kaiser et al., 2011). The pattern of death has prompted a search for upstream triggers that depend on RIP1 (Zhang et al., 2011b) in addition to RIP3, but proceed completely independent of either DAI (Upton et al., 2012) nor TRIF (this work). The range distinct settings where RIP3-dependent cell death becomes unleashed (Mocarski et al., 2011) provides evidence of homeostatic regulation via basal Casp8 activity that remains important throughout life.

Casp8 catalytic activity most likely regulates the formation of a signaling complex that has been variously called the Complex IIB or Ripoptosome, depending on the stimulus involved. When Casp8 activity is compromised, both RIP1 and RIP3 rapidly associate with a detergent insoluble cell fraction consistent with a process of RHIM-dependent oligomerization. This process is concomitant with execution of programmed necrosis. Although Casp8 is able to recognize both RIP1 and RIP3 as substrates (Chan et al., 2003; Feng et al., 2007; Lin et al., 1999), we did not detect cleavage of either protein kinase following TLR3 activation. Casp8 targets many potential regulatory proteins including deubiquitinylases, such as CYLD (O'Donnell et al.,

2011), whose activities depend on RIP1 and RIP3 necrotic signaling. Furthermore, Festivikova et al. (Feoktistova et al., 2011) identified a complex between Casp8 and its non-catalytic partner cFLIP_L that prevented apoptosis that our evidence shows is mediated by TRIF. These observations predict a decision point very similar to death receptor signaling where cFLIP_L regulates cell fate by facilitating basal Casp8 activity that cleaves key mediators to suppress necrosis (Oberst et al., 2011). Additional studies will surely provide further insights into this regulation.

In TNF-signaling, RIP3 is recruited via the RHIM in RIP1 forming an oligomeric complex, mediating necroptosis (Vandenabeele et al., 2010a). In TLR3 signaling, TRIF is the RIP3 partner and RIP1 is dispensable. This situation, like that dependent on DAI-RIP3 complex formation (Upton et al., 2012), suggests that there is no need for a protein kinase like RIP1 upstream of RIP3 to drive programmed necrosis. The situation seems reminiscent of work from Meylan et al (Meylan et al., 2004) where RIP1 and RIP3 were shown to differentially compete for RHIM-dependent binding with TRIF. It is possible that high affinity TRIF-mediated RHIM-dependent interaction with RIP3 overcomes the requirement for RIP1 kinase, and oligomerization is sufficient to trigger RIP3 kinase activity. This would also parallel events that accompany DAI recruitment of RIP3 to induce virus-induced necrosis as a trap door in host defense to eliminate virus-infected cells when Casp8 is naturally inhibited by vICA (Upton et al., 2012). Given the importance of virus-encoded caspase inhibitors in the execution of the DAI-RIP3 pathway, virus-encoded inhibitors are likely to predispose to TRIF-RIP3 as well as RIP1-RIP3 necrosis in natural infections. We predict that a common kinase target is involved no matter which of the three RIP3 complexes initiates oligomerization. Signaling may converge on MLKL and/or PGAM5 in a serine/threonine protein kinase-dependent cascade (Sun L Fau - Wang et al., 2012; Wang Z Fau -

Jiang et al., 2012). In this way, intracellular pathogens may be recognized and eliminated with PRRs and death receptors working in tandem through common cell death pathways.

Strategies used by hosts to detect and eliminate pathogens play out in a range of seemingly related ways. Although activation of cytokines, chemokines and interferon has predominated the observations in TLR signaling as a component of host defense (Kumar et al., 2011), cell fate is also decided (Mocarski et al., 2011). This collaboration at the front lines of innate immunity assures that a common arsenal of effector mechanisms is available no matter the nature of the infectious insult. Plants contend with pathogens by detecting altered biochemical signatures through resistance proteins. These 'guard' proteins sense perturbation of key cellular processes and trigger anti-microbial defenses that include cell death (Medzhitov, 2010). A cognate and comparable mammalian innate immune strategy remains a possibility. RIP3 kinase may function as a sensor of basal Casp8 activity by eliminating cells via necrosis whenever pathogen-associated suppression of Casp8 occurs. Most mammalian DNA viruses encode genes that suppress Casp8 activity to prevent apoptosis (Mocarski et al., 2011). Of course, RIP3 kinase-dependent programmed necrosis was initially revealed when TNF signaling was carried out in the presence of the anti-apoptotic cowpox Casp8 inhibitor CrmA (Vercammen et al., 1998a). This illustrates the natural settings where necrotic death may be called upon to eliminate pathogen-infected cells (Mocarski et al., 2011; Upton et al., 2010, 2012).

Signaling from TLR3 and TLR9 are known to collaborate in restricting systemic MCMV infection *in vivo* (Tabeta et al., 2004). Here, we demonstrate that activation of either receptor leads either directly or indirectly to Casp8-regulation of apoptotic or necrotic death decisions. This virus, like all herpesviruses, is heavily invested in orchestrating cell fate decisions by elaborating an assortment of cell death suppressors, some of which are evolutionarily conserved from mice to humans (Cicin-Sain et al., 2008; Goldmacher et al., 1999; Mack et al., 2008;

McCormick et al., 2005; McCormick et al., 2008; Menard et al., 2003; Skaletskaya et al., 2001; Upton et al., 2008). The conserved vICA binds to the prodomain of Casp8 to prevent homodimerization and autocleavage preceding apoptosis (Skaletskaya et al., 2001). At the same time, this activity predisposes the cell to TNF-driven necroptosis (Kaiser et al., 2011). Here, we have shown that this inhibitor also predisposes to TLR-induced necrosis. Cytomegalovirus pathogenesis in mice requires vIRA suppression of RIP3 (Upton et al., 2010). Although DAI-RIP3 emerged the predominant natural target of vIRA (Mocarski et al., 2011; Upton et al., 2010, 2012), this RHIM inhibitor would prevent TRIP-RIP3 as well as RIP1-RIP3 complex signaling in virus-infected cells. MCMV illustrates the potentially precarious but seemingly successful balance with the entwined necrotic and apoptotic host defense pathways; whereas, another large DNA virus, vaccinia, appears vulnerable to RIP3-dependent pathways that become triggered during infection (Cho et al., 2009). Clearly, viruses exhibit variable levels of success in preventing the TLR and death receptor signaling pathways that employ RIP kinases to sense compromised Casp8 activity and eliminate infected cells. Such is the host-pathogen arms race.

D) MATERIALS AND METHODS

Mice. TRIF mutant (Strain - C57BL/6J-Ticam1^{Lps2}) mice (Hoebe et al., 2003) were from Jackson Laboratory. *RIP3*^{-/-} mice (Newton et al., 2004), *RIP1*^{+/-} mice (Kelliher et al., 1998), *TNF*^{-/-} (Kuprash et al., 2002) and *Casp8*^{+/-} mice (Salmena et al., 2003) were described (Kaiser et al., 2011). Mice were bred and maintained by Emory University Division of Animal Resources where all procedures were approved by the Emory University Institutional Animal Care and Use Committee.

Cell culture, plasmids, transfections and transductions. L929, NIH3T3, 3T3-SA, SVEC4-10, and primary MEFs were maintained in DMEM containing 4.5 g/mL glucose, 10% FBS (Atlanta Biologicals), 2 mM L-glutamine, 100 U/mL penicillin and 100 U/mL streptomycin (Invitrogen). For bone marrow derived macrophage (BMDM) culture, pooled bone marrow cells from flushed tibias and femurs were harvested with PBS containing 0.5 mM EDTA, and then cultured for at least 18 h in DMEM containing 10% FBS prior to differentiation for 5 to 7 days in DMEM containing 20% FBS and 20% L929-conditioned medium to provide macrophage colony-stimulating factor (M-CSF). Where indicated, cells were stimulated with murine IFN β (Chemicon) or TNF (Peprotech) or were stimulated in the presence of anti-TNF α (R&D Systems). The following compounds were employed: necrostatin (Nec)-1 (Calbiochem) and z-VAD-fmk (Enzo Life Sciences), Bafilomycin A₁ (Sigma) and cycloheximide (CHX; Sigma), poly(I:C) (GE healthcare), and LPS, Pam3CysK, and CpG DNA (Invivogen). Flagellin was kindly provided by Andrew Gewirtz (Georgia State University). Selective, small molecule RIP3 kinase inhibitors GSK'843 and GSK'872 were identified through compound screening and optimization efforts (P. Gough, C. Sehon, R Marquis and J. Bertin, manuscript in preparation). Transient transfections were performed using Effectene (Qiagen) according to the manufacturer's protocol. The pLKO.1-based RIP3 shRNA

constructs were obtained from Open Biosystems (TRCN0000022535). The pLKO.1 control scramble shRNA vector, lentiviral/retroviral vector production, infection, and selection of transduced cells as well as all other plasmids have been described (Kaiser and Offermann, 2005; Kaiser et al., 2011; Kaiser et al., 2008; Upton et al., 2008, 2010).

Immunoblot and immunoprecipitations. Immunoblotting, preparation of protein extracts, and immunoprecipitations (Kaiser and Offermann, 2005; Upton et al., 2010) employed the following antibodies: mouse anti- β -actin (clone AC-74; Sigma), mouse anti-RIP1 (clone 38; BD Biosciences), rabbit anti-RIP3 (Imgenex), goat anti-RIP3 (clone C-16; Santa Cruz), rabbit anti-I κ B α (Santa Cruz), rabbit anti-phospho-I κ B α (Cell Signaling Technology), anti-mouse IgG-HRP (Vector Laboratories), and anti-rabbit IgG-HRP (Vector Laboratories). For IP analyses, goat anti-RIP3 anti-body and protein A/G agarose (Santa Cruz) were used.

Cell viability assays. Viability of L929 cells (5000 cells/well), BMDM (30,000 cells/well), NIH3T3 (10,000 cells/well), 3T3-SA (10,000 cells/well), SVEC4-10 (10,000 cells/well) were seeded into Corning 96-well tissue culture plates (3610). Cell viability was determined indirectly by measuring the intracellular levels of ATP using the Cell Titer-Glo Luminescent Cell Viability Assay kit (Promega) according to the manufacturer's instructions and was graphed relative to control cultures. Luminescence was measured on a Synergy HT Multi-Detection Microplate Reader (BioTek). Where indicated, an alternative viability assay was employed to determine the levels of cell death following transient transfection of 3T3-SA cells. This EGFP positive cell viability assay involved enumerating the number of EGFP-positive cells at 24 h post-transfection with the indicated TRIF expression plasmids. Loss of EGFP positivity was determined from the ratio of EGFP in experimental versus empty vector expressing control cells (x 100). **E) FIGURES AND**

FIGURE LEGENDS

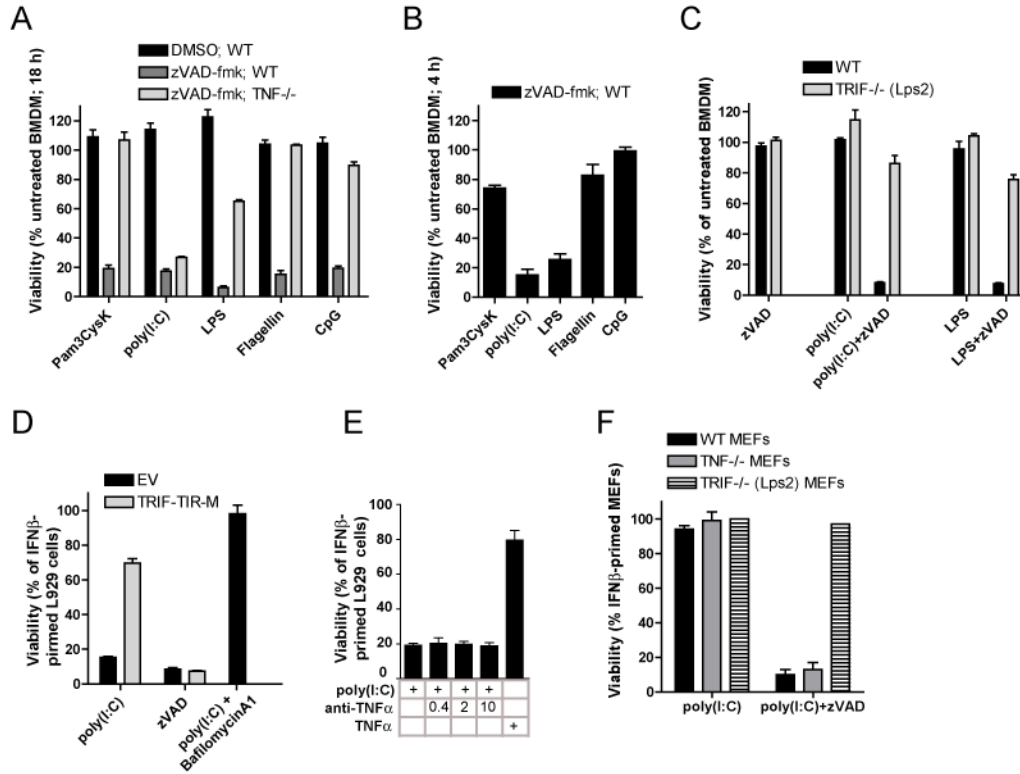


Figure 5.1. TLR stimulation in the presence of caspase inhibitor triggers cell death. (A) Viability of WT and TNF^{-/-} BMDM at 18 h after stimulation with Pam3CysK (1 μ g/mL), poly(I:C) (25 μ g/mL), LPS (500 ng/mL), flagellin (500 ng/mL), or CpG (1 μ g/mL) in the presence of zVAD-fmk (25 μ M) or vehicle (DMSO) control. **(B)** Viability of WT BMDM at 6 h after stimulation with the indicated TLR ligands in the presence of zVAD-fmk. **(C)** Viability of WT or TRIF mutant (*Lps2/Lps2*) BMDM at 18 h after stimulation with poly(I:C) or LPS in the presence or absence of zVAD-fmk. **(D)** Viability of IFN β -primed L929 cells stably expressing a dominant negative TRIF-TIR domain-only construct (TRIF-TIR-M) or vector only control (EV). Cells were first primed with

(Figure 5.1 continued) IFN β (50 units/mL) for 24 hours and then stimulated with poly(I:C) in the absence or presence of zVAD-fmk, or with poly(I:C) and Bafilomycin A₁ (500 nM) for 18h, as indicated. **(E)** Viability of IFN β -primed L929 cells stimulated with poly(I:C) in the presence of the indicated concentration of either TNF-neutralizing antibody (anti-TNF) or treated with TNF (10 μ g/mL) alone. **(F)** Viability of WT, TNF^{-/-}, or TRIF^{Lps2/Lps2} MEFs at 18 h after stimulation with TLR3 agonist poly(I:C) in the presence of zVAD-fmk. Cell viability was assessed by determining ATP levels (CellTiterGlo, Promega). Error bars, SD.

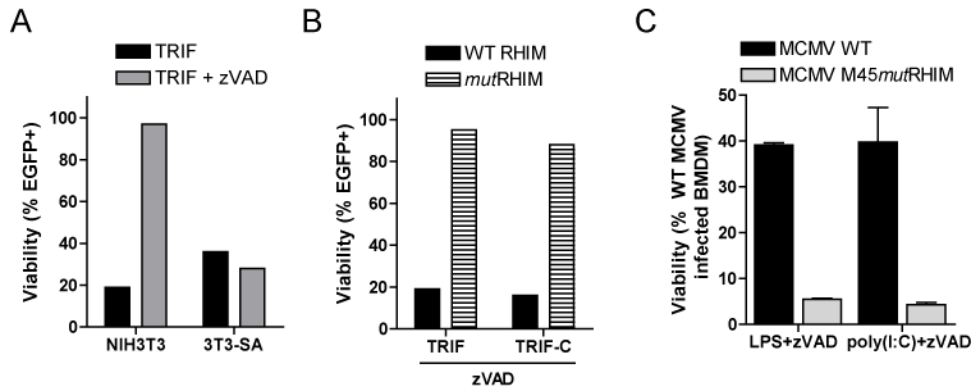


Figure 5.2. TLR3 stimulation triggers programmed necrosis dependent on TRIF and inhibited by

MCMV vIRA. (A) The EGFP positive cell assay described in the Material and Methods was used to assess viability of necrosis-insensitive NIH3T3 or necrosis-sensitive 3T3-SA fibroblasts at 24 h after transfection with plasmids expressing TRIF together with EGFP marker, in the absence or presence of zVAD-fmk. **(B)** The EGFP positive cell assay was used to assess viability of 3T3-SA cells transfected with plasmids expressing TRIF, TRIF-mutRHIM, TRIF-C, or TRIF-C-mutRHIM in the presence of zVAD-fmk. **(C)** The Cell Titer Glo Assay was used to assess viability of BMDM after infection with either WT or M45mutRHIM (vIRAmutRHIM) MCMV (multiplicity of infection of 5) for 18 h followed by treatment with either LPS or poly(I:C) in the presence of zVAD-fmk. Error bars, SD.

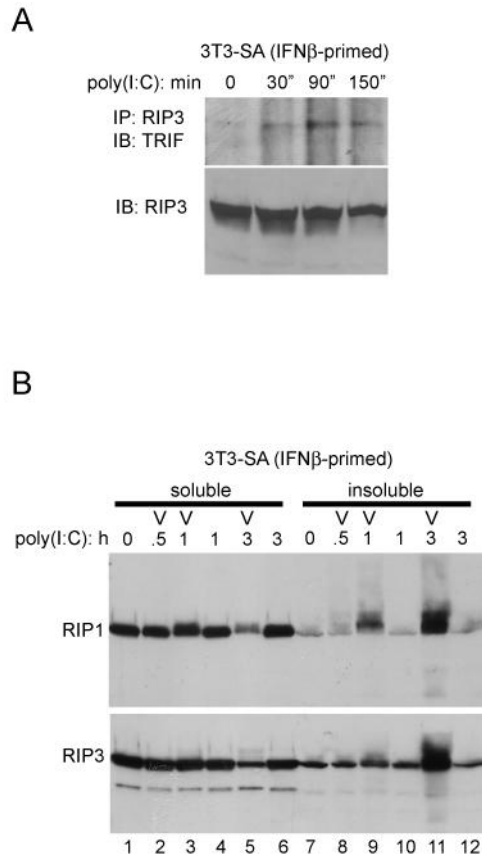


Figure 5.3. TLR3 activation induces a TRIF-RIP1 and TRIF-RIP3 complex. (A) Following priming of 3T3-SA cells for 24h, cells were stimulated with poly(I:C) (25 μ g/mL) RIP3 was immunoprecipitated (IP) from cell lysates to detect an interaction with TRIF. **(B)** Immunoblot detecting RIP1 and RIP3 present in the soluble (1% Triton) and insoluble (pellet) fraction following stimulation of 3T3-SA cells with poly(I:C) for the indicated times (h) in the absence or presence (V) of the caspase inhibitor zVAD-fmk.

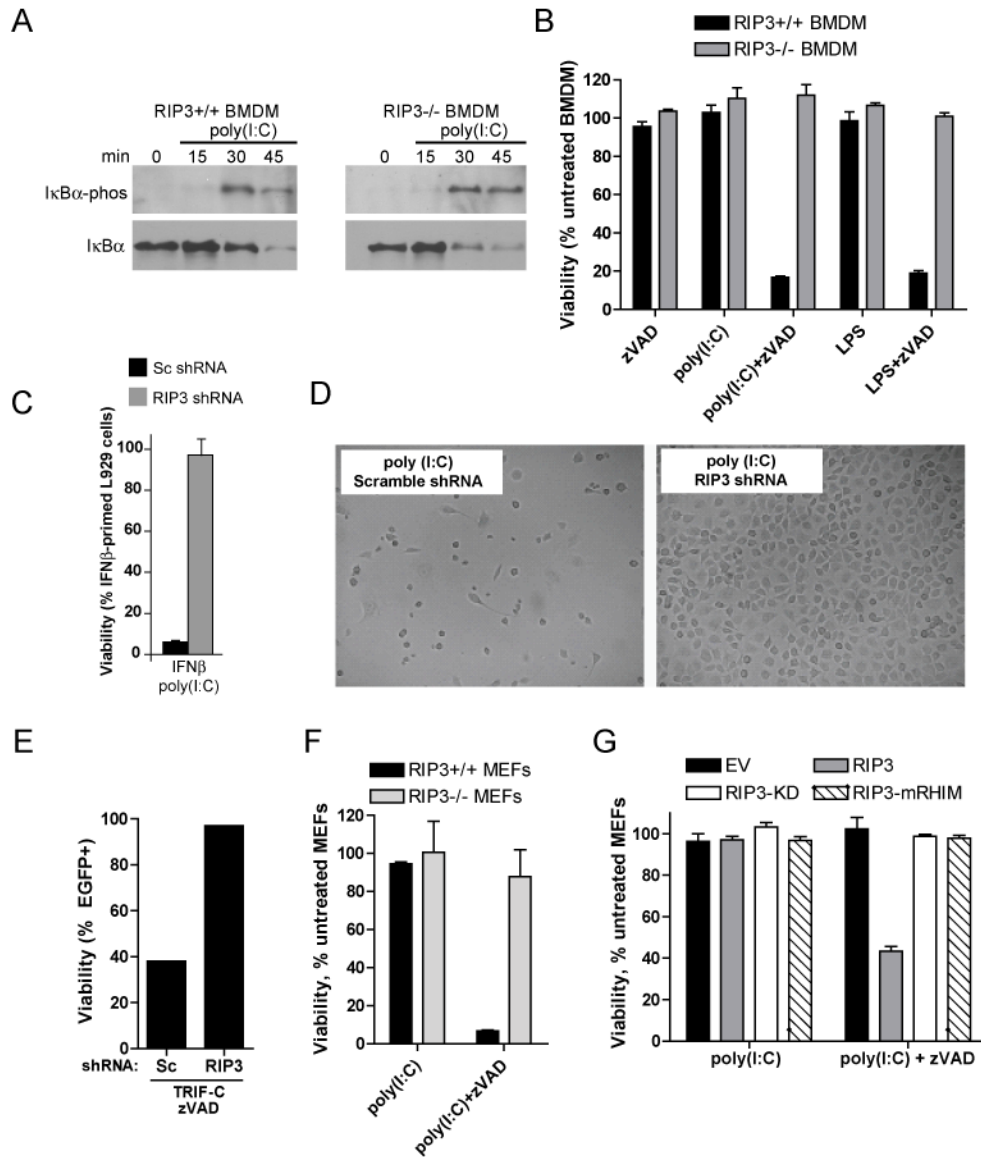


Figure 5.4. TLR3 induced programmed necrosis requires RIP3. (A) Immunoblot detection of total and phosphorylated IκBα in WT (RIP3^{+/+}; left panel) or RIP3^{-/-} (right panel) BMDM following stimulation for the indicated times (min) with poly(I:C). **(B-F)** Viability of WT (RIP3^{+/+}) or RIP3^{-/-} BMDM **(B)**, IFNβ-primed L929 cells expressing control scramble (Sc) or RIP3-specific shRNA **(C)**, IFNβ-primed 3T3-SA cells expressing Sc shRNA or RIP3-specific shRNA at 24 h post-transfection

(Figure 5.4 continued) with TRIF-C plasmid **(D)**, IFN β -primed WT (RIP3^{+/+}) or RIP3^{-/-} MEFs **(E)**, RIP3^{-/-} MEFs reconstituted with WT RIP3, RIP3-KD, or RIP3-mRHIM **(F)**, all at 18 h after stimulation with poly(I:C) in the presence of zVAD-fmk. Photomicrographs of Sc shRNA or RIP3-specific shRNA-expressing L929 cells stimulated for 18 h with poly(I:C) in zVAD-fmk. Cell viability in panels B, C, E and F was determined by ATP assay described in Figure 1 and, in panel D, the EGFP viability assay described in Figure 2 was employed.

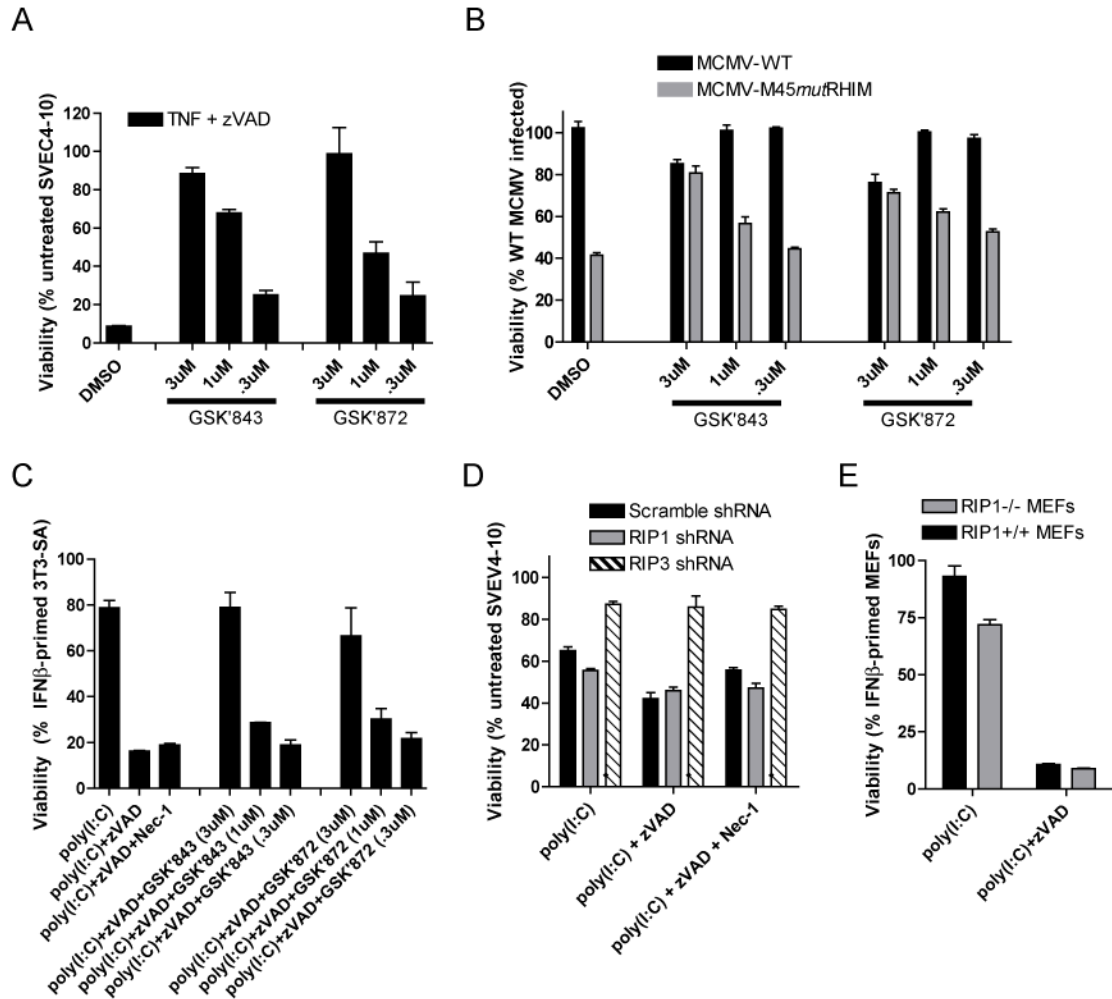


Figure 5.5. Role of RIP3 kinase in TLR3-induced programmed necrosis. (A) Viability of 3T3-SA cells at 18 h after treatment with TNF in the presence of zVAD-fmk in vehicle control (DMSO) or treated with the indicated concentrations of RIP3 kinase inhibitors, GSK'843 or GSK'872. **(B)** Viability of SVEC4-10 cells at 18 h post infection with WT or M45mutRHIM MCMV in vehicle control (DMSO) or treated with the indicated concentrations of RIP3 kinase inhibitors, GSK'843 or GSK'872. **(C)** Viability of IFNβ-primed 3T3-SA cells at 18 h after stimulation with poly(I:C) in the absence or presence of zVAD-fmk, as indicated, and treatment with Nec-1 (30 μM) or the indicated concentrations of RIP3 kinase inhibitors, GSK'843 or GSK'872. **(D)** Viability of IFNβ-primed SVEC4-10 cells expressing control scramble, RIP1-specific or RIP3-specific shRNA in the

(Figure 5.5 continued) absence or presence of zVAD-fmk and Nec-1 (30 μ M), as indicated. **(E)** IFN β -primed WT (RIP3^{+/+}) or RIP3^{-/-} MEFs at 18 h after stimulation with poly(I:C) in the absence or presence of zVAD-fmk. Cell viability was determined by the ATP assay described in Figure 1. Inquiries about RIP3 kinase inhibitors GSK'843 and GSK'872 should be directed to P. G. (peter.j.gough@gsk.com).

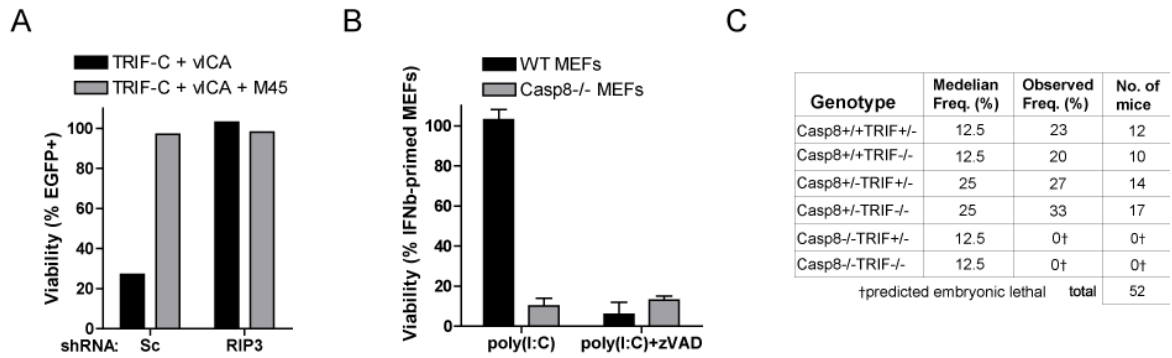


Figure 5.6. Casp8 suppression of TLR3-mediated TRIF- and RIP3-dependent programmed necrosis. (A) The viability of 3T3-SA cells stably expressing a control Sc or RIP3-specific shRNA at 24 h post-transfection with plasmids expressing TRIF-C and vICA together with either vIRA (M45) or a vector control, as indicated. The EGFP cell viability assay was used to determine cell viability at 24 h post-transfection. **(B)** Viability of WT or Casp8^{-/-} MEFs at 18 h after stimulation with poly(I:C) in the absence or presence of zVAD-fmk. Cell viability was determined by ATP levels as described in Figure 1. Error bars, SD. **(C)** Epistatic analysis of mice born following a Casp8^{+/-} TRIF^{+/-}Lps2 X Casp8^{+/-}TRIF^{Lps2/Lps2} intercross with predicted and observed frequencies.

Chapter 6: General Discussion and Future Directions⁵

Pathogens specifically target both Casp8-dependent apoptotic as well as RIP1- and RIP3-dependent necrotic death pathways. The fundamental co-regulation of these important host defense cell death pathways emerged when we found that the midgestational death of mice deficient in Casp8 was prevented by elimination of RIP1 or RIP3, indicating a far more expansive and entwined relationship of these death pathways than previously appreciated. Thus, mammalian life demands Casp8 activity to suppress the kinases RIP1-RIP3 as part of the dialogue between two distinct death processes that together fulfill reinforcing roles in the host defense against intracellular pathogens such as herpesviruses. Clearly Casp8-regulated pathways exist in mammals for host defense purposes. The many examples where Casp8 deficiency leads to inadvertent activation of RIP3-dependent tissue damage where both Casp8 and RIP3 are dispensable for life is a lesson. An impact on development and tissue homeostasis can occur though dysregulation of cell death pathways intended to deal with pathogens. It would not be surprising to see that these underlie disease pathogenesis in many settings.

Investigators struggled for a decade to explain why mice with germline disruption of Casp8, FADD, or cellular or cFLIP die at embryonic day 10 (E10) to E11). This death implied a crucial coordinate non-apoptotic activity of Casp8–FADD–cFLIP complexes (Kang et al., 2004; Kang et al., 2008; Sakamaki et al., 2002; Varfolomeev et al., 1998). Since RIP1-RIP3-dependent programmed necrosis is unveiled when Casp8 activity is compromised (Vandenabeele et al., 2010b), we investigated in Chapter 3 whether aberrant RIP3 activity contributed to the

⁵ The chapter derives from a published paper entitled “Viral infection and the evolution of caspase 8-regulated apoptotic and necrotic death pathways Pathogen subversion of RIP3-dependent necrosis” (Mocarski et al. 2011). Sections of this chapter have been reproduced in whole, or in part, with permission from the publisher.

embryonic lethality of mice deficient in Casp8. *Casp8^{-/-}Rip3^{-/-}* DKO mice were viable and fertile revealing an essential embryonic role of Casp8 activity in suppressing necroptosis (Kaiser et al., 2011; Oberst et al., 2011). Moreover, RIP1- and/or RIP3- dependent programmed necrosis may arise independent of TNF family death receptors, during virus infection (Chapter 2 & 4) or following activation of Toll-like receptors (TLRs) (Chapter 5) (Moquin and Chan, 2010; Vandenabeele et al., 2010a; You et al., 2008) as well as in settings of genotoxic stress (Tenev et al., 2011).

The constellation of phenotypes that emerge when Casp8 or FADD are eliminated in specific mouse tissues must now be viewed with the understanding that a Casp8-FADD complex controls RIP1–RIP3-mediated necroptosis (Kaiser et al., 2011; Oberst et al., 2011; Zhang et al., 2011b). Remarkably, despite a pattern of midgestational death in *Casp8^{-/-}* mice, the combined disruption of *Casp8* and *Rip3* resulted in embryos with functioning hearts, organized yolk sac endothelial architecture and normal levels of hematopoiesis. These mice appear normal and complete gestation to become fertile adults with no abnormal inflammation (Kaiser et al., 2011; Oberst et al., 2011), similar to *Rip3^{-/-}* mice (Newton et al., 2004). *Fadd^{-/-}Rip1^{-/-}* embryos appear normal throughout gestation but succumb soon after birth due to the absence of RIP1 (Zhang et al., 2011b). Casp8-mediated control of apoptosis is important for T cell homeostasis in adult *Casp8^{-/-}Rip3^{-/-}* mice (Kaiser et al., 2011; Oberst et al., 2011), as well as in mice with T cell-specific disruption of Casp8 or FADD on a *Rip3^{-/-}* background (Ch'en et al., 2011; Lu et al., 2011). Our data presented in Chapters 3 and 5 suggest that the defects and proliferation and premature death of Casp8-null B cells (CD19) following TLR3 and TLR4 stimulation is due to dysregulated RIP3 activation (Beisner et al., 2005; Imtiyaz et al., 2006). Defects in hematopoietic development previously observed in Casp8-null settings were reversed in the absence of RIP3 (Ben Moshe et al., 2007; Imtiyaz et al., 2006; Kaiser et al., 2011; Kang et al., 2004; Rosenberg et

al., 2011). Additionally, the severe inflammatory abnormalities that arise when Casp8 (or FADD) is compromised (Beisner et al., 2005; Ben Moshe et al., 2007; Imtiyaz et al., 2006; Kang et al., 2004; Kovalenko et al., 2009; Lee et al., 2009; Li et al., 2010; Rosenberg et al., 2011) are also the consequence of unleashed necroptosis. Recent demonstration that RIP3-deficiency rescues epithelial necroptosis (Bonnet et al., 2011; Gunther et al., 2011; Welz et al., 2011) reinforces this fact. Thus, the viability of *Casp8^{-/-}Rip3^{-/-}* mice establishes that Casp8 is largely dispensable for mammalian development and tissue homeostasis, leaving the many settings where Casp8 has been implicated in essential non-apoptotic processes ripe for reexamination.

Roles of Casp8 in TCR signaling. The successful rescue of T cell function in *Casp8^{-/-}Rip3^{-/-}* mice (Kaiser et al., 2011; Oberst et al., 2011), in mice carrying *Fadd^{-/-}Rip1^{-/-}* hematopoietic cells (Zhang et al., 2011b), and in mice where T cell-specific Casp8 or FADD deficiency is crossed to a *Rip3^{-/-}* background (Ch'en et al., 2011; Lu et al., 2011) indicates that necroptosis underlies T cell loss in Casp8- or FADD-deficient settings. Early evidence associating NF- κ B and autophagy in this death is not supported by current data (Hedrick et al., 2010). TCR activation in Casp8- or FADD-deficient T cells promotes RIP1-RIP3 dependent necroptosis (Ch'en et al., 2008; Ch'en et al., 2011; Hedrick et al., 2010; Lu et al., 2011). The CARMA–BCL10–MALT1 (CBM) complex (Figure 1.1), activates NF- κ B downstream of the TCR (Gaide et al., 2002; Ruefli-Brasse et al., 2003; Ruland et al., 2001), but also forms a complex with Casp8, cFLIP_L, and RIP1 (Kawadler et al., 2008; Misra et al., 2007). Despite the fact that FADD and Casp8 are critical for T cell proliferation, T cell activation does not result in apoptosis. The explanation provided in 2008 (Ch'en et al., 2008) for the induction of necroptosis in antigen stimulated T cells lacking Casp8 or FADD remains most consistent with the fact that TCR activation requires Casp8 activity to inactivate the necrosome. Whether T cell activation engages necroptotic pathways in natural settings remains to be fully elaborated.

RIP1-independent, DAI/RIP3-dependent programmed necrosis. RIP3 is necessary for necroptosis as well as for murine cytomegalovirus (MCMV)-induced necrosis (Upton et al., 2010) but does not contribute directly to TNFR- or TLR-induced NF- κ B activation or apoptosis (Newton et al., 2004). Despite the inability to support necroptosis (Cho et al., 2009; He et al., 2009; Zhang et al., 2009) or MCMV-induced programmed necrosis (Upton et al., 2010), *Rip3*^{-/-} mice lack obvious developmental or immunological abnormalities (Newton et al., 2004). These animals are resistant to natural mouse pathogens, MCMV (Upton et al., 2010), murine hepatitis virus (Lu et al., 2011) or lymphocytic choriomeningitis virus (Ch'en et al., 2011). However, RIP3-deficient mice are remarkably susceptible to infection with the poxvirus vaccinia (Cho et al., 2009). Thus, sufficient evidence supports a role for RIP3-dependent necrosis pathways in host defense against viral infection. However, these RIP3-dependent pathways may have evolved at a cost, as abnormal levels of necrosis may underlie sterile (Challa and Chan, 2010), as well as pathogen-induced (Gunther et al., 2011; Welz et al., 2011) inflammatory disease.

Although MCMV-induced necrosis requires RIP3 kinase activity and RHIM-dependent interactions (Upton et al., 2010), it is independent of RIP1 and so distinct from necroptosis (Cho et al., 2009; He et al., 2009; Zhang et al., 2009). MCMV-induced necrotic death rapidly eliminates infected cells, cutting short infection before viral replication, reinforcing a role in host defence (Upton et al., 2010). The RHIM-containing adapter proteins RIP1 and TRIF are not involved (Upton et al., 2010). Instead, MCMV-induced programmed necrosis requires interaction with the DNA-dependent activator of interferon regulatory factors (DAI, also known as ZBP1) (Takaoka et al., 2007; Upton et al., 2012) (Figure 6.1). DAI and RIP3 form a RHIM interaction-dependent complex, and the MCMV encoded viral inhibitor of RIP activation (vIRA) blocks this complex (Kaiser et al., 2008; Rebsamen et al., 2009). DAI is a cytosolic DNA sensor (Takaoka and Taniguchi, 2007) potentially contributing to host defense against human CMV

(DeFilippis et al., 2010b). Although DAI-deficient mice lack any obvious developmental phenotype and retain the ability to recognize cytosolic DNA (Ishii et al., 2008), vIRA mutant virus replication is normalized in either RIP3^{-/-} or DAI^{-/-} mice indicating that a DAI-RIP3 complex is the natural target of vIRA to suppress MCMV-induced programmed necrosis.

Viral control of programmed necrosis. Programmed necrosis becomes unveiled only when Casp8 activity is compromised, suggesting the abundance of viral Casp8 inhibitors (Table 1.1) may have driven the counteradaptation of programmed necrosis in host defence (Chan et al., 2003; Cho et al., 2009; Upton et al., 2010). The few viral inhibitors of programmed necrosis have been identified (Upton et al., 2010) (Table 1.1, Figure 1.3) may soon be joined by additional examples. The evolutionary adaptation of necrotic death as host a defence pathway may have driven the acquisition of vIRA by murine CMV (and rat CMV), even though this acquisition did not extend to primate CMVs. Once a primordial vertebrate evolved to execute programmed necrosis in response to pathogen-encoded caspase inhibitors, the arms race became elevated as the pathogen evolved to counteract the additional death pathway. The fact that vICA targets Casp8 (McCormick et al., 2003; Skaletskaya et al., 2001), sensitizing cells to necroptosis (Kaiser et al., 2011) or MCMV-induced necrosis that can be suppressed by vIRA (Upton et al., 2010) fit with this scenario. To formally assess the biological interplay of the cell death suppressors M36 and M45 during MCMV infection, we have generated a series of bacmid-derived mutant viruses harboring mutation in M45, M36, or both and we plan to behavior evaluate the behavior of these viruses in infected cells and animals to formally test whether the DAI-RIP3 necrotic pathway is regulated by Casp8.

Cycles of adaptation and counteradaptation play out through evolution (Paterson et al., 2010), and in the case of herpesviruses, co-survival involves a continually renegotiated battle

over the lifetime of an individual as well as a war that wages over time in populations. In addition to vIRA, the vFLIP homologs from molluscum contagiosum MC159, equine herpesvirus 1 E8, and Kaposi's sarcoma herpesvirus (human herpesvirus 8) K13 also have the capacity to block both apoptosis and necroptosis (Akira and Sato, 2003), indicating that viruses have evolved to encode proteins functionally analogous to cFLIP_L (Moquin and Chan, 2010; Oberst et al., 2011; Upton et al., 2010), although the biochemical mechanisms by which vFLIPs function to inhibit apoptosis and necroptosis remain to be established. As only two distinct strategies are known to subvert necrotic death, the absence of a RHIM-dependent inhibitor like vIRA in primate CMVs may be due to an independent adaptation of a vFLIP-like activity as observed in a few herpesviruses and poxviruses.

Role of cell death pathways in immunity. In addition to its role in natural host defence through elimination of infected cells, programmed cell death plays an important role in shaping host immune responses (Ferguson et al., 2011). While apoptosis is generally viewed as immunologically tolerogenic and necrosis as inherently immunogenic (Thompson, 1995), questions remain as to how different modes of death, particularly programmed necrosis, influences these responses. Despite the absence of Casp8-dependent and RIP3-dependent death pathways, *Casp8^{-/-}Rip3^{-/-}* mice mount immune responses during viral infection (Kaiser et al., 2011), so these mice provide a tool for understanding the contribution of extrinsic apoptosis and necrosome-dependent cell death-induced danger signals (Matzinger, 2002) in innate and adaptive immunity. In addition to the immune competence shown by *Casp8^{-/-}Rip3^{-/-}* mice in controlling MCMV infection (Kaiser et al., 2011), mice reconstituted with *Fadd^{-/-}Rip1^{-/-}* hematopoietic progenitors (Zhang et al., 2011b) or with T cells expressing dominant-negative FADD (Lu et al., 2011) or lacking Casp8 (Ch'en et al., 2011) in a *Rip3^{-/-}* background control RNA virus infections. These observations combined indicate that basic innate and adaptive immune

responses to natural pathogens are sustained despite the elimination of extrinsic apoptosis and programmed necrosis. In *Casp8^{-/-}Rip3^{-/-}* mice, intrinsic apoptosis and inflammatory responses are presumably sufficient for direct elimination of infected cells via programmed cell death, for cross presentation of antigens, for elimination of pathogen-infected cells by activated T cells and for the contraction phase of the immune response as well as for immune memory. It will be important to determine precise apoptotic and inflammatory responses that contribute to immune control of infections and immune regulation in the absence of both Casp8-dependent apoptosis and RIP3-dependent necrosis, given the potential for either pathway to influence adaptive immunity (Galluzzi et al., 2010; Krysko et al., 2006)

T cells naturally exhibit the greatest proliferative capacity of any mammalian cell type. Multiple types of cell death are involved in T cell homeostasis, activation and contraction. FAS-dependent apoptosis mediates the elimination of excess T cells that accumulate over the course of life (Strasser et al., 2009). The importance of FAS signaling in homeostatic T cell control has been evident since the occurrence of abnormal CD3⁺CD4⁻CD8⁻B220⁺ lymphocytes, lymphadenopathy and splenomegaly, were first reported in aging FAS-deficient *lpr/lpr* (Watanabe-Fukunaga et al., 1992) or FAS-ligand-deficient *gld/gld* mice (Nagata and Suda, 1995). A deficit in Casp8 or FADD alone in T cells does not recapitulate this phenotype (Hedrick et al., 2010), although modest lymphoproliferation is sometimes noted (Salmena and Hakem, 2005). Progressive abnormal T cell accumulation similar to that observed in FAS-signaling deficient mice is observed in *Casp8^{-/-}Rip3^{-/-}* mice (Kaiser et al., 2011; Oberst et al., 2011), presumably because Casp8 activation lies directly downstream of FAS in the apoptotic pathway (Strasser et al., 2009). Similar defects are observed in mice with T cell-specific disruption of Casp8 or FADD on a *Rip3^{-/-}* background (Ch'en et al., 2011; Lu et al., 2011). These defects do not compromise T

cell responses toward a variety of viral infections (Bertrand and Vandenabeele, 2011; Ch'en et al., 2011; Kaiser et al., 2011).

RIP1–RIP3-dependent necroptosis underlies murine T cell loss in Casp8- or FADD-deficient settings (Ch'en et al., 2008; Hedrick et al., 2010). T cell response is rescued when necrosome components are eliminated (Bertrand and Vandenabeele, 2011; Ch'en et al., 2011; Cho et al., 2011; Kaiser et al., 2011; Oberst et al., 2011), suggesting regulation of the antigen-specific T cell response may be metered out by necroptosis. However, extrapolating these findings to human biology is complicated by the presence of Caspase 10 (Casp10), a Casp8 paralog not present in mice. Interestingly, different T cell defects are found in individuals with mutant Casp8 or Casp10; Casp8 mutations result in immunodeficiency (Chun et al., 2002), while Casp10 deficiency results in lymphadenopathy, splenomegaly, and autoimmunity (Wang et al., 1999). Thus, human Casp8 and Casp10 may have overlapping function during human embryonic development, as individuals with either mutation have been identified, but have different roles in lymphocyte homeostasis, with Casp8 predicted to control apoptosis and necroptosis and Casp10 predicted to be restricted to apoptosis. The contribution that the two human orthologs make to control of apoptotic and necrotic death in development, host defense, cancer, immunity and disease requires closer comparative evaluation.

Searching for core necrotic cell death machinery. A molecular machinery similar to that described for apoptosis has yet to emerge for programmed necrosis except that RIP3 is a master regulator. How RIP3 executes a necrotic cell death program remains shrouded, though glimmers of a possible core pathway surfaced recently in two recent reports identifying the first phosphorylation targets of RIP3, MLKL and DGAM5 (Sun L Fau - Wang et al., 2012; Wang Z Fau - Jiang et al., 2012). MLKL appears to bridge RIP3 to DGAM5, a phosphorylase that triggers

mitochondrial fission. It is unclear whether these substrates direct necrosis in a cell type specific manner or in response to necrotic stimuli other than TNF stimulation. It will be important to determine whether MLKL and PGAM5 are required for DAI- and TLR3/4-induced necrosis (Figure 6.1). The mechanism by which Casp8 suppresses RIP3 pronecrotic complexes as well as the identity of the players and targets downstream of RIP1/3 remain elusive and warrant intense investigation.

Conclusions. It is now clear that programmed necrosis and apoptosis have complementary roles in host defence against pathogens. One form of programmed necrosis, necroptosis, is dependent on RIP1 and RIP3 and is triggered via death receptors, PRRs, TCR or genotoxic stress, as well as during midgestational development, when Casp8 activity is compromised. Necroptosis has a role in host defence during infection with intracellular pathogens that encode Casp8 inhibitors and contributes to disease pathogenesis in acute or chronic bacterial inflammation. By contrast, MCMV- and TLR3/4- induced programmed necrosis is independent of RIP1 but dependent on RIP3. This virus encodes a RHIM-dependent inhibitor of necroptosis and MCMV-induced programmed necrosis as well as a Casp8 inhibitor that sensitizes infected cells to programmed necrosis. Thus, viral infections, and viral cell death suppressors, may have influenced the evolution of programmed necrosis as an alternative mechanism of host defence.

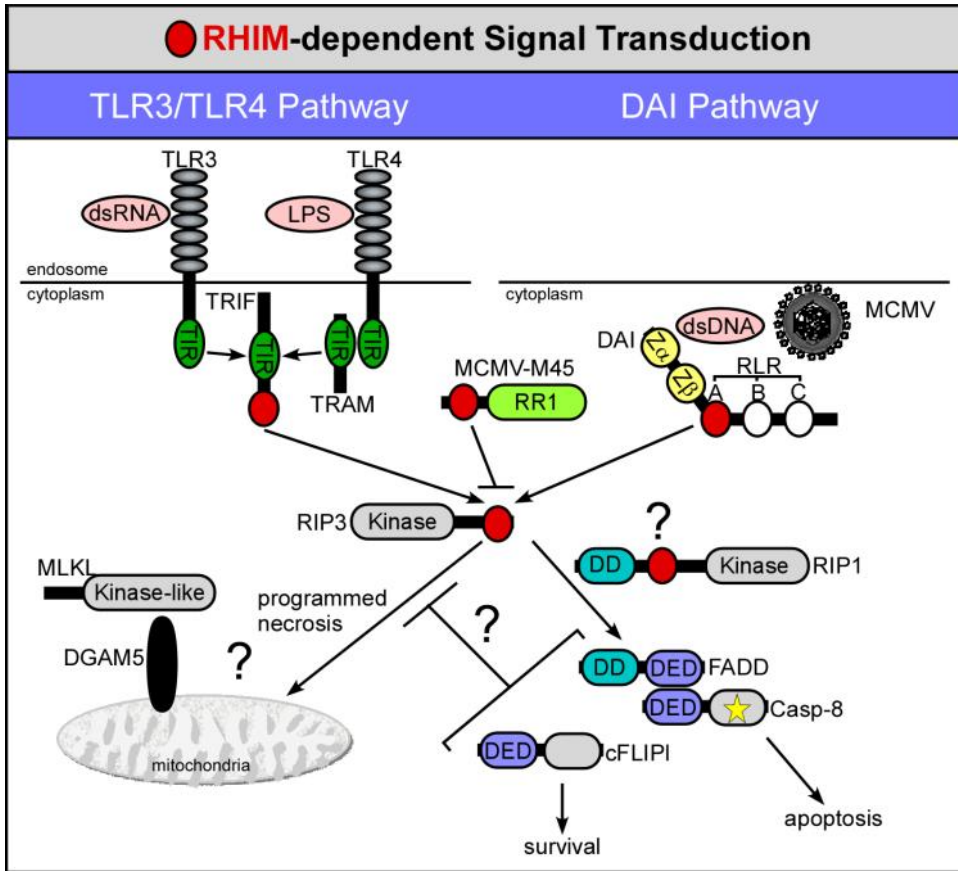


Figure. 6.1. Schematic of RHIM-dependent (red circles) signal transduction induced by TLR3/4 and DAI.

REFERENCES

- Ablasser, A., Bauernfeind, F., Hartmann, G., Latz, E., Fitzgerald, K.A., and Hornung, V. (2009). RIG-I-dependent sensing of poly(dA:dT) through the induction of an RNA polymerase III-transcribed RNA intermediate. *Nat Immunol* 10, 1065-72.
- Akira, S., and Sato, S. (2003). Toll-like receptors and their signaling mechanisms. *Scand J Infect Dis* 35, 555-562.
- Alexopoulou, L., Holt, A.C., Medzhitov, R., and Flavell, R.A. (2001). Recognition of double-stranded RNA and activation of NF-kappaB by Toll-like receptor 3. *Nature* 413, 732-738.
- Ashkenazi, A., and Dixit, V.M. (1998). Death receptors: signaling and modulation. *Science* 281, 1305-1308.
- Balkwill, F. (2009). Tumour necrosis factor and cancer. *Nat Rev Cancer* 9, 361-371.
- Beisner, D.R., Ch'en, I.L., Kolla, R.V., Hoffmann, A., and Hedrick, S.M. (2005). Cutting edge: innate immunity conferred by B cells is regulated by caspase-8. *J Immunol* 175, 3469-3473.
- Belo, J.A., Bouwmeester, T., Leyns, L., Kertesz, N., Gallo, M., Follettie, M., and De Robertis, E.M. (1997). Cerberus-like is a secreted factor with neutralizing activity expressed in the anterior primitive endoderm of the mouse gastrula. *Mech Dev* 68, 45-57.
- Ben Moshe, T., Barash, H., Kang, T.B., Kim, J.C., Kovalenko, A., Gross, E., Schuchmann, M., Abramovitch, R., Galun, E., and Wallach, D. (2007). Role of caspase-8 in hepatocyte response to infection and injury in mice. *Hepatology* 45, 1014-1024.
- Benedict, C.A. (2003). Viruses and the TNF-related cytokines, an evolving battle. *Cytokine Growth Factor Rev* 14, 349-357.
- Benedict, C.A., Angulo, A., Patterson, G., Ha, S., Huang, H., Messerle, M., Ware, C.F., and Ghazal, P. (2004). Neutrality of the canonical NF-kappaB-dependent pathway for human and murine cytomegalovirus transcription and replication in vitro. *J Virol* 78, 741-750.
- Benedict, C.A., Banks, T.A., and Ware, C.F. (2003). Death and survival: viral regulation of TNF signaling pathways. *Curr Opin Immunol* 15, 59-65.
- Benedict, C.A., Norris, P.S., and Ware, C.F. (2002). To kill or be killed: viral evasion of apoptosis. *Nat Immunol* 3, 1013-1018.
- Bertrand, M.J., Milutinovic, S., Dickson, K.M., Ho, W.C., Boudreault, A., Durkin, J., Gillard, J.W., Jaquith, J.B., Morris, S.J., and Barker, P.A. (2008). cIAP1 and cIAP2 facilitate cancer cell survival by functioning as E3 ligases that promote RIP1 ubiquitination. *Mol Cell* 30, 689-700.
- Bertrand, M.J., and Vandenabeele, P. (2011). The ripoptosome: death decision in the cytosol. *Mol Cell* 43, 323-325.

- Best, S.M. (2008). Viral subversion of apoptotic enzymes: escape from death row. Annual review of microbiology 62, 171-192.
- Bidere, N., Su, H.C., and Lenardo, M.J. (2006). Genetic disorders of programmed cell death in the immune system. Annu Rev Immunol 24, 321-352.
- Biton, S., and Ashkenazi, A. (2011). NEMO and RIP1 control cell fate in response to extensive DNA damage via TNF-alpha feedforward signaling. Cell 145, 92-103.
- Boatright, K.M., Deis, C., Denault, J.B., Sutherlin, D.P., and Salvesen, G.S. (2004). Activation of caspases-8 and -10 by FLIP(L). Biochem J 382, 651-657.
- Bonnet, M.C., Preukschat, D., Welz, P.S., van Loo, G., Ermolaeva, M.A., Bloch, W., Haase, I., and Pasparakis, M. (2011). The Adaptor Protein FADD Protects Epidermal Keratinocytes from Necroptosis In Vivo and Prevents Skin Inflammation. Immunity 35, 572-582.
- Bowie, A.G., and Unterholzner, L. (2008). Viral evasion and subversion of pattern-recognition receptor signalling. Nature reviews Immunology 8, 911-922.
- Brune, W. (2011). Inhibition of programmed cell death by cytomegaloviruses. Virus Res 157, 144-150.
- Brune, W., Menard, C., Heesemann, J., and Koszinowski, U.H. (2001). A ribonucleotide reductase homolog of cytomegalovirus and endothelial cell tropism. Science 291, 303-305.
- Brune, W., Nevels, M., and Shenk, T. (2003). Murine cytomegalovirus m41 open reading frame encodes a Golgi-localized antiapoptotic protein. J Virol 77, 11633-11643.
- Bubic, I., Wagner, M., Krmpotic, A., Saulig, T., Kim, S., Yokoyama, W.M., Jonjic, S., and Koszinowski, U.H. (2004). Gain of virulence caused by loss of a gene in murine cytomegalovirus. J Virol 78, 7536-7544.
- Bump, N.J., Hackett, M., Hugunin, M., Seshagiri, S., Brady, K., Chen, P., Ferenz, C., Franklin, S., Ghayur, T., Li, P., et al. (1995). Inhibition of ICE family proteases by baculovirus antiapoptotic protein p35. Science 269, 1885-1888.
- Burke, J.R., Pattoli, M.A., Gregor, K.R., Brassil, P.J., MacMaster, J.F., McIntyre, K.W., Yang, X., Iotzova, V.S., Clarke, W., Strnad, J., et al. (2003). BMS-345541 is a highly selective inhibitor of I kappa B kinase that binds at an allosteric site of the enzyme and blocks NF-kappa B-dependent transcription in mice. J Biol Chem 278, 1450-1456.
- Cam, M., Handke, W., Picard-Maureau, M., and Brune, W. (2010). Cytomegaloviruses inhibit Bak- and Bax-mediated apoptosis with two separate viral proteins. Cell Death Differ 17, 655-665.
- Carswell, E.A., Old, L.J., Kassel, R.L., Green, S., Fiore, N., and Williamson, B. (1975). An endotoxin-induced serum factor that causes necrosis of tumors. Proceedings of the National Academy of Sciences of the United States of America 72, 3666-3670.

- Ch'en, I.L., Beisner, D.R., Degterev, A., Lynch, C., Yuan, J., Hoffmann, A., and Hedrick, S.M. (2008). Antigen-mediated T cell expansion regulated by parallel pathways of death. *Proc Natl Acad Sci U S A* 105, 17463-17468.
- Ch'en, I.L., Tsau, J.S., Molkenin, J.D., Komatsu, M., and Hedrick, S.M. (2011). Mechanisms of necroptosis in T cells. *The Journal of experimental medicine* 208, 633-641.
- Challa, S., and Chan, F.K. (2010). Going up in flames: necrotic cell injury and inflammatory diseases. *Cell Mol Life Sci* 67, 3241-3253.
- Chan, F.K., Shisler, J., Bixby, J.G., Felices, M., Zheng, L., Appel, M., Orenstein, J., Moss, B., and Lenardo, M.J. (2003). A role for tumor necrosis factor receptor-2 and receptor-interacting protein in programmed necrosis and antiviral responses. *J Biol Chem* 278, 51613-51621.
- Chen, P., Tian, J., Kovesdi, I., and Bruder, J.T. (1998). Interaction of the adenovirus 14.7-kDa protein with FLICE inhibits Fas ligand-induced apoptosis. *J Biol Chem* 273, 5815-5820.
- Chipuk, J.E., Moldoveanu, T., Llambi, F., Parsons, M.J., and Green, D.R. (2010). The BCL-2 family reunion. *Mol Cell* 37, 299-310.
- Chiu, Y.H., Macmillan, J.B., and Chen, Z.J. (2009). RNA polymerase III detects cytosolic DNA and induces type I interferons through the RIG-I pathway. *Cell* 138, 576-591.
- Cho, Y., McQuade, T., Zhang, H., Zhang, J., and Chan, F.K. (2011). RIP1-Dependent and Independent Effects of Necrostatin-1 in Necrosis and T Cell Activation. *PLoS One* 6, e23209.
- Cho, Y.S., Challa, S., Moquin, D., Genga, R., Ray, T.D., Guildford, M., and Chan, F.K. (2009). Phosphorylation-driven assembly of the RIP1-RIP3 complex regulates programmed necrosis and virus-induced inflammation. *Cell* 137, 1112-1123.
- Christofferson, D.E., and Yuan, J. (2009). Necroptosis as an alternative form of programmed cell death. *Curr Opin Cell Biol*.
- Chun, H.J., Zheng, L., Ahmad, M., Wang, J., Speirs, C.K., Siegel, R.M., Dale, J.K., Puck, J., Davis, J., Hall, C.G., *et al.* (2002). Pleiotropic defects in lymphocyte activation caused by caspase-8 mutations lead to human immunodeficiency. *Nature* 419, 395-399.
- Cicin-Sain, L., Podlech, J., Messerle, M., Reddehase, M.J., and Koszinowski, U.H. (2005). Frequent coinfection of cells explains functional in vivo complementation between cytomegalovirus variants in the multiply infected host. *J Virol* 79, 9492-9502.
- Cicin-Sain, L., Ruzsics, Z., Podlech, J., Bubic, I., Menard, C., Jonjic, S., Reddehase, M.J., and Koszinowski, U.H. (2008). Dominant-negative FADD rescues the in vivo fitness of a cytomegalovirus lacking an antiapoptotic viral gene. *J Virol* 82, 2056-2064.
- Clem, R.J. (2005). The role of apoptosis in defense against baculovirus infection in insects. *Curr Top Microbiol Immunol* 289, 113-129.

- Clem, R.J., Fechheimer, M., and Miller, L.K. (1991). Prevention of apoptosis by a baculovirus gene during infection of insect cells. *Science* 254, 1388-1390.
- Crook, N.E., Clem, R.J., and Miller, L.K. (1993). An apoptosis-inhibiting baculovirus gene with a zinc finger-like motif. *J Virol* 67, 2168-2174.
- D'Agostino, D.M., Bernardi, P., Chieco-Bianchi, L., and Ciminale, V. (2005). Mitochondria as functional targets of proteins coded by human tumor viruses. *Adv Cancer Res* 94, 87-142.
- Danial, N.N., and Korsmeyer, S.J. (2004). Cell death: critical control points. *Cell* 116, 205-219.
- Datta, S., Costantino, N., and Court, D.L. (2006). A set of recombineering plasmids for gram-negative bacteria. *Gene* 379, 109-115.
- Declercq, W., Vanden Berghe, T., and Vandenabeele, P. (2009). RIP kinases at the crossroads of cell death and survival. *Cell* 138, 229-232.
- DeFilippis, V.R., Alvarado, D., Sali, T., Rothenburg, S., and Fruh, K. (2010a). Human cytomegalovirus induces the interferon response via the DNA sensor ZBP1. *J Virol* 84, 585-598.
- DeFilippis, V.R., Sali, T., Alvarado, D., White, L., Bresnahan, W., and Fruh, K.J. (2010b). Activation of the interferon response by human cytomegalovirus occurs via cytoplasmic double-stranded DNA but not glycoprotein B. *J Virol* 84, 8913-8925.
- Degterev, A., Hitomi, J., Gemscheid, M., Ch'en, I.L., Korkina, O., Teng, X., Abbott, D., Cuny, G.D., Yuan, C., Wagner, G., *et al.* (2008). Identification of RIP1 kinase as a specific cellular target of necrostatins. *Nat Chem Biol* 4, 313-321.
- Degterev, A., Huang, Z., Boyce, M., Li, Y., Jagtap, P., Mizushima, N., Cuny, G.D., Mitchison, T.J., Moskowitz, M.A., and Yuan, J. (2005). Chemical inhibitor of nonapoptotic cell death with therapeutic potential for ischemic brain injury. *Nat Chem Biol* 1, 112-119.
- Degterev, A., and Yuan, J. (2008). Expansion and evolution of cell death programmes. *Nat Rev Mol Cell Biol* 9, 378-390.
- Dillon, C.P., Oberst, A., Weinlich, R., Janke, L.J., Kang, T.B., Ben-Moshe, T., Mak, T.W., Wallach, D., and Green, D.R. (2012). Survival function of the FADD-CASPASE-8-cFLIP(L) complex. *Cell reports* 1, 401-407.
- Feng, S., Yang, Y., Mei, Y., Ma, L., Zhu, D.E., Hoti, N., Castanares, M., and Wu, M. (2007). Cleavage of RIP3 inactivates its caspase-independent apoptosis pathway by removal of kinase domain. *Cell Signal* 19, 2056-2067.
- Feoktistova, M., Geserick, P., Kellert, B., Dimitrova, D.P., Langlais, C., Hupe, M., Cain, K., Macfarlane, M., Hacker, G., and Leverkus, M. (2011). cIAPs Block Ripoptosome Formation, a RIP1/Caspase-8 Containing Intracellular Cell Death Complex Differentially Regulated by cFLIP Isoforms. *Mol Cell* 43, 449-463.

Ferguson, T.A., Choi, J., and Green, D.R. (2011). Armed response: how dying cells influence T-cell functions. *Immunol Rev* 241, 77-88.

Fernandes-Alnemri, T., Yu, J.W., Datta, P., Wu, J., and Alnemri, E.S. (2009). AIM2 activates the inflammasome and cell death in response to cytoplasmic DNA. *Nature* 458, 509-513.

Festjens, N., Vanden Berghe, T., Cornelis, S., and Vandenabeele, P. (2007). RIP1, a kinase on the crossroads of a cell's decision to live or die. *Cell Death Differ* 14, 400-410.

Festjens, N., Vanden Berghe, T., and Vandenabeele, P. (2006). Necrosis, a well-orchestrated form of cell demise: signalling cascades, important mediators and concomitant immune response. *Biochim Biophys Acta* 1757, 1371-1387.

Friedman, H.M., Wang, L., Fishman, N.O., Lambris, J.D., Eisenberg, R.J., Cohen, G.H., and Lubinski, J. (1996). Immune evasion properties of herpes simplex virus type 1 glycoprotein gC. *J Virol* 70, 4253-4260.

Fu, Y., Comella, N., Tognazzi, K., Brown, L.F., Dvorak, H.F., and Kocher, O. (1999). Cloning of DLM-1, a novel gene that is up-regulated in activated macrophages, using RNA differential display. *Gene* 240, 157-163.

Furr, S.R., Chauhan, V.S., Moerdyk-Schauwecker, M.J., and Marriott, I. (2011). A role for DNA-dependent activator of interferon regulatory factor in the recognition of herpes simplex virus type 1 by glial cells. *Journal of neuroinflammation* 8, 99.

Gaide, O., Favier, B., Legler, D.F., Bonnet, D., Brissoni, B., Valitutti, S., Bron, C., Tschopp, J., and Thome, M. (2002). CARMA1 is a critical lipid raft-associated regulator of TCR-induced NF-kappa B activation. *Nat Immunol* 3, 836-843.

Galluzzi, L., Brenner, C., Morselli, E., Touat, Z., and Kroemer, G. (2008). Viral control of mitochondrial apoptosis. *PLoS Pathog* 4, e1000018.

Galluzzi, L., Kepp, O., Morselli, E., Vitale, I., Senovilla, L., Pinti, M., Zitvogel, L., and Kroemer, G. (2010). Viral strategies for the evasion of immunogenic cell death. *J Intern Med* 267, 526-542.

Galluzzi, L., and Kroemer, G. (2008). Necroptosis: a specialized pathway of programmed necrosis. *Cell* 135, 1161-1163.

Gentle, I.E., Wong, W.W., Evans, J.M., Bankovacki, A., Cook, W.D., Khan, N.R., Nachbur, U., Rickard, J., Anderton, H., Moulin, M., *et al.* (2011). In TNF-stimulated cells, RIPK1 promotes cell survival by stabilizing TRAF2 and cIAP1, which limits induction of non-canonical NF-kappaB and activation of caspase-8. *The Journal of biological chemistry* 286, 13282-13291.

Gerlach, B., Cordier, S.M., Schmukle, A.C., Emmerich, C.H., Rieser, E., Haas, T.L., Webb, A.I., Rickard, J.A., Anderton, H., Wong, W.W., *et al.* (2011). Linear ubiquitination prevents inflammation and regulates immune signalling. *Nature* 471, 591-596.

Goldmacher, V.S. (2005). Cell death suppression by cytomegaloviruses. *Apoptosis* 10, 251-265.

Goldmacher, V.S., Bartle, L.M., Skaletskaya, A., Dionne, C.A., Kedersha, N.L., Vater, C.A., Han, J.W., Lutz, R.J., Watanabe, S., Cahir McFarland, E.D., *et al.* (1999). A cytomegalovirus-encoded mitochondria-localized inhibitor of apoptosis structurally unrelated to Bcl-2. *Proc Natl Acad Sci U S A* *96*, 12536-12541.

Gunther, C., Martini, E., Wittkopf, N., Amann, K., Weigmann, B., Neumann, H., Waldner, M.J., Hedrick, S.M., Tenzer, S., Neurath, M.F., *et al.* (2011). Caspase-8 regulates TNF-alpha-induced epithelial necroptosis and terminal ileitis. *Nature* *477*, 335-339.

He, S., Liang, Y., Shao, F., and Wang, X. (2011). Toll-like receptors activate programmed necrosis in macrophages through a receptor-interacting kinase-3-mediated pathway. *Proc Natl Acad Sci U S A* *108*, 20054-20059.

He, S., Wang, L., Miao, L., Wang, T., Du, F., Zhao, L., and Wang, X. (2009). Receptor interacting protein kinase-3 determines cellular necrotic response to TNF-alpha. *Cell* *137*, 1100-1111.

Hedrick, S.M., Ch'en, I.L., and Alves, B.N. (2010). Intertwined pathways of programmed cell death in immunity. *Immunol Rev* *236*, 41-53.

Hengartner, M.O. (2000). The biochemistry of apoptosis. *Nature* *407*, 770-776.

Hida, S., Ogasawara, K., Sato, K., Abe, M., Takayanagi, H., Yokochi, T., Sato, T., Hirose, S., Shirai, T., Taki, S., *et al.* (2000). CD8(+) T cell-mediated skin disease in mice lacking IRF-2, the transcriptional attenuator of interferon-alpha/beta signaling. *Immunity* *13*, 643-655.

Hitomi, J., Christofferson, D.E., Ng, A., Yao, J., Degterev, A., Xavier, R.J., and Yuan, J. (2008). Identification of a molecular signaling network that regulates a cellular necrotic cell death pathway. *Cell* *135*, 1311-1323.

Hoebe, K., Du, X., Georgel, P., Janssen, E., Tabeta, K., Kim, S.O., Goode, J., Lin, P., Mann, N., Mudd, S., *et al.* (2003). Identification of Lps2 as a key transducer of MyD88-independent TIR signalling. *Nature* *424*, 743-748.

Holler, N., Zaru, R., Micheau, O., Thome, M., Attinger, A., Valitutti, S., Bodmer, J.L., Schneider, P., Seed, B., and Tschopp, J. (2000). Fas triggers an alternative, caspase-8-independent cell death pathway using the kinase RIP as effector molecule. *Nat Immunol* *1*, 489-495.

Hsu, H., Huang, J., Shu, H.B., Baichwal, V., and Goeddel, D.V. (1996). TNF-dependent recruitment of the protein kinase RIP to the TNF receptor-1 signaling complex. *Immunity* *4*, 387-396.

Ikner, A., and Ashkenazi, A. (2011). TWEAK Induces Apoptosis through a Death-signaling Complex Comprising Receptor-interacting Protein 1 (RIP1), Fas-associated Death Domain (FADD), and Caspase-8. *J Biol Chem* *286*, 21546-21554.

Imtiyaz, H.Z., Rosenberg, S., Zhang, Y., Rahman, Z.S., Hou, Y.J., Manser, T., and Zhang, J. (2006). The Fas-associated death domain protein is required in apoptosis and TLR-induced proliferative responses in B cells. *J Immunol* *176*, 6852-6861.

Irmiler, M., Thome, M., Hahne, M., Schneider, P., Hofmann, K., Steiner, V., Bodmer, J.L., Schroter, M., Burns, K., Mattmann, C., *et al.* (1997). Inhibition of death receptor signals by cellular FLIP. *Nature* **388**, 190-195.

Irrinki, K.M., Mallilankaraman, K., Thapa, R.J., Chandramoorthy, H.C., Smith, F.J., Jog, N.R., Gandhirajan, R.K., Kelsen, S.G., Houser, S.R., May, M.J., *et al.* (2011). Requirement of FADD, NEMO, and BAX/BAK for aberrant mitochondrial function in tumor necrosis factor alpha-induced necrosis. *Mol Cell Biol* **31**, 3745-3758.

Ishii, K.J., Kawagoe, T., Koyama, S., Matsui, K., Kumar, H., Kawai, T., Uematsu, S., Takeuchi, O., Takeshita, F., Coban, C., *et al.* (2008). TANK-binding kinase-1 delineates innate and adaptive immune responses to DNA vaccines. *Nature* **451**, 725-729.

Janssens, S., Tinel, A., Lippens, S., and Tschopp, J. (2005). PIDD mediates NF-kappaB activation in response to DNA damage. *Cell* **123**, 1079-1092.

Kaiser, W.J., and Offermann, M.K. (2005). Apoptosis induced by the toll-like receptor adaptor TRIF is dependent on its receptor interacting protein homotypic interaction motif. *J Immunol* **174**, 4942-4952.

Kaiser, W.J., Upton, J.W., Long, A.B., Livingston-Rosanoff, D., Daley-Bauer, L.P., Hakem, R., Caspary, T., and Mocarski, E.S. (2011). RIP3 mediates the embryonic lethality of caspase-8-deficient mice. *Nature* **471**, 368-372.

Kaiser, W.J., Upton, J.W., and Mocarski, E.S. (2008). Receptor-interacting protein homotypic interaction motif-dependent control of NF-kappa B activation via the DNA-dependent activator of IFN regulatory factors. *J Immunol* **181**, 6427-6434.

Kalai, M., Van Loo, G., Vanden Berghe, T., Meeus, A., Burm, W., Saelens, X., and Vandenabeele, P. (2002). Tipping the balance between necrosis and apoptosis in human and murine cells treated with interferon and dsRNA. *Cell Death Differ* **9**, 981-994.

Kang, T.B., Ben-Moshe, T., Varfolomeev, E.E., Pewzner-Jung, Y., Yogev, N., Jurewicz, A., Waisman, A., Brenner, O., Haffner, R., Gustafsson, E., *et al.* (2004). Caspase-8 serves both apoptotic and nonapoptotic roles. *J Immunol* **173**, 2976-2984.

Kang, T.B., Oh, G.S., Scandella, E., Bolinger, B., Ludewig, B., Kovalenko, A., and Wallach, D. (2008). Mutation of a self-processing site in caspase-8 compromises its apoptotic but not its nonapoptotic functions in bacterial artificial chromosome-transgenic mice. *J Immunol* **181**, 2522-2532.

Kantari, C., and Walczak, H. (2011). Caspase-8 and bid: caught in the act between death receptors and mitochondria. *Biochim Biophys Acta* **1813**, 558-563.

Kapadia, S.B., Levine, B., Speck, S.H., and Virgin, H.W.t. (2002). Critical role of complement and viral evasion of complement in acute, persistent, and latent gamma-herpesvirus infection. *Immunity* **17**, 143-155.

Karayel, E., Burckstummer, T., Bilban, M., Durnberger, G., Weitzer, S., Martinez, J., and Superti-Furga, G. (2009). The TLR-independent DNA recognition pathway in murine macrophages: Ligand features and molecular signature. *Eur J Immunol* *39*, 1929-1936.

Kasof, G.M., Prosser, J.C., Liu, D., Lorenzi, M.V., and Gomes, B.C. (2000). The RIP-like kinase, RIP3, induces apoptosis and NF-kappaB nuclear translocation and localizes to mitochondria. *FEBS Lett* *473*, 285-291.

Katdare, M., Efimova, E.V., Labay, E., Khodarev, N.N., Darga, T.E., Garofalo, M., Nakamura, S., Kufe, D.W., Posner, M.C., and Weichselbaum, R.R. (2007). Diverse TNFalpha-induced death pathways are enhanced by inhibition of NF-kappaB. *International journal of oncology* *31*, 1519-1528.

Kaufmann, T., Jost, P.J., Pellegrini, M., Puthalakath, H., Gugasyan, R., Gerondakis, S., Cretney, E., Smyth, M.J., Silke, J., Hakem, R., *et al.* (2009). Fatal hepatitis mediated by tumor necrosis factor TNFalpha requires caspase-8 and involves the BH3-only proteins Bid and Bim. *Immunity* *30*, 56-66.

Kawadler, H., Gantz, M.A., Riley, J.L., and Yang, X. (2008). The paracaspase MALT1 controls caspase-8 activation during lymphocyte proliferation. *Mol Cell* *31*, 415-421.

Kawai, T., and Akira, S. (2007). TLR signaling. *Semin Immunol* *19*, 24-32.

Kawai, T., and Akira, S. (2011). Toll-like receptors and their crosstalk with other innate receptors in infection and immunity. *Immunity* *34*, 637-650.

Kelliher, M.A., Grimm, S., Ishida, Y., Kuo, F., Stanger, B.Z., and Leder, P. (1998). The death domain kinase RIP mediates the TNF-induced NF-kappaB signal. *Immunity* *8*, 297-303.

Kepp, O., Senovilla, L., Galluzzi, L., Panaretakis, T., Tesniere, A., Schlemmer, F., Madeo, F., Zitvogel, L., and Kroemer, G. (2009). Viral subversion of immunogenic cell death. *Cell Cycle* *8*, 860-869.

Kielczewska, A., Pyzik, M., Sun, T., Krmpotic, A., Lodoen, M.B., Munks, M.W., Babic, M., Hill, A.B., Koszinowski, U.H., Jonjic, S., *et al.* (2009). Ly49P recognition of cytomegalovirus-infected cells expressing H2-Dk and CMV-encoded m04 correlates with the NK cell antiviral response. *J Exp Med* *206*, 515-523.

Kovalenko, A., Kim, J.C., Kang, T.B., Rajput, A., Bogdanov, K., Dittrich-Breiholz, O., Kracht, M., Brenner, O., and Wallach, D. (2009). Caspase-8 deficiency in epidermal keratinocytes triggers an inflammatory skin disease. *J Exp Med* *206*, 2161-2177.

Krysko, D.V., Denecker, G., Festjens, N., Gabriels, S., Parthoens, E., D'Herde, K., and Vandenabeele, P. (2006). Macrophages use different internalization mechanisms to clear apoptotic and necrotic cells. *Cell Death Differ* *13*, 2011-2022.

Kumar, H., Kawai, T., and Akira, S. (2009). Toll-like receptors and innate immunity. *Biochem Biophys Res Commun* *388*, 621-625.

- Kumar, H., Kawai, T., and Akira, S. (2011). Pathogen recognition by the innate immune system. *Int Rev Immunol* 30, 16-34.
- Kuprash, D.V., Alimzhanov, M.B., Tumanov, A.V., Grivennikov, S.I., Shakhov, A.N., Drutskaya, L.N., Marino, M.W., Turetskaya, R.L., Anderson, A.O., Rajewsky, K., *et al.* (2002). Redundancy in tumor necrosis factor (TNF) and lymphotoxin (LT) signaling in vivo: mice with inactivation of the entire TNF/LT locus versus single-knockout mice. *Mol Cell Biol* 22, 8626-8634.
- Lagunoff, M., and Carroll, P.A. (2003). Inhibition of apoptosis by the gamma-herpesviruses. *Int Rev Immunol* 22, 373-399.
- Lamkanfi, M., and Dixit, V.M. (2010). Manipulation of host cell death pathways during microbial infections. *Cell Host Microbe* 8, 44-54.
- Laouar, Y., and Ezine, S. (1994). In vivo CD4+ lymph node T cells from lpr mice generate CD4-CD8-B220+TCR-beta low cells. *J Immunol* 153, 3948-3955.
- Laster, S.M., Wood, J.G., and Gooding, L.R. (1988). Tumor necrosis factor can induce both apoptotic and necrotic forms of cell lysis. *Journal of immunology* 141, 2629-2634.
- Lee, P., Lee, D.J., Chan, C., Chen, S.W., Ch'en, I., and Jamora, C. (2009). Dynamic expression of epidermal caspase 8 simulates a wound healing response. *Nature* 458, 519-523.
- Leib, D.A., Machalek, M.A., Williams, B.R., Silverman, R.H., and Virgin, H.W. (2000). Specific phenotypic restoration of an attenuated virus by knockout of a host resistance gene. *Proc Natl Acad Sci U S A* 97, 6097-6101.
- Lembo, D., and Brune, W. (2009). Tinkering with a viral ribonucleotide reductase. *Trends Biochem Sci* 34, 25-32.
- Lembo, D., Donalizio, M., Hofer, A., Cornaglia, M., Brune, W., Koszinowski, U., Thelander, L., and Landolfo, S. (2004). The ribonucleotide reductase R1 homolog of murine cytomegalovirus is not a functional enzyme subunit but is required for pathogenesis. *J Virol* 78, 4278-4288.
- Li, C., Lasse, S., Lee, P., Nakasaki, M., Chen, S.W., Yamasaki, K., Gallo, R.L., and Jamora, C. (2010). Development of atopic dermatitis-like skin disease from the chronic loss of epidermal caspase-8. *Proc Natl Acad Sci U S A* 107, 22249-22254.
- Li, M., and Beg, A.A. (2000). Induction of necrotic-like cell death by tumor necrosis factor alpha and caspase inhibitors: novel mechanism for killing virus-infected cells. *J Virol* 74, 7470-7477.
- Lin, Y., Devin, A., Rodriguez, Y., and Liu, Z.G. (1999). Cleavage of the death domain kinase RIP by caspase-8 prompts TNF-induced apoptosis. *Genes Dev* 13, 2514-2526.
- Lippmann, J., Rothenburg, S., Deigendesch, N., Eitel, J., Meixenberger, K., van Laak, V., Slevogt, H., N'Guessan P, D., Hippenstiel, S., Chakraborty, T., *et al.* (2008). IFNbeta responses induced by

intracellular bacteria or cytosolic DNA in different human cells do not require ZBP1 (DLM-1/DAI). *Cell Microbiol* *10*, 2579-2588.

Lu, J.V., Weist, B.M., van Raam, B.J., Marro, B.S., Srinivas, P., Bell, B.D., Luhrs, K.A., Lane, T.E., Salvesen, G.S., and Walsh, C.M. (2011). Complementary roles of FADD and RIPK3 in T cell homeostasis and antiviral immunity. *Proc Natl Acad Sci U S A* *108*, 15312-15317.

Lubinski, J., Wang, L., Mastellos, D., Sahu, A., Lambris, J.D., and Friedman, H.M. (1999). In vivo role of complement-interacting domains of herpes simplex virus type 1 glycoprotein gC. *J Exp Med* *190*, 1637-1646.

Lubinski, J.M., Wang, L., Soulika, A.M., Burger, R., Wetsel, R.A., Colten, H., Cohen, G.H., Eisenberg, R.J., Lambris, J.D., and Friedman, H.M. (1998). Herpes simplex virus type 1 glycoprotein gC mediates immune evasion in vivo. *J Virol* *72*, 8257-8263.

Mack, C., Sickmann, A., Lembo, D., and Brune, W. (2008). Inhibition of proinflammatory and innate immune signaling pathways by a cytomegalovirus RIP1-interacting protein. *Proc Natl Acad Sci U S A* *105*, 3094-3099.

Manzur, M., Fleming, P., Huang, D.C., Degli-Esposti, M.A., and Andoniou, C.E. (2009). Virally mediated inhibition of Bax in leukocytes promotes dissemination of murine cytomegalovirus. *Cell Death Differ* *16*, 312-320.

Matzinger, P. (2002). The danger model: a renewed sense of self. *Science* *296*, 301-305.
McCartney, S.A., and Colonna, M. (2009). Viral sensors: diversity in pathogen recognition. *Immunol Rev* *227*, 87-94.

McCormick, A.L. (2008). Control of apoptosis by human cytomegalovirus. *Curr Top Microbiol Immunol* *325*, 281-295.

McCormick, A.L., Meiering, C.D., Smith, G.B., and Mocarski, E.S. (2005). Mitochondrial cell death suppressors carried by human and murine cytomegalovirus confer resistance to proteasome inhibitor-induced apoptosis. *J Virol* *79*, 12205-12217.

McCormick, A.L., Roback, L., and Mocarski, E.S. (2008). HtrA2/Omi terminates cytomegalovirus infection and is controlled by the viral mitochondrial inhibitor of apoptosis (vMIA). *PLoS Pathog* *4*, e1000063.

McCormick, A.L., Skaletskaya, A., Barry, P.A., Mocarski, E.S., and Goldmacher, V.S. (2003). Differential function and expression of the viral inhibitor of caspase 8-induced apoptosis (vICA) and the viral mitochondria-localized inhibitor of apoptosis (vMIA) cell death suppressors conserved in primate and rodent cytomegaloviruses. *Virology* *316*, 221-233.

Medzhitov, R. (2010). Innate immunity: quo vadis? *Nature immunology* *11*, 551-553.
Menard, C., Wagner, M., Ruzsics, Z., Holak, K., Brune, W., Campbell, A.E., and Koszinowski, U.H. (2003). Role of murine cytomegalovirus US22 gene family members in replication in macrophages. *J Virol* *77*, 5557-5570.

- Meylan, E., Burns, K., Hofmann, K., Blancheteau, V., Martinon, F., Kelliher, M., and Tschopp, J. (2004). RIP1 is an essential mediator of Toll-like receptor 3-induced NF-kappa B activation. *Nat Immunol* 5, 503-507.
- Meylan, E., and Tschopp, J. (2005). The RIP kinases: crucial integrators of cellular stress. *Trends Biochem Sci* 30, 151-159.
- Michallet, M.C., Meylan, E., Ermolaeva, M.A., Vazquez, J., Rebsamen, M., Curran, J., Poeck, H., Bscheider, M., Hartmann, G., Konig, M., *et al.* (2008). TRADD Protein Is an Essential Component of the RIG-like Helicase Antiviral Pathway. *Immunity*. 28, 651-61
- Micheau, O., Thome, M., Schneider, P., Holler, N., Tschopp, J., Nicholson, D.W., Briand, C., and Grutter, M.G. (2002). The long form of FLIP is an activator of caspase-8 at the Fas death-inducing signaling complex. *J Biol Chem* 277, 45162-45171.
- Micheau, O., and Tschopp, J. (2003). Induction of TNF Receptor I-Mediated Apoptosis via Two Sequential Signaling Complexes. *Cell* 114, 181-190.
- Misra, R.S., Russell, J.Q., Koenig, A., Hinshaw-Makepeace, J.A., Wen, R., Wang, D., Huo, H., Littman, D.R., Ferch, U., Ruland, J., *et al.* (2007). Caspase-8 and c-FLIPL associate in lipid rafts with NF-kappaB adaptors during T cell activation. *J Biol Chem* 282, 19365-19374.
- Mitjavila-Garcia, M.T., Cailleret, M., Godin, I., Nogueira, M.M., Cohen-Solal, K., Schiavon, V., Lecluse, Y., Le Pesteur, F., Lagrue, A.H., and Vainchenker, W. (2002). Expression of CD41 on hematopoietic progenitors derived from embryonic hematopoietic cells. *Development* 129, 2003-2013.
- Miura, M., Zhu, H., Rotello, R., Hartwig, E.A., and Yuan, J. (1993). Induction of apoptosis in fibroblasts by IL-1 beta-converting enzyme, a mammalian homolog of the *C. elegans* cell death gene *ced-3*. *Cell* 75, 653-660.
- Mocarski, E.S. (2007). Betaherpes viral genes and their functions. In *Human Herpesviruses: Biology, Therapy and Immunoprophylaxis*, E.S.M. A. M. Arvin, P. Moore, R. Whitley, K. Yamanishi, G. Campadelli-Fiume, B. Roizman. , ed. (Cambridge, UK: Cambridge Press), pp. 204-230.
- Mocarski, E.S., Upton, J.W., and Kaiser, W.J. (2011). Viral infection and the evolution of caspase 8-regulated apoptotic and necrotic death pathways. *Nature reviews Immunology* 12, 79-88.
- Mocarski, E.S., Upton, J. W., Kaiser, W.J. (2011). Viral infection and the evolution of caspase 8-regulated apoptotic and necrotic death pathways. *Nature reviews Immunology*. 12, 79-88.
- Moquin, D., and Chan, F.K. (2010). The molecular regulation of programmed necrotic cell injury. *Trends Biochem Sci* 35, 434-441.
- Nagata, S., and Suda, T. (1995). Fas and Fas ligand: *lpr* and *gld* mutations. *Immunol Today* 16, 39-43.

- Newton, K., Sun, X., and Dixit, V.M. (2004). Kinase RIP3 is dispensable for normal NF-kappa B signaling by the B-cell and T-cell receptors, tumor necrosis factor receptor 1, and Toll-like receptors 2 and 4. *Mol Cell Biol* 24, 1464-1469.
- O'Donnell, M.A., Perez-Jimenez, E., Oberst, A., Ng, A., Massoumi, R., Xavier, R., Green, D.R., and Ting, A.T. (2011). Caspase 8 inhibits programmed necrosis by processing CYLD. *Nature cell biology*.
- O'Donnell, S.M., Hansberger, M.W., Connolly, J.L., Chappell, J.D., Watson, M.J., Pierce, J.M., Wetzel, J.D., Han, W., Barton, E.S., Forrest, J.C., *et al.* (2005). Organ-specific roles for transcription factor NF-kappaB in reovirus-induced apoptosis and disease. *J Clin Invest* 115, 2341-2350.
- Oberst, A., Dillon, C.P., Weinlich, R., McCormick, L.L., Fitzgerald, P., Pop, C., Hakem, R., Salvesen, G.S., and Green, D.R. (2011). Catalytic activity of the caspase-8-FLIP(L) complex inhibits RIPK3-dependent necrosis. *Nature* 471, 363-367.
- Oberst, A., Pop, C., Tremblay, A.G., Blais, V., Denault, J.B., Salvesen, G.S., and Green, D.R. (2010). Inducible dimerization and inducible cleavage reveal a requirement for both processes in caspase-8 activation. *J Biol Chem* 285, 16632-16642.
- Palm, N.W., and Medzhitov, R. (2009). Pattern recognition receptors and control of adaptive immunity. *Immunol Rev* 227, 221-233.
- Paterson, S., Vogwill, T., Buckling, A., Benmayor, R., Spiers, A.J., Thomson, N.R., Quail, M., Smith, F., Walker, D., Libberton, B., *et al.* (2010). Antagonistic coevolution accelerates molecular evolution. *Nature* 464, 275-278.
- Pazdernik, N.J., Donner, D.B., Goebel, M.G., and Harrington, M.A. (1999). Mouse receptor interacting protein 3 does not contain a caspase-recruiting or a death domain but induces apoptosis and activates NF-kappaB. *Mol Cell Biol* 19, 6500-6508.
- Pollock, J.L., and Virgin, H.W.t. (1995). Latency, without persistence, of murine cytomegalovirus in the spleen and kidney. *J Virol* 69, 1762-1768.
- Pop, C., Oberst, A., Drag, M., Van Raam, B.J., Riedl, S.J., Green, D.R., and Salvesen, G.S. (2011). FLIP(L) induces caspase 8 activity in the absence of interdomain caspase 8 cleavage and alters substrate specificity. *Biochem J* 433, 447-457.
- Pop, C., and Salvesen, G.S. (2009). Human caspases: activation, specificity, and regulation. *J Biol Chem* 284, 21777-21781.
- Rahman, M.M., and McFadden, G. (2011). Modulation of NF-kappaB signalling by microbial pathogens. *Nat Rev Microbiol* 9, 291-306.

Ray, C.A., Black, R.A., Kronheim, S.R., Greenstreet, T.A., Sleath, P.R., Salvesen, G.S., and Pickup, D.J. (1992). Viral inhibition of inflammation: cowpox virus encodes an inhibitor of the interleukin-1 beta converting enzyme. *Cell* 69, 597-604.

Rebsamen, M., Heinz, L.X., Meylan, E., Michallet, M.C., Schroder, K., Hofmann, K., Vazquez, J., Benedict, C.A., and Tschopp, J. (2009). DAI/ZBP1 recruits RIP1 and RIP3 through RIP homotypic interaction motifs to activate NF-kappaB. *EMBO Rep* 10, 916-922.

Redwood, A.J., Messerle, M., Harvey, N.L., Hardy, C.M., Koszinowski, U.H., Lawson, M.A., and Shellam, G.R. (2005). Use of a murine cytomegalovirus K181-derived bacterial artificial chromosome as a vaccine vector for immunocontraception. *J Virol* 79, 2998-3008.

Rosenberg, S., Zhang, H., and Zhang, J. (2011). FADD deficiency impairs early hematopoiesis in the bone marrow. *J Immunol* 186, 203-213.

Roue, G., Perez-Galan, P., Lopez-Guerra, M., Villamor, N., Campo, E., and Colomer, D. (2007). Selective inhibition of IkappaB kinase sensitizes mantle cell lymphoma B cells to TRAIL by decreasing cellular FLIP level. *J Immunol* 178, 1923-1930.

Roy, C.R., and Mocarski, E.S. (2007). Pathogen subversion of cell-intrinsic innate immunity. *Nat Immunol* 8, 1179-1187.

Ruefli-Brasse, A.A., French, D.M., and Dixit, V.M. (2003). Regulation of NF-kappaB-dependent lymphocyte activation and development by paracaspase. *Science* 302, 1581-1584.

Ruland, J., Duncan, G.S., Elia, A., del Barco Barrantes, I., Nguyen, L., Plyte, S., Millar, D.G., Bouchard, D., Wakeham, A., Ohashi, P.S., *et al.* (2001). Bcl10 is a positive regulator of antigen receptor-induced activation of NF-kappaB and neural tube closure. *Cell* 104, 33-42.

Saederup, N., Aguirre, S.A., Sparer, T.E., Bouley, D.M., and Mocarski, E.S. (2001). Murine cytomegalovirus CC chemokine homolog MCK-2 (m131-129) is a determinant of dissemination that increases inflammation at initial sites of infection. *J Virol* 75, 9966-9976.

Saederup, N., Lin, Y.C., Dairaghi, D.J., Schall, T.J., and Mocarski, E.S. (1999). Cytomegalovirus-encoded beta chemokine promotes monocyte-associated viremia in the host. *Proc Natl Acad Sci U S A* 96, 10881-10886.

Saito, T., and Gale, M., Jr. (2007). Principles of intracellular viral recognition. *Curr Opin Immunol* 19, 17-23.

Sakamaki, K., Inoue, T., Asano, M., Sudo, K., Kazama, H., Sakagami, J., Sakata, S., Ozaki, M., Nakamura, S., Toyokuni, S., *et al.* (2002). Ex vivo whole-embryo culture of caspase-8-deficient embryos normalize their aberrant phenotypes in the developing neural tube and heart. *Cell Death Differ* 9, 1196-1206.

Salmena, L., and Hakem, R. (2005). Caspase-8 deficiency in T cells leads to a lethal lymphoinfiltrative immune disorder. *J Exp Med* 202, 727-732.

Salmena, L., Lemmers, B., Hakem, A., Matsiyak-Zablocki, E., Murakami, K., Au, P.Y., Berry, D.M., Tambllyn, L., Shehabeldin, A., Migon, E., *et al.* (2003). Essential role for caspase 8 in T-cell homeostasis and T-cell-mediated immunity. *Genes Dev* *17*, 883-895.

Sapin, V., Blanchon, L., Serre, A.F., Lemery, D., Dastugue, B., and Ward, S.J. (2001). Use of transgenic mice model for understanding the placentation: towards clinical applications in human obstetrical pathologies? *Transgenic Res* *10*, 377-398.

Sarbassov, D.D., Guertin, D.A., Ali, S.M., and Sabatini, D.M. (2005). Phosphorylation and regulation of Akt/PKB by the rictor-mTOR complex. *Science* *307*, 1098-1101.

Shultz, L.D., Lyons, B.L., Burzenski, L.M., Gott, B., Chen, X., Chaleff, S., Kotb, M., Gillies, S.D., King, M., Mangada, J., *et al.* (2005). Human lymphoid and myeloid cell development in NOD/LtSz-scid IL2R gamma null mice engrafted with mobilized human hemopoietic stem cells. *J Immunol* *174*, 6477-6489.

Silke, J. (2011). The regulation of TNF signalling: what a tangled web we weave. *Curr Opin Immunol* *23*, 620-626.

Skaletskaya, A., Bartle, L.M., Chittenden, T., McCormick, A.L., Mocarski, E.S., and Goldmacher, V.S. (2001). A cytomegalovirus-encoded inhibitor of apoptosis that suppresses caspase-8 activation. *Proc Natl Acad Sci U S A* *98*, 7829-7834.

Stanger, B.Z., Leder, P., Lee, T.H., Kim, E., and Seed, B. (1995). RIP: a novel protein containing a death domain that interacts with Fas/APO-1 (CD95) in yeast and causes cell death. *Cell* *81*, 513-523.

Strasser, A., Jost, P.J., and Nagata, S. (2009). The many roles of FAS receptor signaling in the immune system. *Immunity* *30*, 180-192.

Strasser, A., O'Connor, L., and Dixit, V.M. (2000). Apoptosis signaling. *Annu Rev Biochem* *69*, 217-245.

Sun L Fau - Wang, H., Wang H Fau - Wang, Z., Wang Z Fau - He, S., He S Fau - Chen, S., Chen S Fau - Liao, D., Liao D Fau - Wang, L., Wang L Fau - Yan, J., Yan J Fau - Liu, W., Liu W Fau - Lei, X., Lei X Fau - Wang, X., *et al.* (2012). Mixed Lineage Kinase Domain-like Protein Mediates Necrosis Signaling Downstream. *Cell* *148*, 213-227.

Sun, X., Lee, J., Navas, T., Baldwin, D.T., Stewart, T.A., and Dixit, V.M. (1999). RIP3, a novel apoptosis-inducing kinase. *J Biol Chem* *274*, 16871-16875.

Sun, X., Yin, J., Starovasnik, M.A., Fairbrother, W.J., and Dixit, V.M. (2002). Identification of a novel homotypic interaction motif required for the phosphorylation of receptor-interacting protein (RIP) by RIP3. *J Biol Chem* *277*, 9505-9511.

Tabeta, K., Georgel, P., Janssen, E., Du, X., Hoebe, K., Crozat, K., Mudd, S., Shamel, L., Sovath, S., Goode, J., *et al.* (2004). Toll-like receptors 9 and 3 as essential components of innate immune defense against mouse cytomegalovirus infection. *Proc Natl Acad Sci U S A* *101*, 3516-3521.

Takaoka, A., and Taniguchi, T. (2007). Cytosolic DNA recognition for triggering innate immune responses. *Adv Drug Deliv Rev*.

Takaoka, A., Wang, Z., Choi, M.K., Yanai, H., Negishi, H., Ban, T., Lu, Y., Miyagishi, M., Kodama, T., Honda, K., *et al.* (2007). DAI (DLM-1/ZBP1) is a cytosolic DNA sensor and an activator of innate immune response. *Nature* *448*, 501-505.

Takeuchi, O., and Akira, S. (2009). Innate immunity to virus infection. *Immunol Rev* *227*, 75-86.

Tandon, R., and Mocarski, E.S. (2008). Control of cytoplasmic maturation events by cytomegalovirus tegument protein pp150. *J Virol* *82*, 9433-9444.

Taylor, J.M., and Barry, M. (2006). Near death experiences: poxvirus regulation of apoptotic death. *Virology* *344*, 139-150.

Tenev, T., Bianchi, K., Darding, M., Broemer, M., Langlais, C., Wallberg, F., Zachariou, A., Lopez, J., Macfarlane, M., Cain, K., *et al.* (2011). The Ripoptosome, a Signaling Platform that Assembles in Response to Genotoxic Stress and Loss of IAPs. *Mol Cell* *43*, 432-448.

Thome, M., Schneider, P., Hofmann, K., Fickenscher, H., Meinel, E., Neipel, F., Mattmann, C., Burns, K., Bodmer, J.L., Schroter, M., *et al.* (1997). Viral FLICE-inhibitory proteins (FLIPs) prevent apoptosis induced by death receptors. *Nature* *386*, 517-521.

Thome, M., and Tschopp, J. (2001). Regulation of lymphocyte proliferation and death by FLIP. *Nature reviews Immunology* *1*, 50-58.

Thompson, C.B. (1995). Apoptosis in the pathogenesis and treatment of disease. *Science* *267*, 1456-1462.

Thornberry, N.A., and Lazebnik, Y. (1998). Caspases: enemies within. *Science* *281*, 1312-1316.

Ting, A.T., Pimentel-Muinos, F.X., and Seed, B. (1996). RIP mediates tumor necrosis factor receptor 1 activation of NF-kappaB but not Fas/APO-1-initiated apoptosis. *EMBO J* *15*, 6189-6196.

Unterholzner, L., Keating, S.E., Baran, M., Horan, K.A., Jensen, S.B., Sharma, S., Sirois, C.M., Jin, T., Latz, E., Xiao, T.S., *et al.* (2010). IFI16 is an innate immune sensor for intracellular DNA. *Nat Immunol* *11*, 997-1004.

Upton, J.W., Kaiser, W.J., and Mocarski, E.S. (2008). Cytomegalovirus M45 cell death suppression requires receptor-interacting protein (RIP) homotypic interaction motif (RHIM)-dependent interaction with RIP1. *J Biol Chem* *283*, 16966-16970.

Upton, J.W., Kaiser, W.J., and Mocarski, E.S. (2010). Virus inhibition of RIP3-dependent necrosis. *Cell Host Microbe* *7*, 302-313.

- Upton, J.W., Kaiser, W.J., and Mocarski, E.S. (2012). DAI/ZBP1/DLM-1 Complexes with RIP3 to Mediate Virus-Induced Programmed Necrosis that Is Targeted by Murine Cytomegalovirus vIRA. *Cell Host Microbe* *11*, 290-297.
- Van Antwerp, D.J., Martin, S.J., Kafri, T., Green, D.R., and Verma, I.M. (1996). Suppression of TNF-alpha-induced apoptosis by NF-kappaB. *Science* *274*, 787-789.
- Vanden Berghe, T., Kalai, M., Denecker, G., Meeus, A., Saelens, X., and Vandenabeele, P. (2006). Necrosis is associated with IL-6 production but apoptosis is not. *Cell Signal* *18*, 328-335.
- Vandenabeele, P., Declercq, W., Van Herreweghe, F., and Vanden Berghe, T. (2010a). The role of the kinases RIP1 and RIP3 in TNF-induced necrosis. *Sci Signal* *3*, re4.
- Vandenabeele, P., Galluzzi, L., Vanden Berghe, T., and Kroemer, G. (2010b). Molecular mechanisms of necroptosis: an ordered cellular explosion. *Nat Rev Mol Cell Biol* *11*, 700-714.
- Vanlangenakker, N., Vanden Berghe, T., Bogaert, P., Laukens, B., Zobel, K., Deshayes, K., Vucic, D., Fulda, S., Vandenabeele, P., and Bertrand, M.J. (2011). cIAP1 and TAK1 protect cells from TNF-induced necrosis by preventing RIP1/RIP3-dependent reactive oxygen species production. *Cell death and differentiation* *18*, 656-665.
- Varfolomeev, E., Goncharov, T., Fedorova, A.V., Dynek, J.N., Zobel, K., Deshayes, K., Fairbrother, W.J., and Vucic, D. (2008). c-IAP1 and c-IAP2 are critical mediators of tumor necrosis factor alpha (TNFalpha)-induced NF-kappaB activation. *J Biol Chem* *283*, 24295-24299.
- Varfolomeev, E.E., Schuchmann, M., Luria, V., Chiannikulchai, N., Beckmann, J.S., Mett, I.L., Rebrikov, D., Brodianski, V.M., Kemper, O.C., Kollet, O., *et al.* (1998). Targeted disruption of the mouse Caspase 8 gene ablates cell death induction by the TNF receptors, Fas/Apo1, and DR3 and is lethal prenatally. *Immunity* *9*, 267-276.
- Ventura, A., Kirsch, D.G., McLaughlin, M.E., Tuveson, D.A., Grimm, J., Lintault, L., Newman, J., Reczek, E.E., Weissleder, R., and Jacks, T. (2007). Restoration of p53 function leads to tumour regression in vivo. *Nature* *445*, 661-665.
- Vercammen, D., Beyaert, R., Denecker, G., Goossens, V., Van Loo, G., Declercq, W., Grooten, J., Fiers, W., and Vandenabeele, P. (1998a). Inhibition of caspases increases the sensitivity of L929 cells to necrosis mediated by tumor necrosis factor. *J Exp Med* *187*, 1477-1485.
- Vercammen, D., Brouckaert, G., Denecker, G., Van de Craen, M., Declercq, W., Fiers, W., and Vandenabeele, P. (1998b). Dual signaling of the Fas receptor: initiation of both apoptotic and necrotic cell death pathways. *J Exp Med* *188*, 919-930.
- Versteeg, G.A., and Garcia-Sastre, A. (2010). Viral tricks to grid-lock the type I interferon system. *Curr Opin Microbiol* *13*, 508-516.
- Vince, J.E., Pantaki, D., Feltham, R., Mace, P.D., Cordier, S.M., Schmukle, A.C., Davidson, A.J., Callus, B.A., Wong, W.W., Gentle, I.E., *et al.* (2009). TRAF2 must bind to cellular inhibitors of

apoptosis for tumor necrosis factor (tnf) to efficiently activate nf- κ b and to prevent tnf-induced apoptosis. *The Journal of biological chemistry* 284, 35906-35915.

Vivarelli, M.S., McDonald, D., Miller, M., Cusson, N., Kelliher, M., and Geha, R.S. (2004). RIP links TLR4 to Akt and is essential for cell survival in response to LPS stimulation. *J Exp Med* 200, 399-404.

Vucic, D., Dixit, V.M., and Wertz, I.E. (2011). Ubiquitylation in apoptosis: a post-translational modification at the edge of life and death. *Nat Rev Mol Cell Biol* 12, 439-452.

Wajant, H., and Scheurich, P. (2011). TNFR1-induced activation of the classical NF-kappaB pathway. *The FEBS journal* 278, 862-876.

Walczak, H. (2011). TNF and ubiquitin at the crossroads of gene activation, cell death, inflammation, and cancer. *Immunol Rev* 244, 9-28.

Wang, F., Gao, X., Barrett, J.W., Shao, Q., Bartee, E., Mohamed, M.R., Rahman, M., Werden, S., Irvine, T., Cao, J., *et al.* (2008a). RIG-I mediates the co-induction of tumor necrosis factor and type I interferon elicited by myxoma virus in primary human macrophages. *PLoS Pathog* 4, e1000099.

Wang, J., Zheng, L., Lobito, A., Chan, F.K., Dale, J., Sneller, M., Yao, X., Puck, J.M., Straus, S.E., and Lenardo, M.J. (1999). Inherited human Caspase 10 mutations underlie defective lymphocyte and dendritic cell apoptosis in autoimmune lymphoproliferative syndrome type II. *Cell* 98, 47-58.

Wang, L., Du, F., and Wang, X. (2008b). TNF-alpha induces two distinct caspase-8 activation pathways. *Cell* 133, 693-703.

Wang, Z., Choi, M.K., Ban, T., Yanai, H., Negishi, H., Lu, Y., Tamura, T., Takaoka, A., Nishikura, K., and Taniguchi, T. (2008c). Regulation of innate immune responses by DAI (DLM-1/ZBP1) and other DNA-sensing molecules. *Proc Natl Acad Sci U S A*.

Wang Z Fau - Jiang, H., Jiang H Fau - Chen, S., Chen S Fau - Du, F., Du F Fau - Wang, X., and Wang, X. (2012). The Mitochondrial Phosphatase PGAM5 Functions at the Convergence Point of. *Cell* 148, 228-243.

Watanabe-Fukunaga, R., Brannan, C.I., Copeland, N.G., Jenkins, N.A., and Nagata, S. (1992). Lymphoproliferation disorder in mice explained by defects in Fas antigen that mediates apoptosis. *Nature* 356, 314-317.

Welz, P.S., Wullaert, A., Vlantis, K., Kondylis, V., Fernandez-Majada, V., Ermolaeva, M., Kirsch, P., Sterner-Kock, A., van Loo, G., and Pasparakis, M. (2011). FADD prevents RIP3-mediated epithelial cell necrosis and chronic intestinal inflammation. *Nature* 477, 330-334.

White, E. (2006). Mechanisms of apoptosis regulation by viral oncogenes in infection and tumorigenesis. *Cell Death Differ* 13, 1371-1377.

- Wilson, N.S., Dixit, V., and Ashkenazi, A. (2009). Death receptor signal transducers: nodes of coordination in immune signaling networks. *Nat Immunol* 10, 348-355.
- Wong, W.W., Gentle, I.E., Nachbur, U., Anderton, H., Vaux, D.L., and Silke, J. (2010). RIPK1 is not essential for TNFR1-induced activation of NF-kappaB. *Cell Death Differ.* 17, 482-487.
- Yamamoto, M., Sato, S., Mori, K., Hoshino, K., Takeuchi, O., Takeda, K., and Akira, S. (2002). Cutting edge: a novel Toll/IL-1 receptor domain-containing adapter that preferentially activates the IFN-beta promoter in the Toll-like receptor signaling. *J Immunol* 169, 6668-6672.
- Yang, P., An, H., Liu, X., Wen, M., Zheng, Y., Rui, Y., and Cao, X. (2010). The cytosolic nucleic acid sensor LRRFIP1 mediates the production of type I interferon via a beta-catenin-dependent pathway. *Nat Immunol* 11, 487-494.
- You, Z., Savitz, S.I., Yang, J., Degterev, A., Yuan, J., Cuny, G.D., Moskowitz, M.A., and Whalen, M.J. (2008). Necrostatin-1 reduces histopathology and improves functional outcome after controlled cortical impact in mice. *J Cereb Blood Flow Metab* 28, 1564-1573.
- Yu, L., Alva, A., Su, H., Dutt, P., Freundt, E., Welsh, S., Baehrecke, E.H., and Lenardo, M.J. (2004). Regulation of an ATG7-beclin 1 program of autophagic cell death by caspase-8. *Science* 304, 1500-1502.
- Yu, P.W., Huang, B.C., Shen, M., Quast, J., Chan, E., Xu, X., Nolan, G.P., Payan, D.G., and Luo, Y. (1999). Identification of RIP3, a RIP-like kinase that activates apoptosis and NFkappaB. *Curr Biol* 9, 539-542.
- Yuan, J., and Kroemer, G. (2010). Alternative cell death mechanisms in development and beyond. *Genes Dev* 24, 2592-2602.
- Zhang, D.W., Shao, J., Lin, J., Zhang, N., Lu, B.J., Lin, S.C., Dong, M.Q., and Han, J. (2009). RIP3, an Energy Metabolism Regulator that Switches TNF-Induced Cell Death from Apoptosis to Necrosis. *Science*. 325(5938), 332-336.
- Zhang, D.W., Zheng, M., Zhao, J., Li, Y.Y., Huang, Z., Li, Z., and Han, J. (2011a). Multiple death pathways in TNF-treated fibroblasts: RIP3- and RIP1-dependent and independent routes. *Cell Res* 21, 368-371.
- Zhang, H., Zhou, X., McQuade, T., Li, J., Chan, F.K., and Zhang, J. (2011b). Functional complementation between FADD and RIP1 in embryos and lymphocytes. *Nature* 471, 373-376.
- Zhang, X., Brann, T.W., Zhou, M., Yang, J., Oguariri, R.M., Lidie, K.B., Imamichi, H., Huang, D.W., Lempicki, R.A., Baseler, M.W., *et al.* (2011c). Cutting edge: Ku70 is a novel cytosolic DNA sensor that induces type III rather than type I IFN. *J Immunol* 186, 4541-4545.
- Zhang, Z., Yuan, B., Bao, M., Lu, N., Kim, T., and Liu, Y.J. (2011d). The helicase DDX41 senses intracellular DNA mediated by the adaptor STING in dendritic cells. *Nat Immunol* 12, 959-965.

Zhao, J., Jitkaew, S., Cai, Z., Choksi, S., Li, Q., Luo, J., and Liu, Z.G. (2012). Mixed lineage kinase domain-like is a key receptor interacting protein 3 downstream component of TNF-induced necrosis. *Proc Natl Acad Sci U S A* *109*, 5322-5327.